AN UNCERTAINTY FRAMEWORK FOR IMPROBABLE SLOPE FAILURE

by

Omar Barghouthi

in partial fulfillment of the requirements for the degree of

Master of Science
in Civil Engineering

at the Delft University of Technology,
to be defended publicly on Monday August 28, 2017 at 9:00 AM.

Supervisor:	Prof. dr. M. A. Hicks	TU Delft
Thesis committee:	Dr. A. P. van den Eijnden,	TU Delft
	Dr. P. J. Vardon,	TU Delft
	Dr. M. Schweckendiek,	TU Delft

An electronic version of this thesis is available at http://repository.tudelft.nl/.

TU Delft Delft University of Technology

ABSTRACT

Soil properties used to determine the stability of soil structures are variable in nature. Uncertainty in soil can be attributed to its inherent variability, as well as sources of error encountered while estimating the magnitude of its properties. The modelling of these uncertainties will produce more meaningful solutions when evaluating stability. This is especially relevant when quantifying the probability and risk associated with a rare event of failure.

An uncertainty framework is implemented in this report to evaluate improbable slope failure. A slope stability program using a modified subset simulation approach (van den Eijnden and Hicks, 2017) is expanded to account for cross-correlation between cohesion, friction angle and unit weight of soil. The mean of the three soil properties and their correlation coefficients are treated as random variables in the analysis. A parametric study is performed to evaluate the influence of the mean and correlation coefficients of these properties on the probability of failure. The influence of randomising these properties is also evaluated in the analysis. The implemented method is applied for a practical slope example, based on values reported in literature for the expected variability in the mentioned soil properties.

Results demonstrate that modelling the mean of c, ϕ and γ as a random variable leads to a significant increase in the probability of failure for a slope. While treating the correlation coefficients as random in the analysis will lead to very little changes in the outcome, some generated correlation matrices may lead to a notable decrease in probability of failure. The stability of the slope is heavily influenced by the input parameters used in the analysis. Furthermore, a proper choice for coefficient of variation of each property and the horizontal and vertical scales of fluctuation is necessary to avoid inaccurate results in the analysis. Other inputs investigated include the type of distribution for each soil property and the range of possible values for their means. Different distribution types are tested in the analysis to identify which of these properly model the variability in the parameter.

By evaluating generated samples within each subset level, it is evident that a combination of low mean values for c and positive correlation between ϕ and γ is required for failure at low probability of failure levels. Although the influence of set means of c, ϕ and γ on the calculated proability of failure is similar, the same conclusion cannot be made when the means of the properties are random. At low probability of failure levels, the outcome is very sensitive to changes in the minimum possible value for c and less to changes in ϕ and γ. Furthermore, it is demonstrated that the mode of failure may be overestimated when analysing stability by reducing the strength of the slope. Shallow failures are encountered when slope is failing under a strength reduction factor of 1, which is a more likely mode of failure in spatially variable soil.

PREFACE

I would like to take the opportunity to thank my daily supervisor Bram van den Eijnden for his continued support and input during this whole process; the rest of my thesis committee Michael Hicks, Phil Vardon and Timo Schweckendiek for their confidence and guidance; and my friends and family for keeping me motivated and supporting me during this period.

Omar Barghouthi
Delft, August 2017

CONTENTS

NOMENCLATURE

Ω^i	subset
$\xi^{Ms}{}_i$	zero mean non-skewed random numbers
α_x	reduction factor
β	reliability Index
γ	Unit weight
γ_m	partial safety factor
μ	mean
Ω^0	total sample space
$\overline{P}_f$	Sample mean for p_f
Φ	cumaltive standard normal distribution
ϕ	friction angle
σ	standard deviation
θ	scale of fluctuation
θ_h	Horizontal scale of fluctuation
θ_i	samples in MMH
θ_v	Vertical scale of fluctuation
θ^*	proposal sample in MMH
θ^s	seed sample in MMH
$\tilde{x}$	Antithetic sample
p_f	probability of failure
c	cohesion
$c_{0,1}$	computation cost
CDF	cumulative density function
COV	Coefficient of Variation
D	demand (load)
D_f	failure zones
D_s	safe zones
DOF	Degrees of freedom
E[]	expected Value
F(x)	cumulative density function
f(x)	probability density function
$F_{1,2,..,m}$	Intermediate failure events
FORM	First Order Reliability Method
FOSM	First Order Second Moment Method
I_F	indicator function
ISD	importance sampling density
MCMC	Markov chain Monte Carlo
MCS	Monte Carlo Simulation
MH	Metropolis-Hastings algorithm
MMH	Modified Metropolis Algorithm
N	total number of samples
N_F	samples in failure domain
p()	conditional PDF values
PDF	robability density function
q()	PDF values
R	resistance
r_a	acceptance ratio in MMH
RFEM	Random Finite Element Method
S	load
S_u	undrained shear strength
SRF	strength reduction factor
SS	Subset Simulation
U	standard normal variables
X	random variables
X_D	design property value
X_K	charectaristic property value
Z	limit state

1

General Introduction

When determining the stability of a soil slope, any calculation requires knowledge about soil parameters, geometry of the structure and other properties that are needed as input in the analysis. This knowledge is usually based on site investigations, lab testing and engineering judgement. The acquired information is then applied in a calculation model to evaluate the problem. In classical geo-technical analysis, deterministic methods have been used to determine the stability of slopes and other geo-structures. In these methods, single representative values are chosen for material properties to come up with a global factor of safety. The soil is considered as homogeneous and is only represented by one set of parameters. However, these type of methods fail to take into account the inherent uncertainty that is a part of any geo-technical system. Rather than modelling such uncertainty, deterministic methods make use of partial factors that scale the uncertain parameters, which is found to be conservative.

There are different sources of soil uncertainty but it mainly stems from the fact that soil is in itself variable. Soil investigations rely on in-situ and lab testing before transforming test results using models to estimate soil properties. This process will lead to more uncertainty, due to measurement error in testing, and uncertainty in the transformation model. Furthermore, studies have shown that correlation exists between different soil properties. Such dependence between parameters may influence stability results and therefore should be investigated as part of an uncertainty analysis(Fenton and Griffiths (2003); Javankhoshdel and Bathurst (2015); Cho and Park (2010)). In recent times, probabilistic methods have been applied to take into account such uncertainty. Simple probabilistic approaches include modelling parameters as random variables by only using their statistical properties (mean and standard deviation). While these methods take into account the uncertainty in determining such parameters, the soil is still considered homogeneous and is represented by one set of values. This neglects the spatial variability of soil material properties. In reality, soil is a heterogeneous material and therefore material properties vary spatially in both the vertical and horizontal direction. This is mainly due to the deposition process that lead to the formation of the soil body in question.

Therefore, advanced probabilistic methods have been introduced, where soil properties are modelled as random fields. In these approaches, both the statistical properties and the spatial variability of soil parameters is taken into account in the analysis. By combing deterministic and stochastic approaches, probabilistic methods represent the structure response using either probability of failure or its complement, reliability. This will require multiple simulations of possible random fields and will produce a more meaningful definition of stability than in the case with a factor of safety (Hicks and Samy, 2002).One way to carry out such an analysis is with the use of Monte

Carlo simulations. Based on the stastistical properties and spatial variability of soil parameters, a number of realisations are generated and their stability is evaluated. The probability of failure is then simply the ratio of failing realisations over total realisations.

In the case of rare events of failure, traditional sampling techniques such as a Monte Carlo Simulation become computationally expensive to carry out. This lead to the development of variance reduction techniques that can achieve the same outcome but with lower computational costs or lower variance. Subset simulation is such a method that was first developed by Au and Beck (2001). It uses properties of conditional probability to determine reliability with a reduced number of samples. van den Eijnden and Hicks (2017) carried out an analysis to investigate slope stability of cohesive slopes using a modified approach of subset simulation. This was performed using the Random Finite Element Method (Griffiths and Fenton, 2004) and cohesion was modelled as a random variable in the analysis.

1.1. AIM OF REPORT

The aim of this report is to expand on this approach by implementing a method that takes into account uncertainty in multiple soil properties in the procedure of subset simulation. This includes:

1. Modelling cohesion, friction angle and unit weight as spatially variable properties
2. Modelling the mean of c ,ϕ and γ as random variables
3. Introducing cross-correlation between the three properties and modelling correlation coefficients as random variables

This requires the implementation of an uncertainty framework within subset simulation. After implementation, the method can be applied to compute the probability of failure for rare events of slope instability. By doing so, it becomes possible to examine the most critical combinations of parameters that lead to failure at such low probability levels.

1.2. RESEARCH QUESTIONS

Recent studies have incorporated subset simulation to evaluate improbable slope failure events. While some reported on the effect of introducing cross-correlation between c and ϕ (eg. Javankhoshdel and Bathurst (2015)), none have considered correlation between three or more properties in the analysis. Furthermore, uncertainty in the magnitude of the mean of properties is examined in numerous studies but means have rarely been modelled as random variables. This is also the case for the magnitude of correlation coefficients between such properties. For this uncertainty framework, the following research questions are identified:

1. How can cross-correlation be implemented within Subset Simulation?
2. How can uncertainty in means and correlation coefficients of soil properties be implemented within Subset Simulation ?
3. What is the effect of type and range of distribution for these random parameters?
4. What are the most critical combinations of parameters that lead to failure?
5. Does it make sense to apply such an uncertainty framework?

1.3. OUTLINE OF REPORT

This report presents a framework for modelling uncertainty in the procedure of subset simulation. This includes an evaluation of the influence of all random variables on the calculated probability of failure. Furthermore, a practical example for an ideal slope is carried out to identify the most critical combinations of parameters that lead to failure. The report begins with a theory review to identify key concepts, conventions and procedures that are required for a slope stability analysis using subset simulation. Therefore, the report is divided in to the following chapters:

1. Theory review
2. Implementation
3. Sensitivity analysis
4. Practical example

The first chapter includes a literature review for uncertainty in general, and modelling soil uncertainty in particular. The different probabilistic methods that can be applied to evaluate reliability of a structure are also identified. Furthermore variance reduction methods are discussed before examining in detail the procedure of subset simulation. Finally an overview of slope stability methods and the Random Finite Element Method is carried out before investigating theory for how cross-correlation can be achieved between input parameters.

The implementation chapter describes how uncertainty is included in the analysis. The original code used in this analysis was developed by van den Eijnden and Hicks (2017). The section details how slope stability is evaluated in this code and the additions required to achieve the aims identified previously in this section. This includes flow charts to illustrate how cross-correlation and uncertainty will be implemented within the framework of subset simulation. A detailed explanation of the different distributions used in the analysis is also be provided.

A sensitivity analysis is then performed to identify the influence of different input parameters on the outcome of the results. This includes the sensitivity of probability of failure to changes in mean values (c ,ϕ and γ), correlation coefficients, and scales of fluctuation. The influence of randomising these parameters is also investigated within this chapter before evaluating the effect of their distribution type on the outcome. The final chapter includes results for a practical example in order to evaluate the most critical combination of parameters at different failure levels. The input used for this example is based on values reported in literature for the variability of soil parameters. The results of this section in combination with the sensitivity analysis are used to answer the last three research questions identified.

2

THEORY REVIEW

2.1. INTRODUCTION

Before attempting to answer the research questions identified in the beginning of this paper, it is necessary to gain better understanding about the different topics that are related to the subject in question. This includes a review of soil uncertainty, subset simulation and slope stability. Available literature is examined to identify methods that have been previously applied, conventions and equations needed for the analysis, and possible limitations for the scope of the research. By examining all the components related to this subset simulation approach, it becomes possible to identify the modifications required to introduce an uncertainty framework and how these additions can be implemented in the analysis.

First the different sources of uncertainty are highlighted before defining how they can and are modelled in literature. Next, the different methods of reliability are elaborated before identifying a need for advanced sampling techniques. The subset simulation approach is then described in detail and its different components are analysed. To link the approach to a real life application, slope stability is defined and its most common methods in literature are introduced. Furthermore, the Random Finite Element Method (RFEM) is evaluated to illustrate how reliability methods, slope stability and subset simulation can be applied together in practice. Finally, cross-correlation is included to investigate the procedure of achieving correlation between soil parameters.

2.2. UNCERTAINTY

Most engineering problems that assess reliability and risk do so within the framework of a model universe. This universe includes the physical and probabilistic sub-models that are used to evaluate an engineering problem to reach a solution. The model universe will have inherent uncertainty as well as added uncertainty that stems from the physical and probabilistic sub-models in the analysis. These sources of uncertainty can be characterised into either aleatory or epistemic and together they can be referred to as global uncertainty. The word aleatory comes from the latin word *alea* which means a roll of the dice. On the other hand epistemic derives from *episteme* which means knowledge. Therefore, aleatory uncertainty refers to inherent randomness and epistemic uncertainty refers to a lack of knowledge (Kiureghian and Ditlevsen, 2007). Most engineering problems will involve a combination of both uncertainties and this is heavily dependant on the set-up of the models.

2.2.1. SOURCES OF UNCERTAINTY

According to Kiureghian and Ditlevsen (2007), general sources of uncertainty of the model universe in the framework of a reliability analysis are:

1. Inherent uncertainty of the basic random variables
2. Uncertain modelling error resulting from the form of the probabilistic model and the selection of the physical model
3. Statistical uncertainty in determining parameters of both physical and probabilistic models
4. Uncertainty in measurements used as input for sub-models
5. Uncertainty in modelling the system response due to approximations and computation errors.

For the first source of error, it is necessary to distinguish between basic and derived variables. In the model, a decision is made to whether a variable is set as basic and therefore is fit with a probabilistic model, or, the variable is derived from another more basic variable. In the latter case, the uncertainty in deriving the variable should be attributed to model uncertainty rather than variable uncertainty. For a basic variable, the uncertainty is considered to be epistemic if its possible to test samples to improve on the knowledge about the property. However, basic variables with uncertainty that cannot be improved upon (inherent) should be categorised as aleatory.

In the case of uncertainty due to model error, in many cases it can be improved upon with better approximates and refinement. Therefore, a large portion of the error can be attributed to epistemic uncertainty. On the other hand, in certain cases limited scientific knowledge can not be improved upon and therefore some of the error is categorised as aleatory. Furthermore, the uncertainty in model parameters is strictly epistemic (Kiureghian and Ditlevsen, 2007) as it decreases with more and better measurements.

2.2.2. SOIL UNCERTAINTY

According to Kulhawy (1992), uncertainty in soil can be attributed to three different sources:

- Variability of soil parameters
- Measurement errors
- Transformation errors and uncertainty

Figure 2.18 shows how these sources lead to an uncertainty in measuring soil properties. The first source, the inherent variability of soil can be attributed to the deposition processes that lead to the formation of the soil, and ongoing geological processes that continue to alter the soil body. This uncertainty source is charectarized as aleatory. Measurement errors on the other hand arise from equipment error and other random effects. Measurement error can be improved upon and therefore falls under epistemic uncertainty. Inherent variability and measurement errors together can be characterised as data scatter. The last source of uncertainty is attributed to the transformation of results from in situ and lab parameters to design parameters which is also categorised as epistemic.

The global uncertainty, due to the three sources of error heavily depends on site specific conditions (Elkateb et al., 2002). It is necessary to distinguish between global uncertainty and inherent

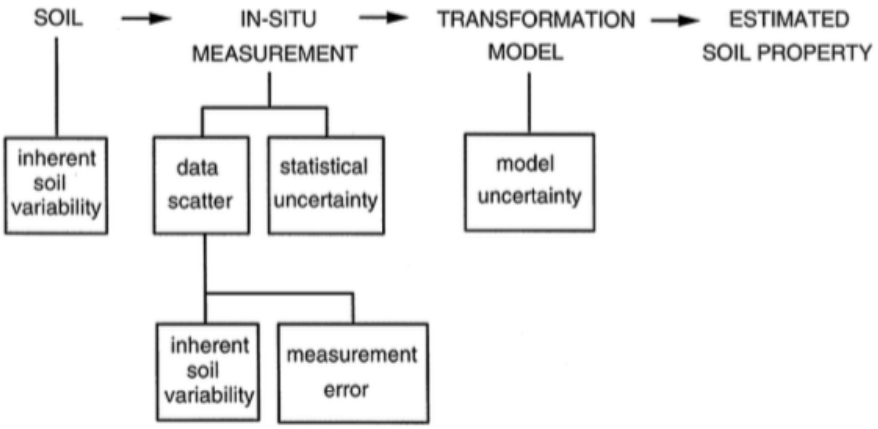

Figure 2.1: sources of uncertainty(Kulhawy, 1992)

soil uncertainty. Global or total uncertainty includes all sources of error that may lead to an uncertain output. This includes the site specific soil properties as well as the equipment and correlation models used in the analysis. The total global uncertainty can be improved with better field measurements. However, for this report no field measurements will be included and therefore only the inherent soil variability will be taken into account. As illustrated in the next section, this will be modelled using the coefficient of variation (COV) and the scale of fluctuation of soil parameters.

2.3. MODELLING OF UNCERTAIN SOIL PARAMETERS

Modelling the inherent variability of the soil can be done with the use of simplified probabilistic approaches. The variability of soil parameters is considered by using their statistical properties, mean μ and standard deviation σ, this is referred to as point statistics. Another way to represent these properties is with the use of coefficient of variation (COV) which is defined as the ratio between μ and σ (COV= σ/μ). In this simplified approach, in every stochastic realisation the soil is considered homogeneous with a set of parameters determined based on their COV. This fails to take into account the spatial variability that characterises a soil in both the horizontal and vertical direction, referred to as spatial statistics.

Advanced probabilistic approaches can be applied where the spatial variability is included and parameters are modelled with the use of random fields. This is achieved by introducing a statistical parameter referred to as the scale of fluctuation θ. Figure 2.2(a) (Hicks and Samy 2002) indicates how θ in the vertical direction is determined for undrained cohesion based on results of cone penetration tests (CPT). Figure 2.2(b) is the probability distribution function for the undrained cohesion based on μ and σ (COV). In this section, typical values from literature for COV and θ are summarised.

2.3.1. COEFFICIENT OF VARIATION

COV is a non-dimensional statistical parameter that can describe the dispersion of a probabilistic distribution relative to μ. Phoon and Kulhawy (1999) concluded that most COVs reported in literatures are that of total uncertainty and not just inherent soil variability. For this report, COV will only be based on soil parameter variability, which means that values reported could be overestimated as they include measurement and transformation uncertainty. For determining COV based on lab and field measurements, the overestimation can be minimised by:

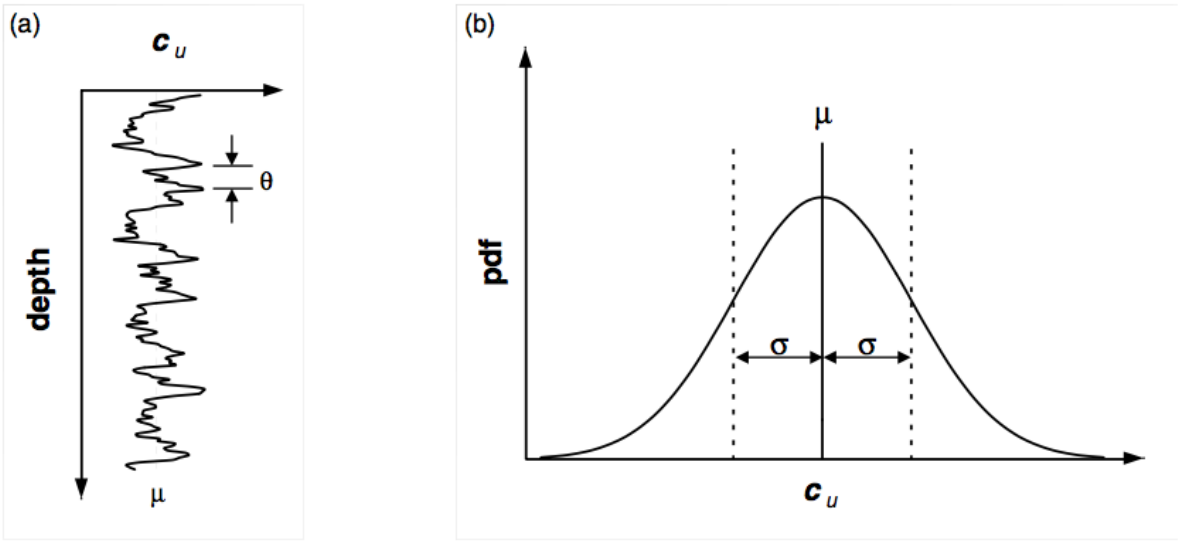

Figure 2.2: (a) S_u varying with depth, (b) PDF of S_u (Hicks and Samy, 2002)

1. Classifying data into separate geological units
2. Separating measurement error from soil variability
3. removing any depth trends if visible
4. removing time trends for samples

Figure 2.3 is a table that summarises COV results for soil parameters based on available literature. The parameters in question are the undrained shear strength of soil S_u and friction angle ϕ. Little or no literature is available regarding the COV of other soil properties such as unit weight γ.

Property[a]	Soil type	No. of data groups	No. of tests per group		Property value		Property COV (%)	
			Range	Mean	Range	Mean	Range	Mean
s_u(UC) (kN/m^2)	Fine grained	38	2–538	101	6–412	100	6–56	33
s_u(UU) (kN/m^2)	Clay, silt	13	14–82	33	15–363	276	11–49	22
s_u(CIUC) (kN/m^2)	Clay	10	12–86	47	130–713	405	18–42	32
s_u (kN/m^2)[b]	Clay	42	24–124	48	8–638	112	6–80	32
$\bar{\phi}$ (°)	Sand	7	29–136	62	35–41	37.6	5–11	9
$\bar{\phi}$ (°)	Clay, silt	12	5–51	16	9–33	15.3	10–50	21
$\bar{\phi}$ (°)	Clay, silt	9	—	—	17–41	33.3	4–12	9
tan $\bar{\phi}$ (TC)	Clay, silt	4	—	—	0.24–0.69	0.509	6–46	20
tan $\bar{\phi}$ (DS)	Clay, silt	3	—	—	—	0.615	6–46	23
tan $\bar{\phi}$[b]	Sand	13	6–111	45	0.65–0.92	0.744	5–14	9

[a] s_u, undrained shear strength; $\bar{\phi}$, effective stress friction angle; TC, triaxial compression test; UC, unconfined compression test; UU, unconsolidated–undrained triaxial compression test; CIUC, consolidated isotropic undrained triaxial compression test; DS, direct shear test.
[b] Laboratory test type not reported.

Figure 2.3: Variability of strength properties
(Phoon et al., 1995)

An analysis of the extensive literature review for COV of S_u indicates that the lower bound of COV remains constant at around 10% regardless of the mean. The upper bound however decreases with an increase in mean S_u. It was also found that the type of laboratory test used to determine COV of S_u has a direct effect on the range of values. For example, COV results from unconfined compression (UC) tests for S_u range between 20-55% while results from unconsolidated undrained

(UU) tests range between 10-30%. The general range of COV values of S_u reported in literature are between 10% and 40% with type of soil having little effect on reported values.

In the case of friction angle ϕ, COV results indicate a different story. The COV of ϕ of clay is generally higher than that of sand. For clayey and sandy soils, the σ of ϕ is constant while μ for clay soils tends to be much lower. Phoon and Kulhawy (1999) show that for a constant σ, the COV is inversely proportional to the μ which explains why COV of friction angle of clay is reported to be higher. For a friction angle ϕ between 20° and 40°, reported values of COV from literature range between 5% and 15%.

2.3.2. SCALE OF FLUCTUATION

Reliability of a structure is determined as a function of both point statistics (COV) and a spatial correlation property or autocorrelation function. The autocorrelation function is usually expressed in terms of an exponential decaying function referred to as the scale of fluctuation (θ). θ is defined as the distance beyond which the correlation between soil properties becomes negligible. In other words, it is the measure of distance between adjacent strong or weak zones(Hicks, 2016). Scale of fluctuation θ can be classified further into θ_h and θ_v, horizontal and vertical scale of fluctuation, respectively. Due to deposition processes, the value of θ_h is much bigger than that of θ_v which shows the anisotropy of soil heterogeneity. Many estimates of the autocorrelation function are available in literature (Hicks (2014); Hicks and Samy (2002); Phoon et al. (1995)). For example, Alonso (1976) introduced estimates for a correlation parameter α for different sand and clayey soil properties. Figure 2.4 is a summary of autocorrelation function estimates based on available literature. The table shows that θ_v is typically around 0.5 to 2m and that θ_h is at least an order of magnitude higher at around 40 to 60m.

Property[a]	Soil type	No. of studies	Scale of fluctuation (m) Range	Mean
Vertical fluctuation				
s_u	Clay	5	0.8–6.1	2.5
q_c	Sand, clay	7	0.1–2.2	0.9
q_T	Clay	10	0.2–0.5	0.3
s_u(VST)	Clay	6	2.0–6.2	3.8
N	Sand	1	—	2.4
w_n	Clay, loam	3	1.6–12.7	5.7
w_l	Clay, loam	2	1.6–8.7	5.2
$\bar{\gamma}$	Clay	1	—	1.6
γ	Clay, loam	2	2.4–7.9	5.2
Horizontal fluctuation				
q_c	Sand, clay	11	3.0–80.0	47.9
q_T	Clay	2	23.0–66.0	44.5
s_u(VST)	Clay	3	46.0–60.0	50.7
w_n	Clay	1	—	170.0

[a] s_u and s_u (VST), undrained shear strength from laboratory tests and vane shear tests, respectively; $\bar{\gamma}$, effective unit weight.

Figure 2.4: Summary of θ for some soil properties (Phoon et al., 1995)

The spatial correlation can be modelled with the use of random fields. At any arbitrary point within the soil, properties are unknown and are represented by a random variable characterised by their probability density function (PDF). The combination of all random variables within the soil layer are referred to as a random field. Different algorithms that can be used to generate approximate random fields are described in literature (Vanmarcke, 1983; Fenton and Vanmarcke, 1990; Griffiths and Fenton, 2004) . Local average subdivision (LAS) introduced by Fenton and Vanmarcke (1990) is considered as an efficient method and its use is documented in many geotechnical papers.

2.4. PROBABILISTIC / RELIABILITY ANALYSIS METHODS

The ultimate limit state evaluation of a safety of a structure in its simplest form is expressed as the resistance of a structure (R) versus its load (S). This can also be expressed in terms of a limit state Z where

$$Z = R - S \tag{2.1}$$

Failure of the structure will occur when S > R or in other words Z < 0. A general formation for the limit state Z is

$$g(\underline{X}) = Z = 0 \tag{2.2}$$

where g is the limit state function and the vector $\underline{X}$ consists of n variables such as material properties, loads and geometric properties. Some of these are random variables and therefore must be considered with a probabilistic distribution. On the other hand, some variables have little or no variability in time and space, and therefore can be considered deterministic. Let $f_{\underline{X}}(x)$ be the n-dimensional PDF for the n variables X_i. The failure probability can therefore be expressed as

$$P_f = \int_{g(\underline{X})<0} f_{\underline{X}}(x)\, d\underline{x} \tag{2.3}$$

with $f_{\underline{X}}(x)$ being the n-dimensional PDF of basic variable X_i. If the number of dimensions is 2 (n=2), then the probability of failure can be determined with the use of the joint probability distribution of R and S. The failure probability corresponds to the area where g(X) <0 (figure 2.5).

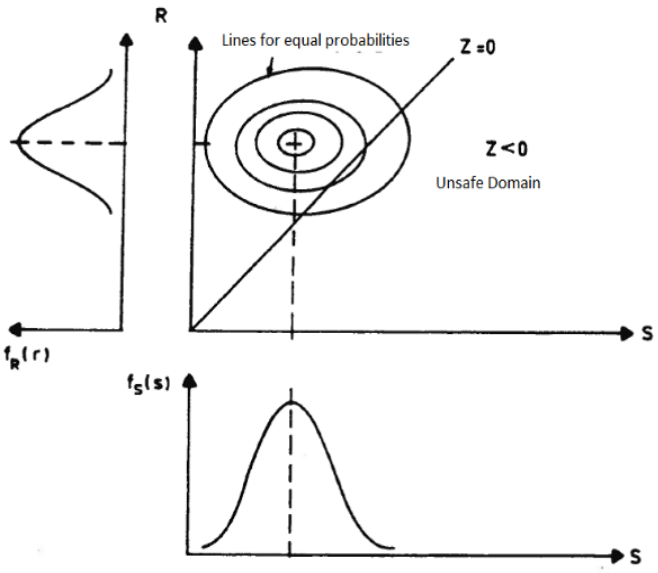

Figure 2.5: Probability of failure for n=2 (Jonkman et al., 2016)

Equation 2.14 can be elaborated or approximated with the use of different available methods, each with a different level of complexity and accuracy. In practice, these methods are referred to as reliability methods. Reliability is the compliment of probability of failure and it expresses the probability of a safe structure. Reliability index β is used as a measure of a safety and was defined by Cornell (1969) as

$$\beta = \frac{0 - \mu_Z}{\sigma_Z} = \frac{1}{COV_Z} \tag{2.4}$$

where COV_z refers to the coefficient of variation of Z. β is directly related to probability of failure and P_f can be expressed as

$$P_f = \Phi(-\beta) \tag{2.5}$$

where Φ is a cumulative standard normal distribution. Methods to elaborate the reliability of a structure can be divided into five different levels (Jonkman et al., 2016)

- **level 0: deterministic methods:** uncertainty is not taken into account and failure is expressed with the use of a factor of safety
- **level I: semi-probabilistic methods:** similar to engineering codes, uncertain parameters are modelled with the use of partial factors and only characteristic value for S and R
- **level II: approximation methods:** uncertain parameters are modelled with the use of their point statistics (COV) and cross-correlation. They are assumed to be normally distributed
- **level III: numerical methods:** uncertain parameters are modelled with the use of the joint PDF and cross correlation. Variables are modelled with a random field. Calculations are numerical and exact
- **level IIII: risk-based methods:** the consequence of failure is taken into account and risk is determined as probability of failure multiplied by the consequence

level 0 does not include any probabilistic calculations and will not be included in the analysis. On the other hand level IIII is similar to level III but with the inclusion of consequences such as cost or volume of sliding material for a slope failure. Therefore the following subsections will focus on reliability methods I, II, and III.

2.4.1. LEVEL I METHODS

In level I methods, uncertain parameters are taken into account with the use of a characteristic property value (X_k). A reliability based X_k is the only value of a material property, which, when used in a deterministic analysis, will gave the same response of a stochastic analysis for a given level of reliability (Hicks, 2016). Based on a mean property value (X_m), X_K is determined with the use of a reduction factor (α_x) as follows

$$X_K = \alpha_x X_m \tag{2.6}$$

α_x is a number between 0 and 1 however in most cases 1 is used as further partial factors are applied. According to Eurocode 7, the design property value is then determined based on a partial safety factor γ_m where

$$X_d = \frac{X_K}{\gamma_m} \tag{2.7}$$

This can be applied both to characteristic values of loads (S_K) and resistance (R_K) as shown in figure 2.6. The partial safety factor γ_m is determined with the use of a probabilistic calculation. This can be either level II or level III methods. However, the use of level III in this case is considered less straightforward (Jonkman et al., 2016). Furthermore, Eurocode 7 provides standardised values for load and resistance factors (α) independent of the specific application in question. These values are determined based on dominant loads and load combinations level II probabilistic approach which is introduced in the next section.

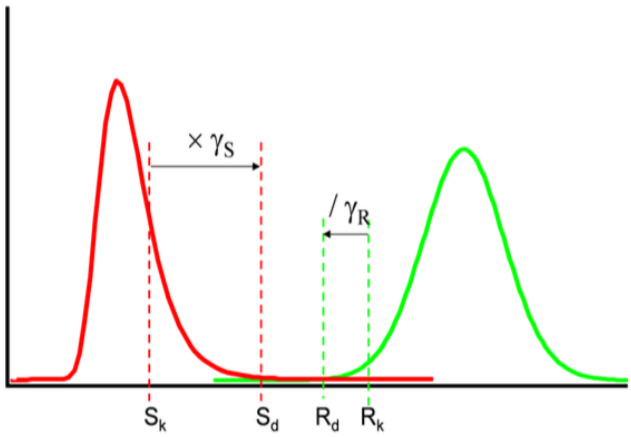

Figure 2.6: level I reliability method (Jonkman et al., 2016)

2.4.2. LEVEL II METHODS

In order to determine failure probability with the use of level II methods, the point statistics and the covariance matrix of the base variables are taken into account. For a linear reliability function with a normal distribution, it is relatively easy to determine the reliability using equation 2.4 for β (reliability index). If the limit state function is non linear, Taylor expansion is used to linearise the equation around the mean value of random parameters.(Jonkman et al., 2016)

$$g(\underline{X}) = Z \cong g(\mu_1, ..., \mu_n) + \sum_{i=1}^{n} \frac{\delta g(\mu_i)}{\delta X_i}(X_i - \mu_i) \tag{2.8}$$

which is a linearised function for the random variables X_i. Now the point statistics μ_z and σ_z can be determined using

$$\mu_z \cong g(\mu_1, ..., \mu_n) \tag{2.9}$$

$$\sigma^2{}_z \cong \sum_{i=1}^{n} \frac{\delta g(\underline{\mu})}{\delta X_i} \frac{\delta g(\underline{\mu})}{\delta X_j} COV[X_i, X_j] \tag{2.10}$$

where COV[X_i,X_j] is the covariance of X_i and X_j. Now, with the point statistics of a linear function, the reliability β once again can be calculated using equation 2.4. In the field of geotechnical engineering, this method is referred to as First Order Second Moment Method (FOSM). Its use has been noted in different reliability based geotechnical papers (Elkateb et al., 2002; Liang et al., 1999; Suchomel and Masin, 2010) as FOSM is easy to formulate as it does not require prior knowledge with regards to the PDF of the input variables. The drawbacks of using such as method is that β will heavily depend on how the limit state function is formulated(Griffiths et al., 2010). This means that results can differ greatly between one person to another.

Hasofer and Lind (1974) introduced a reliability index β that does not depend on the formulation of the limit state. In the case of uncorrelated normally distributed random variables, the variables are normalised to basic variables (μ=0 and σ=1) using

$$U_i = \frac{X_i - \mu_i}{\sigma_i} \tag{2.11}$$

the basic equation g($\underline{X}$) = R-S=0 is now rewritten in terms of the basic variables as

$$g(\underline{U}) = \sigma_R U_R - \sigma_S U_S + (\mu_R - \mu_S) \tag{2.12}$$

This simple case is represented in figure 2.7 where D_s and D_f refer to safe zones and failure zones, respectively. Using Pythagoras and properties of geometry, β can now be determined as the distance between the origin and point A. In this case, Hasofer and Lind (1974)define β as :

> *The reliability index β is equal to the shortest distance from the origin to the surface described by $g(\underline{U}) = 0$ in the space of the normalised basic variables.*

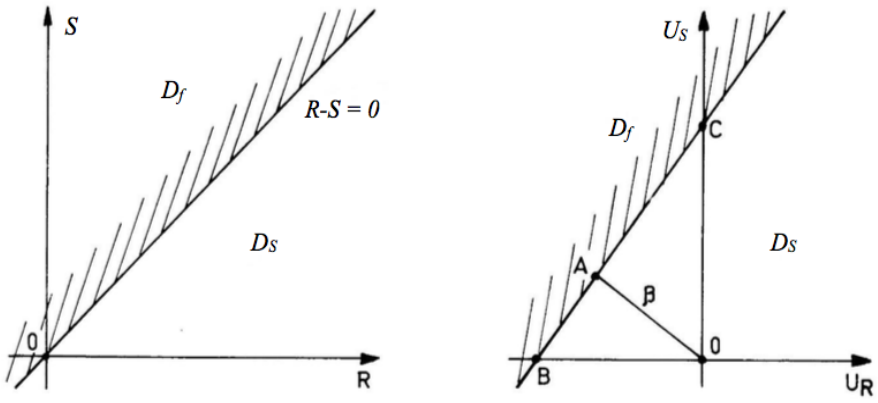

Figure 2.7: Linear limit state equation in the X- and U-space (Jonkman et al., 2016)

In the case of non-linear limit state functions, it becomes necessary to solve for a point referred to as the design point, similar to point A in figure 2.7. Evaluating the reliability index can now be done by one of the following methods:

1. Transformation to normal variables
2. Direct iteration based on limit state function

In the field, evaluating reliability by $\beta_{\text{Hasofer and Lind}}$ is referred to as First Order Reliability Method (FORM). The use of FORM has become popular because contrary to FOSM, β does not depend on how the limit state function is formulated (Griffiths et al., 2010).

2.4.3. LEVEL III METHODS

Level III reliability methods are methods of directly computing the integral of failure probability shown in equation 2.14. These methods are considered accurate because of the exact integration which also makes the methods rather time consuming. The most used methods of level III reliability are:

- Analytical integration
- Numerical integration
- Monte Carlo simulations

ANALYTICAL INTEGRATION

Analytical integration is seldom used as it requires a simple form failure surface with only a few basic variables for it to be applicable (Karandeniz and Vrouwenvelder, 2003). If the limit state function given in equation 2.1 is stated in terms of independent load and resistance variables, the joint PDF is equal to

$$f_X(r,s) = f_R(r) f_S(s) \tag{2.13}$$

With a known limit state or failure domain (R<S), the probability of failure integral can be evaluated based on the expected value (E) of the probability distribution function of R (F_R):

$$P_f = \int_{-\infty}^{\infty} f_S(s)\left(\int_{-\infty}^{S} f_R(r)\,dr\right)ds = \int_{-\infty}^{\infty} F_r(s) f_S(s)\,ds = E[F_R(s)] \tag{2.14}$$

For cases with different distributions and more complex limit state functions, the use of analytical integration is not possible. Therefore other techniques need to be applied to get an exact solution to the probability of failure integral.

NUMERICAL INTEGRATION

Figure 2.8a is a joint probability density function example for a load term (S) and a resistance term (R) (Jonkman et al., 2016). The volume under the joint PDF in the failure region (Z<0) is represented by the integral:

$$P_f = \int_{-\infty}^{\infty}\left[f_R(r)\int_{S=r}^{\infty} f_S(s)\,ds\right]dr \tag{2.15}$$

by dividing the domain into smaller bins (dr in fig 2.8a), the integral can be evaluated analytically as seen in the previous section. However, the integral can also be elaborated using numerical integration. This is achieved by splitting the failure region volume (Z<0) into smaller volumes as depicted in figure 2.8b. The failure probability can now be calculated exactly by using:

$$P_f = \sum_i \sum_i f_{R,S}(r_i, s_i)\Delta r \Delta s \tag{2.16}$$

This can also be achieved for non-linear limit state functions. In such cases, where load and resistance terms are a function of more random variables, the elaboration will include multiple integrals rather than single ones. This becomes more difficult and therefore numerical integration is only feasible up to a limited number of random variables up to a maximum around n=10 (Waarts, 2000). Therefore for problems with a large number of random variables, the computation cost for numerical integration is too high and other probabilistic methods of analysis are required.

MONTE CARLO SIMULATION (MCS)

For cases where numerical integration is not a viable option, a Monte Carlo simulation (MCS) can be used to evaluate the failure probability. The method achieves this by generating random variables, given a certain distribution function for these variables. MCS is one of the most applied methods in literature that is used to evaluate structural and geotechnical reliability, eg. El-Ramly et al. (2002); Griffiths et al. (2009); Hicks (2014). First, random numbers between 0 and 1 are generated from a uniform probability density function, this can be done with ease in any computational program such as Matlab or Excel. The random numbers are then transformed depending on the PDF of the unknown variables. Figure 2.9 shows 200 generated samples for the simple limit state example that has been dealt with in this report.

The general idea is that by sampling variables from their distribution and determining the number of samples that fall in the failure domain N_f, it becomes possible to estimate the probability of failure (Karandeniz and Vrouwenvelder, 2003) using

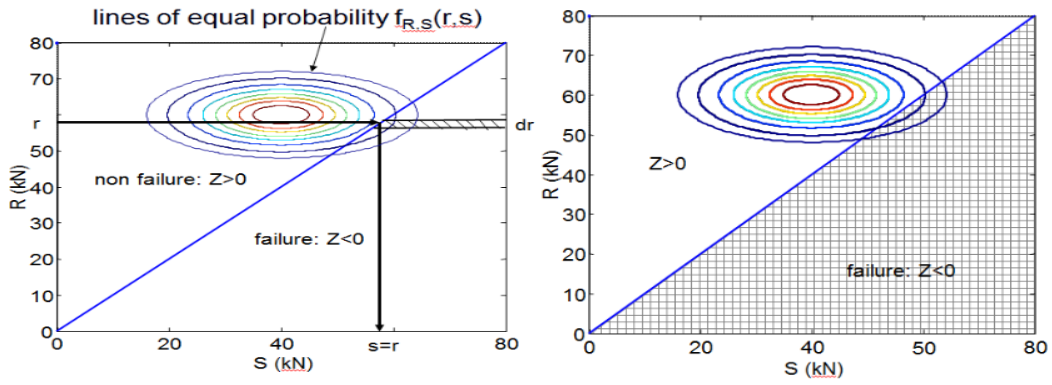

Figure 2.8: a) analytical integration vs b) numerical integration (Jonkman et al., 2016)

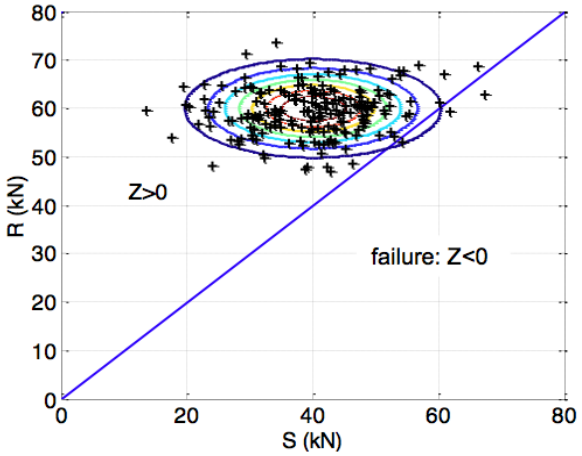

Figure 2.9: 200 generated samples for S and R (Jonkman et al., 2016)

$$\bar{P}_f = \frac{N_f}{N} \approx P_f \tag{2.17}$$

where $\overline{P}_f$ is the sample mean and N is the total number of generated samples.The relative error can be determined by evaluating the coefficient of variation of $\overline{P}_f$

$$COV(\bar{P}_f) = \sqrt{\frac{1-\bar{P}_f}{N\bar{P}_f}} \tag{2.18}$$

Equation 2.18 shows that the accuracy of the method largely depends on the number of random samples generated. As N increases, the relative error (COV) decreases and therefore the result is more accurate. However, generating more samples greatly increases computational time and therefore a balance needs to be achieved with regards to accuracy vs costs. Furthermore, equation 2.18 shows that for a target COV, the number of samples increases as the probability of failure decreases. For rare events (very low P_f) equation 2.18 becomes

$$COV(\bar{P}_f) = \frac{1}{\sqrt{N\bar{P}_f}} \tag{2.19}$$

If a target COV of 0.01 is required for a probability of failure of $1x10^{-6}$, the number of samples required is 10^{10}. This means that MCS is inefficient when considering rare events and techniques

to reduce the variance without the need for a large N need to be applied. These techniques are evaluated in the next section.

2.5. VARIANCE REDUCTION TECHNIQUES

As mentioned in the previous section, in order to evaluate rare failure events with very low probabilities of failure, crude MCS is not an option as the number of samples required becomes too high. This is because assessing low probabilities of failure requires information from rare samples corresponding to the failure. The number of required samples is proportional to $\frac{1}{P_f}$ and therefore many samples will be simulated before witnessing failure (Au and Beck, 2001).

Therefore, other more efficient methods need to be applied to asses such rare events of failure. These methods are referred to as variance reduction techniques, as they reduce the variance (error) rather than increase the number of samples required. By applying such techniques, the same solution produced by an extensive MCS can be achieved but with a smaller variance σ or a lower number of samples N. There are many different techniques that fall into this category such as:

- **Importance sampling:** More realisations are obtained in the failure zone (Z<0) by choosing a sampling function which falls within the domain that contributes the most to P_f. The success of the method depends on the chosen importance sampling density (ISD) which requires knowledge of the system in the failure region (Au and Beck, 2001)
- **Adaptive importance sampling:** The sampling distribution is adaptively improved while in the process of determining the probability of failure. Based on simulated sample paths, the method works by updating and learning an adapted change of measure which emphasises the path to the rare failure event in question (Juneja and Shahabuddin, 2006)
- **Antithetic variates:** An antithetic sample ($\tilde{x}$) is one that gives the opposite value of f(x) expected from x. Each value of x is balanced by $\tilde{x}$ and f(x) is balanced by f($\tilde{x}$). The method reduces both the number of samples N and the variance in sample path. The improvement in efficiency associated with antithetic samples largely depends on the limit state formulation.(Owen, 2013)
- **Stratification (Splitting):** Stratified sampling achieves better efficiency by splitting the domain into smaller sections and taking samples from each section. The samples are then combined and the expected value of the function is estimated.
- **Common random numbers:** If two different functions f and g are closely related, common random numbers method works by first assuming that both functions only sample from X. This assumption is then relaxed and common random numbers are retained which will lead to a decrease in variance.

It is necessary to mention that in order to asses the added value of a variance reduction technique, reduction in variance is not the only factor that determines the success of the method. The success also depends on the cost or computation time associated with the method which includes running time, memory allocated, and required human effort (Owen, 2013). Therefore, Owen (2013) defines the efficiency of a variance reduction technique relative to a standard method as:

$$E = \frac{c_0 {\sigma_0}^2}{c_1 {\sigma_1}^2} \tag{2.20}$$

At a certain level of accuracy, the standard or old method will take E times more work than the variance reduction method. Equation 2.20 has two different factors $\frac{c_0}{c_1}$ and $\frac{{\sigma_0}^2}{{\sigma_1}^2}$ where one is a ratio

of associated costs and the other a ratio of variance, respectively.

2.5.1. THE NEED FOR ADVANCED METHODS

Importance sampling has been used in literature as a variance reduction technique to estimate probability of rare events (Heidelberger, 1995; Shahabuddin, 1995). However, the effectiveness of the technique relies on the ability to choose the right sampling function (Glasserman et al., 1999). This means that a prediction is required for where the rare failure region lies within the domain. Therefore the mentioned importance sampling and variance reduction techniques above are only useful when assessing problems with a limited number of parameters and a simple failure region. For more complex problems, using these techniques becomes challenging.

The complexity of linear limit state systems depends on the number of degrees of freedom (DOF) needed to reach a solution. Schueller and Pardlwarter (2009) provided a measure of "complexity" for linear systems as any that require more than 10^4 DOF. This however does not describe the complexity that is associated with a non-linear system. This lead to the development of more efficient simulation methods such as Subset Simulation (SS). The method is considered appealing as it is wildly applicable if the limit state function is continuous, regardless of the non-linearity or complexity of the problem in hand.

2.6. SUBSET SIMULATION

Subset Simulation was first presented by Au and Beck (2001) as a new simulation approach to evaluate failure probabilities. The idea behind SS goes back to the basics of importance or multilevel splitting techniques (Glasserman et al., 1999). The method has become popular for the evaluation of rare events in structural reliability analysis (Wang et al., 2010; Liu et al., 2017).Furthermore various alterations or modifications have been proposed since 2001, for example Cerou et al. (2012); Brehier et al. (2016); van den Eijnden and Hicks (2017).

The premise of the method is that failure probability can be expressed as a product of larger conditional failure probabilities by the introduction of intermediate failure events $\{F_1, F_2,...,F_m\}$ (figure 2.10). This means that the problem of evaluating P_f is replaced by a sequence of smaller simulations of more frequent events. The analysis is restricted to a subset Ω^i of the total sample space Ω^0 (van den Eijnden and Hicks, 2017). This is achieved by using basic properties of conditional probability.

The probability of a rare failure event occurring is equal to the probability that it occurs, given that a more likely failure event has already happened, multiplied by the probability of that more likely event (Yu and Au, 2014). Let F= [S>C] where in this case S represents the demand (load) and C the capacity (resistance). The sequence of failure events can now be described as F_i= [D>C_i] where $C_1 < C_2 <... < C_m = C$ (figure 2.10). Using properties of conditional probability P_f becomes (Au and Beck, 2001)

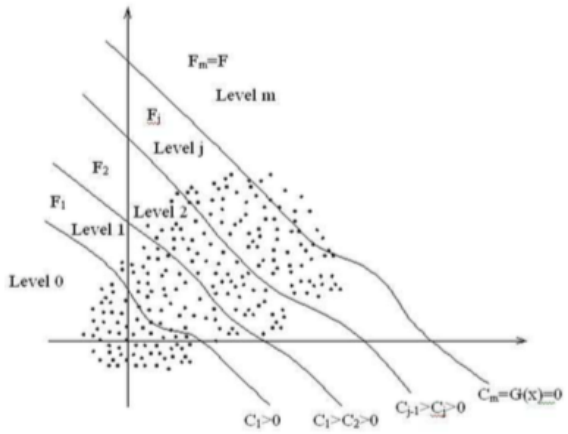

Figure 2.10: Nested failure domain (Soubra and Bastidas-Arteaga, 2014)

$$\begin{aligned} P_{\mathrm{f}} = P(F_{\mathrm{m}}) &= P\Big(\bigcap_{i=1}^{m} F_{\mathrm{i}}\Big) \\ &= P\Big(F_{\mathrm{m}}|\bigcap_{i=1}^{m-1} F_{\mathrm{i}}\Big)P\Big(\bigcap_{i=1}^{m-1} F_{\mathrm{i}}\Big) \\ &= P(F_{\mathrm{m}}|F_{\mathrm{m\text{-}1}})P\Big(\bigcap_{i=1}^{m-1} F_{\mathrm{i}}\Big) \\ &= P(F_1)\prod_{i=1}^{m-1} P(F_{\mathrm{i+1}}|F_{\mathrm{i}}) \end{aligned} \tag{2.21}$$

equation 2.21 indicates how the failure probability is determined as product of $P(F_1)$ and the sequence of conditional failure probabilities. $P(F_1)$ is the unconditional probability term that can be evaluated using a Direct Monte Carlo analysis. This step is essential because the target probability P_f must contain an unconditional probability term (Yu and Au, 2014). Evaluation of $P(F_1)$ is referred to as simulation level 0 of a SS procedure with the conditional probability evaluation being simulation level 1. MCS can be used to evaluate level 0 of the analysis

$$P(F_1) \approx \bar{P}_1 = \frac{1}{N}\sum_{k=1}^{N} I_{F_1}(\theta_{\mathrm{k}}) \tag{2.22}$$

where I_{F_1} is an indicator function (I_F= 1 if $\theta \in$ F and I_F= 0 otherwise) and θ_k are independent and identically distributed samples simulated according to a probability distribution function q (Au and Beck, 2001). Although MCS can also be used to simulate the conditional samples of θ that lie in F_i, it is not an efficient choice due to the required number of samples. Therefore SS uses a more efficient Markov Chain Monte Carlo simulation method to generate the conditional samples.

2.6.1. MARKOV HAIN MONTE CARLO

After simulation level 0 is done, subset simulation requires the generation of additional realisations to gather sufficient samples from each subset. Therefore samples need to be generated from the unknown conditional sampling space referred to as the posterior distribution (van den Eijnden and Hicks, 2017). To generate the conditional samples that lie in subsets F_i, Au and Beck(2001) employ the use of a Modified Metropolis Hastings (MMH) algorithm in combination with a Markov chain Monte Carlo simulation (MCMC). Therefore it is necessary to first define what is a Markov chain and

how its applicable in this framework, before explaining the use of a MH algorithm in combination with MCMC.

> *A Markov chain $\{X^{(t)}\}$ is a sequence of dependant random variables $X^{(0)}$, $X^{(1)}$, $X^{(2)}$, ..., $X^{(t)}$,... such that the probability of distribution of X^t given the past variables depends only on $X^{(t-1)}$* (Robert and Casella, 2010)

The conditional probability distribution is referred to as a Markov kernel K where

$$X^{(t+1)}|X^{(0)}, X^{(1)}, X^{(2)}, ..., X^{(t)} \sim K(X^{(t)}, X^{(t+1)}) \tag{2.23}$$

Markov Chain MCS is a numerical method that simulates a sequence of samples of random variables as a Markov Chain with the joint PDF of the variables as the limiting stationary distribution for the Markov Chain(Cao et al., 2016). In other words, based on a target density *f*, a Markov Kernel is built with stationary distribution *f* and then a Markov chain is generated where *f* is also the limiting distribution of $(X^{(t)})$. MCMC provides a feasible way in generating conditional samples, especially when dealing with a complicated arbitrary distribution. The difficulty of a MCMC method lies in deriving a kernel K associated with the arbitrary density *f*. However, algorithms exist that in combination with MCMC, can overcome this difficulty.

Metropolis-Hastings (MH) is one of the methods that are used to derive such kernels in a way that they become theoretically valid for any arbitrary density (Robert and Casella, 2010). The significance of this method is that samples can be simulated having the conditional distribution $q(.|F_i)$, and then the next state of the sample is simulated using MH will also be distributed according to $q(.|F_i)$. Due to the limiting distribution property, this is the case even if the current sample is not distributed according to $q(.|F_i)$. Although the samples of the Markov Chain are dependant in nature, they can be used as if they were independant and identically distributed samples but with a reduced efficiency(Au and Beck, 2001). When the problem in question is of a high dimension, the MH algorithm is not applicable. This is because as the dimension n of the uncertain parameter space increases, acceptance ratio r_a (see next section) becomes infinitely small and thus most states will be rejected(Cao et al., 2016). This lead to the introduction of new algorithms such as Modified Metropolis-Hastings (MMH).

2.6.2. MODIFIED METROPOLIS-HASTINGS ALGORITHM

The Modified Metropolis-Hastings algorithm (MMH) was introduced by Au and Beck (2001) to be able to deal with high dimensional problems. It differs from the Metropolis algorithm in the way the candidate state is generated.

For a link j>1 in a Markov Chain with samples from conditional space Ω^i with a standard normal distribution $q^{(0)}$, a realisation $\theta_{(k,j)}{}^{(i)}$ is generated as follows:

- The Markov Chain starts at an initial seed $\theta^s=\theta_{(k,j-1)}{}^i$ which is defined by the user.
- The next state of the Markov Chain (θ^2), or in general the *i*th state (θ^i), is then generated from the previous state.
- A candidate sample $\theta^*{}_i$, i=2,3,...,n_{MCMC}, is generated from the proposal PDF $p(\theta^*{}_i/\theta_i{}^s)$. Components $\theta^*{}_i$ are generated from proposal distribution as follows:

$$p(\theta^*{}_i/\theta_i{}^s) = \theta_i{}^s + \xi_i{}^{Ms} \tag{2.24}$$

where $\xi^{Ms}{}_i$ is a column vector of zero mean non-skewed random numbers. The sample is referred to as a candidate sample as it's not necessarily accepted as the *i*th sample of the Markov Chain. This decision depends on a so called "acceptance ratio" calculated as (Cao et al., 2016):

$$r_a = \frac{q_i(\theta^*{}_i)}{q(\theta_{i-1})} * \frac{p(\theta_{i-1}|\theta^*{}_i)}{p(\theta^*{}_i|\theta_{i-1})} \quad for \quad i = 2,3,...,n_{MCMC} \tag{2.25}$$

in which q() are PDF values and p(.1.) are conditional PDF values. For a symmetric proposal PDF, $p(\theta^*{}_i|\theta_{i-1})=p(\theta_{i-1}|\theta^*{}_i)$, MMH and MH reduce to the Metropolis algorithm (Metropolis et al., 1953) and r_a reduces to:

$$r_a = \frac{q(\theta^*{}_i)}{q(\theta_{i-1})} \tag{2.26}$$

- A random number (u) between 0 and 1 is generated from a uniform distribution. If the $u<r_a$ then $\theta^*{}_i$ is accepted as θ_i. Otherwise $\theta^*{}_i$ is rejected and θ_i is set equal to θ_{i-1} from the previous state.
- The updated proposal state is checked to be a part of of the subset Ω_i. If it is not, the proposal state is rejected and the seed state takes place.
- The steps above are repeated n_{MCMC}-1 times in order to generate samples for a Markov Chain that consists of n_{MCMC} samples including the initial.

It is necessary to mention that the key to have an efficient MMA is a balance between high acceptance ratio and large Markov steps in order to limit the correlation between different steps in a chain. The efficiency of the algorithm is also dependant on the definition of the problem (van den Eijnden and Hicks, 2017).

ILLUSTRATIVE EXAMPLE OF MMH

In order to show the importance of the MMH algorithm in MCMC, a simple MATLAB program was created. The aim of the illustration is to show how the MMH algorithm shifts the sampling space towards the failure region. For example consider a limit state function that can be modelled using the quadratic function below:

$$-X^2 + 5 - Y = Z \tag{2.27}$$

Failure is defined to occur when the limit state is exceeded or in other words Z<=0 and depends on the magnitude of values of X and Y. Normally distributed random samples were generated for the two unknown variables (X and Y).These samples will act as the seed samples for each Markov Chain (θ_s). Next, according to the MMH algorithm outlined above, candidate states were generated ($\theta^*{}_i$) from the proposal distribution and were accepted or rejected depending on the acceptance ratio explained above. Figure 2.11 shows the evolution of 15 different Markov chains in X and Y space. As illustrated in the figure, most of the Markov chains begin in the 'safe' region where the constant value is positive. As candidate samples are generated and rejected, the Markov chains move towards the failure region where ultimately, all samples will be accepted.

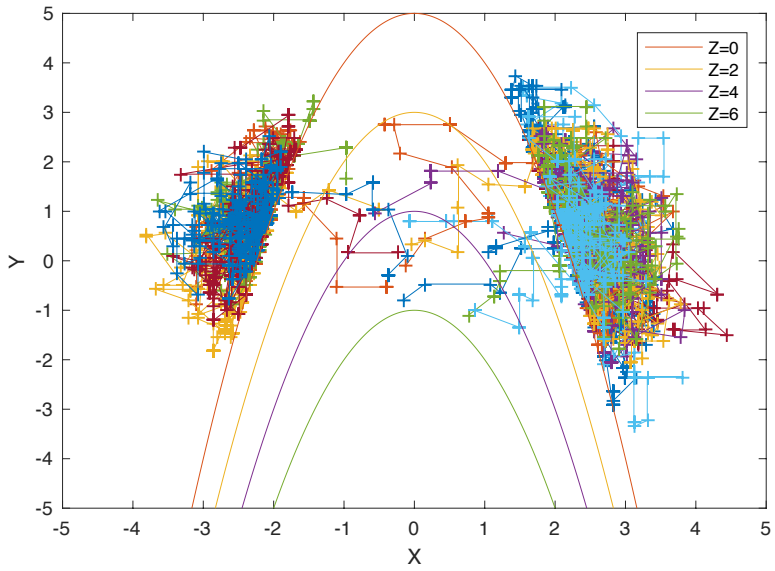

Figure 2.11: Markov chains using MMH for function in eq 2.27

2.6.3. SUBSET SIMULATION PROCEDURE

Let **X**=[X_1,...,X_n] be a set of random independent variables with a joint pdf

$$q(x) = q_1(X_1)....q_n(X_n) \tag{2.28}$$

The scalar response Y=h(X) completely depends on the random variables X. The user chooses values for the level or subset probability p_0 and for the number of samples N per subset so that:

$$N_c = p_0 N \tag{2.29}$$

$$N_s = p_0^{-1} \tag{2.30}$$

where N_c is the number of Markov chains and N_s is the number of samples per chain. Based on the chosen parameters, the following is the standard SS procedure to estimate the sequence of threshold values b_i that correspond to the chosen level exceedance probabilities P(Y>b). This will produce an estimate for the complementary cumulative distribution function (CCDF) of Y . As mentioned before, the procedure is divided into different levels, level 0 and level 1. Level 0 is the initial MCS stage which is followed by the MCMC sampling or level 1. The MCMC with MMH algorithm was outlined in the previous section and therefore will not be included in detail.

LEVEL 0: DIRECT MCS

(Yu and Au, 2014)

1. generate samples [$X_k^{(0)}$:K=1,...,N] according to their PDF and calculate the system response $Y_k^{(0)}$.

2. sort $Y_k^{(0)}$ values in ascending order to generate a list [$b_k^{(0)}$] and estimate threshold values b that correspond to exceedance probability $p_k^{(0)}$= P(Y>b) where

$$p_k^{(0)} = \frac{N-k}{N} \tag{2.31}$$

By plotting ($p_k^{(0)}$, $b_k^{(0)}$:k=1,...,N-N_c), the CCDF is estimated for probabilities ranging up to the chosen level probability p_0. Probabilities below p_0 will be estimated using MCMC.

3. Set

$$b_1 = b_{\text{N-N}_c}{}^{(0)} \tag{2.32}$$

Next, N_c samples of X from level 0 will be used as seeds to generate conditional MCMC samples for level 1.

LEVEL 1: MCMC

Simulation level 1 actually consists of i=1,...,m-1 simulations of MCMC with the following procedure:

1. based on the chosen seeds from level 0, generate N_{s-1} samples with conditional PDF $q(.|F_i)$ per Markov chain. Therefore now we have N_c chains with N_s each.

2. sort $Y_{jk}{}^{(i)}$ (which is evaluated using MCMC) values in ascending order to generate a list $[b_k{}^{(i)}]$ and estimate threshold values b that correspond to exceedance probability $p_k{}^{(i)} = P(Y>b)$ where

$$p_k{}^{(i)} = p_{(0)}{}^{i}\frac{N-k}{N} \tag{2.33}$$

By plotting $(p_k{}^{(i)}, b_k{}^{(i)}:k=1,...,N-N_c)$, the CCDF is estimated for probabilities ranging from $p_0{}^{i}(1-N^{-1})$ to $p_0{}^{i+1}$. If i=m-1 is reached then the values between N and $N-N_c$ should also be plotted.

3. Set

$$b_{i+1} = b_{\text{N-N}_c}{}^{(i)} \tag{2.34}$$

Next, N_c samples of X from level i will be used as seeds to generate conditional MCMC samples for level i+1. Omit this step if highest level is reached (i=m-1).

Figure 2.12 graphically illustrates how the SS procedure works and how different threshold values are determined. First samples from level 0 (MCS) are generated in random variable space X (figure 2.12(a)). Next samples exceeding the user defined first threshold level (or exceedence response value) b_1 are selected as seed samples for the Markov Chains (figure 2.12(b)). Figure 2.12(c) shows the progression of the Markov Chains as samples are accepted or rejected according to the acceptance ratio in equation 2.26. Figure 2.12(c) is a bit misleading as it indicates that all MCMC samples are generated in one direction which is not necessarily the case. Next, Nc samples from figure 2.12(c) that exceed the second threshold level will be used as seeds for Markov Chains for the next level (figure 2.12(d)). This process (figure 2.12(c),(d)) is continued until the highest level is reached. The probability of failure can now be calculated as a product of probability in level 0 and conditional probabilities of simulation levels 1 to *i=m-1* as illustrated in equation 2.21.

2.7. SLOPE STABILITY ANALYSIS

Slope failure is defined as the failure of a soil mass in a slope by movement outward or downward (Das, 2006). Failure can occur in existing or engineered slopes due to various reasons such as increased loading, earthquakes, pore water pressure and removal of material. The evaluation of stability or the determination of the factor of safety (FOS) requires knowledge about soil shear strength parameters. Depending on the shape of the slope, many methods have been developed to analyse stability. These methods range from simple charts for preliminary analysis to comprehensive computer programs for more detailed analysis (Wright et al., 2014). As mentioned in the Probabilistic methods section, some methods are only deterministic and do not consider uncertainty in the soil, while others are stochastic and therefore consider uncertainty and evaluate probability of failure.

The analysis of soil pressures in extreme conditions that lead to failure derive from the the theory of plasticity. To formulate the basic theorems of plasticity theory, two types of analysis are used (Verruijt, 2007):

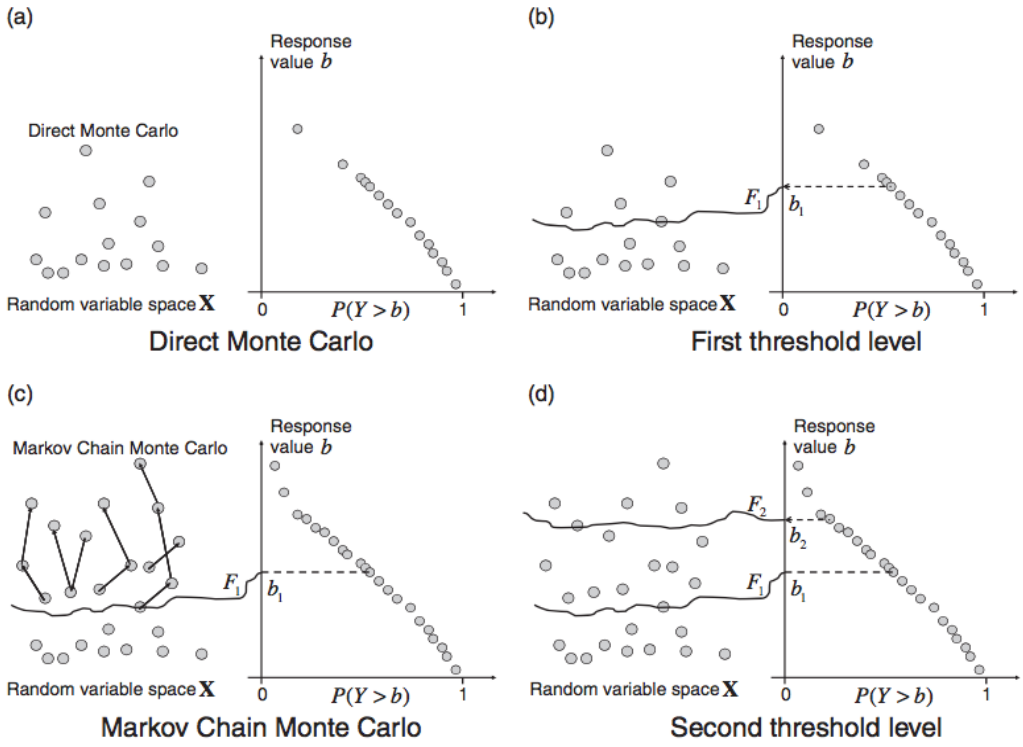

Figure 2.12: illustration of Subset Simulation procedure (Yu and Au, 2014)

- Equilibrium analysis
- Kinematic analysis

Most slope stability methods make use of the Limit Equilibrium methods (LEM). These methods utilise the Mohr-Coulumb criterion to determine the shear strength along a sliding surface in a soil. A state of equilibrium exists when shear strength τ is expressed as follows(Janbu et al., 1973):

$$\tau = \frac{\tau_f}{F} \tag{2.35}$$

where F is the factor of safety and τ_f is the shear strength. The shear strength can be expressed by Coulomb's equation and equation 2.35 becomes

$$\tau = \frac{c + \sigma'_n tan\phi}{F} \tag{2.36}$$

where c is soil cohesion, ϕ is the friction angle and σ'_n is the effective normal stress on the failure surface. Most LEMs assume that the soil fails along a circular slip surface as in figure 2.13. The equation of equilibrium used in this case is that of moment equilibrium with respect to the centre of the circle (Verruijt, 2007) :

$$\Sigma[\gamma hbRsin\alpha] = \Sigma\frac{\tau bR}{cos\alpha} \tag{2.37}$$

where h and b are height and width of slice, respectively, γ is the volumetric weight, R is the radius of the surface and α is the inclination. γbh together refer to the weight (w) of the slice as illustrated in figure 2.13.When all slices have the same width, by combining equation 2.36 and 2.37, the FOS can be expressed as

$$F = \frac{\Sigma[(c + \sigma'_n tan\phi)/cos\alpha]}{\Sigma[\gamma hsin\alpha]} \tag{2.38}$$

Which is the basic formula used by most slope stability LEMs. Variation between one method to the other is usually in the formulation of the effective stress parameter σ'_n (Verruijt, 2007). Some of these methods are summarised in the following section.

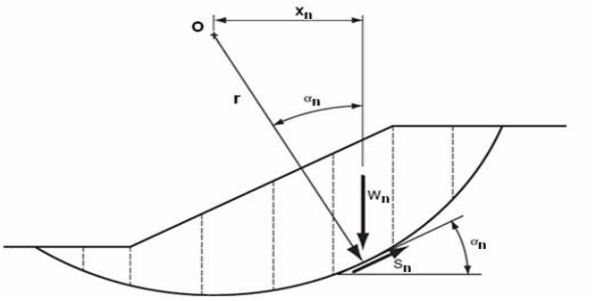

Figure 2.13: Slope stability slip surface

2.7.1. DETERMINISTIC SLOPE STABILITY METHODS

LIMIT EQUILIBRIUM METHODS

Table 2.1 is a summary of the characteristics of four the of the most used LEM slope stability techniques. The forces considered show the small deviations between one method to the other.

Method	*Characteristics*	*Forces considered*
Fellenius	Oldest method of analysis, assumes no forces between slices. Only remaining forces acting on slice are w, σ'_n and τ	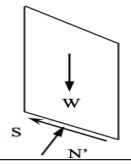
Bishop	Interslice forces are taken into account and it is assumed that their resultant force is horizontal. Method satisfies vertical force equilibrium and moment equilibrium for FOS.	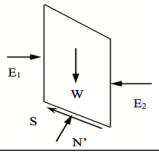
Janbu's generalised method	Considers both vertical and horizontal interslice forces. The method satisfies both force and moment equilibrium. Method is advanced and can handle more difficult geometries.	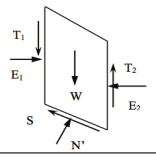
Morgenstern-Price	Satisfies both force and moment equilibrium. Assumes a function for interslice forces and allows selection for it.	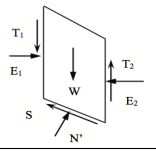

Table 2.1: Common Limit Equilibrium methods for slope stability

FINITE ELEMENT METHOD

Limit Equilibrium methods require that a continuos slip surface passes through the soil for it to fail. This in turn will require assumptions with regards to interslice forces and their directions (Rocscience, 2001). With the advancement of computer softwares, the Finite Element Method (FEM) has

been recently used to analyse the stability of slopes. FEM is a numerical technique that has been developed to be able to solve complex problems with partial equations. The advantages of using FEM for slope stability analysis include:

- The algorithm searches for the most critical slip surface without prior assumptions regarding the shape or location of the surface (Griffiths et al., 2009).
- The concept of slices is not used in the analysis and therefore no assumptions need to be made about interslice forces (Griffiths and Lane, 1999).
- The ability to monitor progressive failures (Griffiths and Lane, 1999).
- The ability to interchange between different soil models and failure criteria.

2.7.2. PROBABILISTIC SLOPE STABILITY METHODS

In order to take into account the inherent uncertainty of soil, deterministic slope stability methods are used in combination with random field theory to evaluate the reliability of the slope. The majority of these studies use LEM as the deterministic function for the problem. Earlier studies only considered the uncertainty by using the point statistics for random soil parameters (Hassan and Wolff, 1999). Other studies analysed slope stability by using a LEM while taking into account the spatial variability of soil (El-Ramly et al., 2002). Some of these methods are described in the Probabilistic methods section and can be either approximate like level II methods (FORM), or exact such as a level III methods (MCS). However, as mentioned before, the limitation of using a LEM is that by predetermining the critical slip surface, the influence of the random field is restricted to the slip surface (Cho, 2010). Therefore recent studies have combined advanced methods such as FEM with the random field theory to model the uncertainty of soil. The Random Finite Element method (RFEM) introduced by Griffiths and Fenton (2004) is one of these advanced probabilistic methods and will be described in the following section.

2.8. RANDOM FINITE ELEMENT METHOD

The Random Finite Element Method (RFEM) is a powerful method that combines FE analysis with random field theory to evaluate the reliability of a soil structure. The method takes into account the uncertainty in the soil parameters in addition to the spatial correlation (see section1.3). RFEM involves the generation of a random field for soil properties and then the mapping of this random field into a finite element(Griffiths et al., 2009). This can be applied to any type of distribution for the soil properties in question (e.g. normal or lognormal). Each value assigned to a finite element is itself a random variable. Figure 2.14 is a typical finite element mesh for the simple case of a slope with foundation (Griffiths and Lane, 1999).

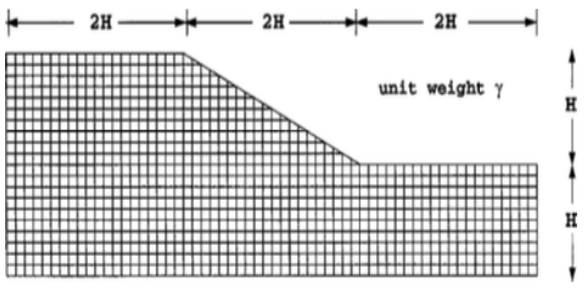

Figure 2.14: Typical mesh for RFEM

RFEM starts by generating realisations depending on the point statistics and spatial correlations chosen for the random parameters. Next, each realisation is evaluated using the deterministic function chosen for the analysis. The resulting factors of safety for each realisation are then used to evaluate the probability of failure or reliability of the slope. This framework was applied in literature for different types of soil. Examples include Hicks and Samy (2002); Griffiths and Fenton (2004) for cohesive soils and Griffiths et al. (2009) for cohesive-frictional soils.

The evaluation of the reliability of the slope is carried out by applying gravity loading which will lead to stress changes at the finite element gauss points. For the example of cohesive clays, the soil model used is a linear elastic perfectly plastic (LEPP) with a Tresca failure criterion. This can differ according to the type of soil used in the analysis. If stresses lead to failure according to the Tresca criterion, stresses are redistributed to neighbouring elements in a iterative process until equilibrium is satisfied at all finite elements (Griffiths and Fenton, 2004). This stress redistribution is done according to a visco-plastic algorithm with 8-node quadrilateral elements (Griffiths and Lane, 1999). The process can be achieved with two different approaches:

- Shear strength reduction (SSR): the stability of the slope is evaluated by introducing strength reduction factors f_s which are iteratively updated. This will reduce the strength of soil by reducing the strength of its shear strength parameters. The lowest f_s leading to failure is considered as the factor of safety.
- Direct stability analysis (DSA):In this case, the stability is determined based on only one strength reduction factor. Rather than a factor of safety, DSA only indicates if slope is stable or has failed.

The probability of failure is then determined by performing a MCS and applying one of these approaches to each realisation.

2.8.1. SPATIAL CORRELATION

In traditional analysis, the spatial correlation length of a random variable is considered to be infinite. This means that the slope is homogeneous which does not represent soil in reality (see section1.3). Defining a smaller correlation length means that spatial uncertainty is taken into account as soil properties will vary spatially within the slope. For a single random variable (cohesion), this is achieved in RFEM with the use of an exponentially decaying Markovian correlation function for spatial correlation length $\theta_{\ln C}$ (Griffiths and Lane, 1999):

$$\rho = e^{-(-2\tau/\theta_{\ln C})} \tag{2.39}$$

where ρ is the familiar correlation coefficient and τ is the absolute distance between two points in a random field. Figure 2.15 is an example random field for cohesion based on a user defined spatial correlation length. This approach can be applied to all random variables considered in the analysis. As mentioned before, the scale of fluctuation of soil differs between the horizontal and vertical direction and this anisotropy can be included in the analysis.

2.8.2. TYPES OF RANDOM FIELDS

The type of random field chosen for the analysis will depend on the number of spatially varying properties. Therefore random fields fall in one of these categories (Hicks, 2016):

1. **Univariate:** single random field with only 1 spatially varying property.

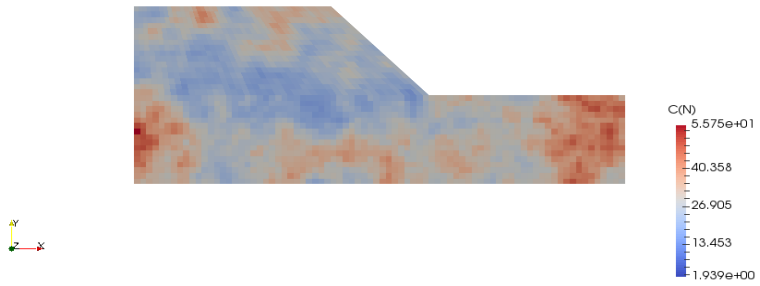

Figure 2.15: Typical random field for cohesion C

2. **Mulitvariate:** more than one spatial property. Therefore, a random field is generated for each and then cross correlated to take into account the dependancy between the parameters.

3. **Reduced variate:** number of random fields generated are minimised by only generating for some properties and then back-figuring other property values later. For example, a random field is generated for one state parameter and other properties are back-figured from this parameter.

Most slope stability studies encountered in literature use a univariate approach with a random field for cohesion C as in figure 2.15. If more than one random property is to be taken into account, either approach 2 or 3 can be applied. In this case, a reduced variate approach is more efficient as the number of random fields generated will be less. Furthermore, it insures proper correlation between back-figured parameters (Hicks, 2016).

2.8.3. DISCRETIZATION OF RANDOM FIELDS

The generation of a random field $X(\vec{x})$ for a stochastic variable X is usually achieved by generating a standard normal random field $Z(\vec{x})$ and then applying a transformation $\Psi(.)$ to acquire the desired distribution for X (van den Eijnden and Hicks, 2017). Different techniques have been proposed in literature for this procedure and mainly fall into two categories:

- **Average discretization methods:** The random variable is calculated as an average of the underlying random field.
- **Series expansion discretization methods:** more exact approximation of the random field with a fixed number of variables.

Local Average Subdivision method (LAS) introduced by (Fenton and Vanmarcke, 1990) is one of the many average discretization methods available in literature.The use of this method is very common in geotechnical engineering due to its high efficiency (Griffiths and Fenton, 2004; Hicks and Samy, 2002). Other more exact techniques based on covariance matrix decomposition have been described in literature. These techniques are more suitable for the application of subset simulation because after discretization, they describe the random field as a set of uncorrelated parameters (van den Eijnden and Hicks, 2017). Karhunen-Loeve (KL) decomposition (Huang et al., 2001) and Covariance Matrix Decomposition (CMD) (Fenton, 2014) are two methods that have been used to generate random fields to describe the spatial variability of soil. The discretization methodology with the use of CMD is described below.

In finite element analysis, discretization of the random field is required to transform a continuos random field into a discrete random field with the number of values equal to the number of integration points in the FE mesh. The finite element is first divided into cells and the integration point is

assigned the average of the cells from the underlying random field as done in local averaging theory (Fenton and Vanmarcke, 1990). Therefore, the variance reduction due to this averaging needs to be taken into account. For random field values z($\vec{x}$) and a cell average $\bar{z}$, the variance reduction factor γ=E[$\bar{z}$]/E[z] can be calculated exactly

$$\gamma = \frac{1}{V^2} \int_{\vec{x}_i \in \Omega} \int_{\vec{x}_j \in \Omega} \rho(\vec{x}_i - \vec{x}_j) dV dV \tag{2.40}$$

where ρ is the spatial correlation function defined in equation2.39. Equation 2.40 can be approximated by Gauss-Legendre quadrature (van den Eijnden and Hicks, 2017). It follows that the correlation between any two points A and B can be evaluated as follows

$$\rho(\Omega_A, \Omega_B) = \frac{1}{V_A V_B} \int_{\Omega_A} \int_{\Omega_B} \rho(\vec{x_B} - \vec{x_A}) dV dV \tag{2.41}$$

Given a discretization *Z*, *C* is defined as the autocovariance matrix between any components of Z. C can be calculated using equation 2.41 to produce

$$C = E[ZZ^T] \tag{2.42}$$

if *C* is a positive definitive covariance matrix, CMD defines the random field as

$$Z = L\xi \tag{2.43}$$

where *L* is a lower triangular matrix satisfying LL^T= C which is obtained using a Cholesky decomposition, and ξ is a n-dimensional vector of uncorrelated standard normal numbers (Fenton, 2014). The decomposition can be achieved using other methods (eigen-decomposition in KL) as Cholesky is prone to numerical instabilities (van den Eijnden and Hicks, 2017). These methods of discretizing the random fields have a high computational costs and other methods such as EOLE method (Sudret and Kiureghian, 2000) are available and employ restrictions on accuracy to limit the computational cost.

2.9. CROSS CORRELATION BETWEEN INPUT PARAMETERS

In a probabilistic analysis of a geotechnical problem, typically a number of input parameters will be needed to compute the response. These include properties such as Young's Modulus, Poisson's ratio, unit weight, cohesion and friction angle. In a probabilistic concept, all these variables can be modelled using random variables or fields. Furthermore, It is often assumed in literature that geotechnical parameters are independent variables. However, even though the geological and other processes that lead to the formation of a soil body may not influence different parameters in the same way, each process does influence more than one parameter at a time. This means that a correlation, either positive or negative, exists between these different soil properties. A positive correlation will indicate that as the first variable increases, so will the second while a negative correlation indicates the opposite, as one increases, the other will decrease.

2.9.1. GENERATING CROSS-CORRELATED RANDOM VARIABLES

In a probabilistic analysis, a single random variable X is generated as follows:

$$X = \sigma Z + \mu \tag{2.44}$$

Where Z is a standard normal variable with mean=0 and standard deviation=1, and σ and μ correspond to the known distribution of the input parameter. In order to generate correlated random variables, it is first necessary to make an assumption about the distribution of these variables. For example, if the two variables in question are normally distributed, then its assumed that the joint distribution for the correlated variables where will be normal as well. This is necessary as the correlation between the variables will be defined according to their gaussian fields.

COVARIANCE MATRIX

In order to measure dependance between continuous variables, covariance is often used. It is a mathematical operator that is a measure of the joint variability of two random variables X and Y, or:

$$Cov(X_1, X_2) = \sigma_{X_1,X_2} = E\big([X_1 - E(X_1)][X_2 - E(X_2)]\big) \tag{2.45}$$

where E is the expected value or mean of the operation in the parenthesis(Jonkman et al., 2016). If the variables in question are independent, than the covariance will be equal to zero. The correlation between two parameters can be represented by a standardised covariance referred to as the correlation coefficient ρ where:

$$\rho = \rho_{X_1,X_2} = \frac{\sigma_{X_1,X_2}}{\sigma_{X_1}\sigma_{X_2}} \tag{2.46}$$

The values of ρ range between [-1,1] where $\rho = 1$ means perfect correlation between two random variables and $\rho = -1$ means perfect inverse or negative correlation. When applying the concept of covariance to n random variables, the multivariate distribution for the variables X=(X_1, X_1, X_2,..., X_n) has a symmetrical nxn covariance matrix as follows (Nguyen and Chowdhury, 1985):

$$\Lambda = \begin{bmatrix} \sigma_{11} & \sigma_{11} & \dots & \sigma_{1n} \\ \sigma_{21} & \sigma_{22} & \dots & \sigma_{2n} \\ \vdots & \vdots & \ddots & \vdots \\ \sigma_{n1} & \sigma_{n2} & & \sigma_{nn} \end{bmatrix} \tag{2.47}$$

where for example σ_{12} refers to the covariance between the random variables X_1 and X_2 such as in equation 2.45. The elements of the main diagonal of the matrix are the variances of the variables. By combining equation 2.45 and the matrix in 2.49, the covariance matrix becomes:

$$\Lambda = \begin{bmatrix} {\sigma^2}_1 & \rho_{1,2}\sigma_1\sigma_2 & \dots & \rho_{1,n}\sigma_1\sigma_n \\ \rho_{1,2}\sigma_1\sigma_2 & {\sigma^2}_2 & \dots & \rho_{2,n}\sigma_2\sigma_n \\ \vdots & \vdots & \ddots & \vdots \\ \rho_{1,n}\sigma_1\sigma_n & \rho_{2,n}\sigma_2\sigma_n & & {\sigma^2}_n \end{bmatrix} \tag{2.48}$$

For standard normal variables ($\mu = 0, \sigma = 1$) then the covariance matrix reduces to:

$$\Lambda = \begin{bmatrix} 1 & \rho_{1,2} & \dots & \rho_{1,n} \\ \rho_{1,2} & 1 & \dots & \rho_{2,n} \\ \vdots & \vdots & \ddots & \vdots \\ \rho_{1,n} & \rho_{2,n} & & 1 \end{bmatrix} \tag{2.49}$$

2.9.2. TRANSFORMATION PROCEDURE

Based on the expected correlation between normal random variables, a transformation is required to generate a set of correlated random variables from a set of uncorrelated numbers. From equation 2.45, it is known that for a set of standard normal uncorrelated vectors Xi and Xj, the covariance equals the expected value of their products. Furthermore, since the elements in X are uncorrelated and have unit distribution

$$E(XX^T) = I \tag{2.50}$$

where I is the identity matrix. Next, different approaches can be applied in order to generate a vector of random numbers with a given correlation matrix Λ.

LINEAR TRANSFORMATION APPROACH

One approach is to apply a linear transformation based on the general linear transformation equation

$$X = AY + B \tag{2.51}$$

where N and Y is the column vector of uncorrelated random variables and A is nxn matrix with constant elements a_{ij} and B is a column vector with constant elements b_i. The linear transformation leads to a set of transformation equations, equations 2.52 and 2.53 are examples of these equations for a 2x2 covariance matrix

$$N_1 = \sigma_1 Y_1 + \mu_1 \tag{2.52}$$

$$N_2 = \rho\sigma_2 Y_1 + \sigma_2(1-\rho^2)^{\frac{1}{2}} Y_2 + \mu_2 \tag{2.53}$$

For the full procedure on how to generate the linear transformation equations, refer to Nguyen and Chowdhury (1985).

CHOLEKSY DECOMPOSITION APPROACH

Another approach to generate a correlated set from an uncorrelated set of random variables is to apply a Cholesky decomposition to the covariance matrix. It is possible to do so since by definition a covariance matrix Λ is positive semi-definitive matrix and therefore a decomposition is possible. Applying Cholesky leads to

$$\Lambda = LL^T \tag{2.54}$$

Next by multiplying the decomposed lower triangular matrix L by the set of uncorrelated numbers N, a correlated set Z is achieved 2.55

$$Z = LN \tag{2.55}$$

Z now has the required covariance matrix Λ. This is true since

$$E(ZZ^T) = E\big((LN)(LN)^T\big) = E(LNN^TL^T) = LE(NN^T)L^T = LIL^T = LL^T = \Lambda \tag{2.56}$$

Which means that Z will have the desired covariance matrix Λ. The operations in 2.56 are possible because expectation (E) is a linear operator.

2.9.3. 1D CORRELATED SOIL PROPERTIES- MATLAB EXAMPLE

In order to illustrate the process of generating correlated random variables, a simple MATLAB code was created to generate correlated soil properties for a simple 1D soil column. It is assumed that correlation exists between cohesion (c), friction angle (ϕ), and unit weight (γ). A negative correlation was assumed between c and ϕ, positive between c and γ and negative between ϕ and γ. The Cholesky decomposition approach, introduced in the previous section, was utilized to discretize the covariance matrix. Figure 2.16 indicates the flow of the code. The flow chart highlights that in order to generate a correlated random field, 3 levels of analysis are required:

1. Generating random variables, covariance and correlation matrices
2. Generating correlated random variables
3. Generating correlated random fields

Figure 2.17 shows the 1D random fields with an arbitrary mean and standard deviation chosen for each material property. The figure clearly indicates where correlation is positive (c and γ) and where it is negative (c and ϕ, ϕ and γ). Although with this particular set of ρ's it was possible to generate correlated random fields, this is not always the case. The covariance matrix must be first positive definitive and this is investigated in the following section.

2.9.4. LIMITS FOR THE CORRELATION MATRIX

By definition a covariance matrix must be positive definite. In numerical terms, this means that it is a symmetrical matrix for which all Eigen values are non-negative. However, this limitation can be backed up by a theoretical explanation as well. In the 1D code, the discretisation of both the spatial correlation matrix and the covariance matrix was performed using Cholesky decomposition. The theoretical limitation of positive definitive can be seen in figure 2.17. If there is negative correlation between c and ϕ and positive between c and γ then intuitively, correlation between ϕ and γ must be negative. This is because if $\rho_{\phi\gamma}$ is positive, then the negative correlation between c and ϕ will be affected. This explains why covariance matrices must be positive semi-definite.

Furthermore, if correlation coefficients between properties are treated as random variables, then the produced correlation matrix in each simulation must be positive definite. This was tested using a MATLAB code and the acceptance (positive definite or not) highly depends on the limits of the correlation coefficients. 10000 samples were generated and acceptance for the absolute value of the limits of ρ was investigated. Figure 2.18 indicates that if the limits for each ρ in a covariance matrix is [-1,1] then the acceptance is only 62%. On the other hand ρ's between [-0.5,0.5] has a 100% acceptance rate.

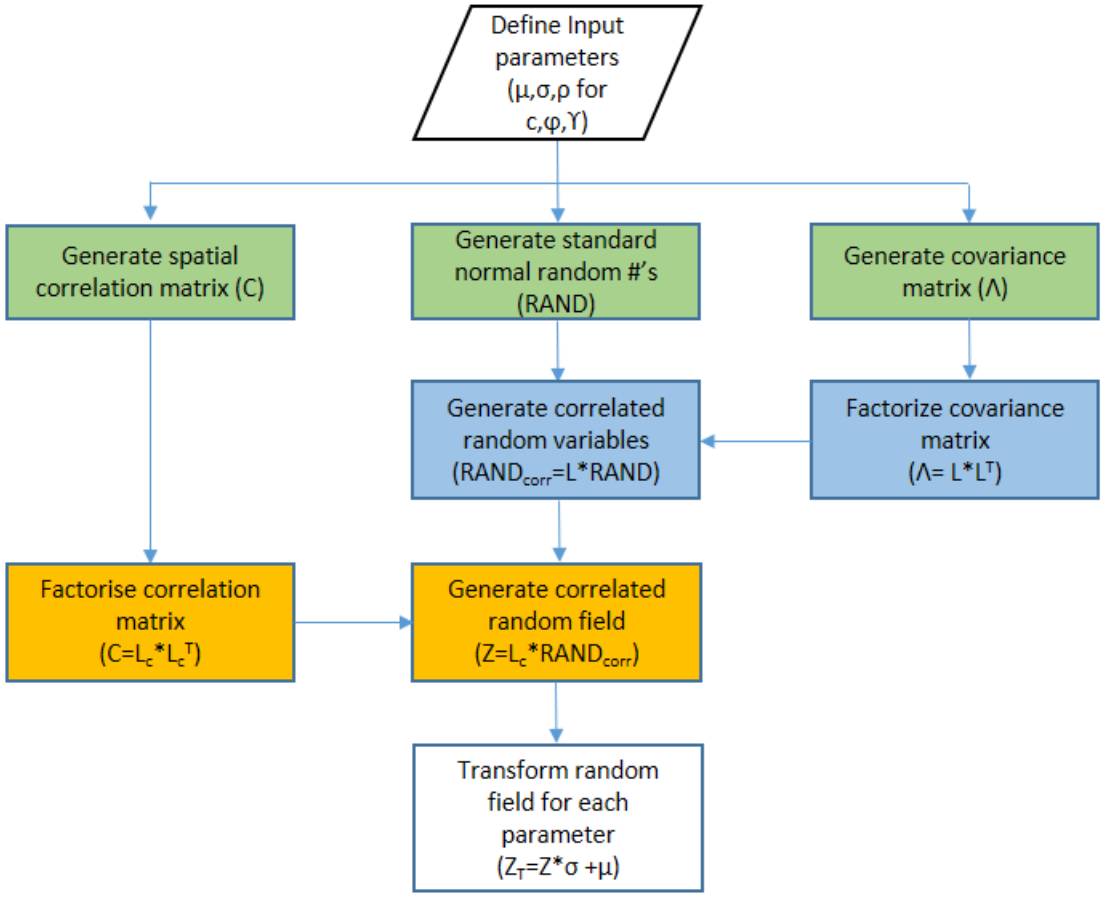

Figure 2.16: Flow chart for generation of cross-correlated random fields

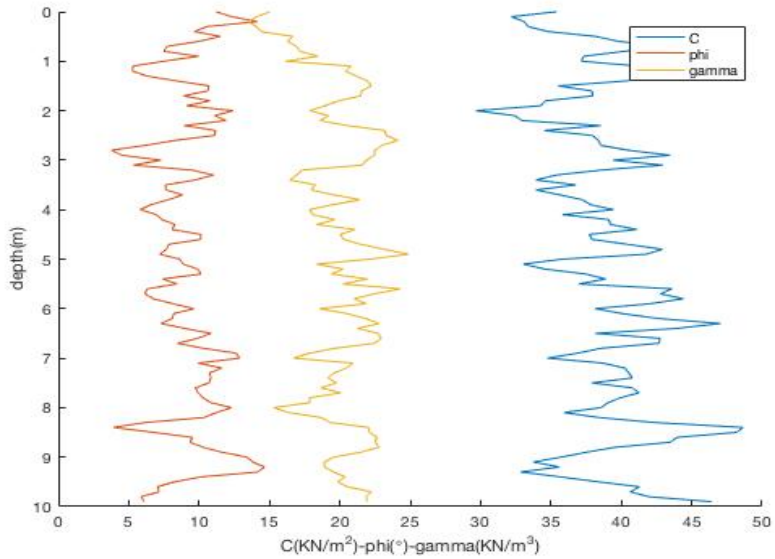

Figure 2.17: 1D correlated soil properties ($\rho_{c,\phi}$=-0.7, $\rho_{c,\gamma}$=0.6 and $\rho_{\phi,\gamma}$=-0.5)

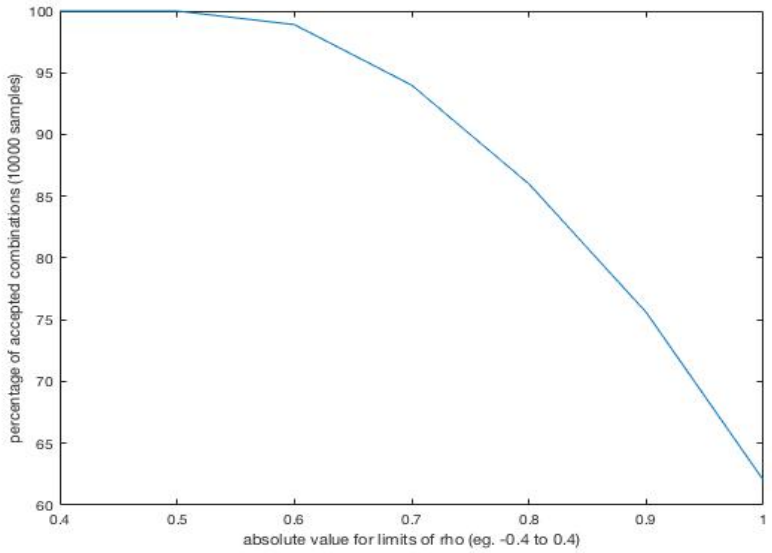

Figure 2.18: Acceptance for positive definite correlation matrix

Figure 2.18 indicates that if the correlation matrix is treated as random, then limitations must exist to insure that it remains positive definite. This can be achieved by using one of two different approaches:

- Limiting the range of values of ρ to [-0.5,0.5], or
- Checking for positive definiteness and accepting/rejecting matrices accordingly

Although limiting the range will require less computation time, correlation between these parameters can vary significantly and all possible combinations must be considered. Therefore, a check for positive definiteness is more appropriate. This can be achieved by a variety of different techniques including determining if either (Zwick, 2012):

- Matrix eigen values
- Pivots of Matrix
- N upper left determinants of matrix

are positive. As an example, consider the correlation matrix A below:

$$A = \begin{bmatrix} 1 & -0.8 & 0.5 \\ -0.8 & 1 & 0.4 \\ 0.5 & 0.4 & 1 \end{bmatrix} \tag{2.57}$$

where $\rho_{c,\phi}$=-0.8, $\rho_{c,\gamma}$=0.5, and $\rho_{\phi,\gamma}$=0.4. The three upper left matrices that exist within A and their determinants are:

$$\begin{aligned} A_1 &= [1], & det(A_1) &= 1 \\ A_2 &= \begin{bmatrix} 1 & -0.8 \\ -0.8 & 1 \end{bmatrix} & det(A_2) &= 0.36 \\ A_3 &= \begin{bmatrix} 1 & -0.8 & 0.5 \\ -0.8 & 1 & 0.4 \\ 0.5 & 0.4 & 1 \end{bmatrix} & det(A_3) &= -0.37 \end{aligned} \tag{2.58}$$

Not all the upper left determinants for A are positive and therefore A is not positive definite and is therefore rejected. The influence this may have on the distribution of ρ's is not investigated in this analysis.

2.10. CONCLUSION

This section has shown the different sources of uncertainty expected when dealing with the subsurface. These include parametric uncertainty, spatial variability and measurement and model errors. Tables are included to illustrate the typical variability in the magnitude of some soil properties, which will be used as input moving forward. Although Monte Carlo simulations can effectively formulate the probability of failure, the computation cost is significant when considering improbable events of failure. There are many different approaches than can be applied to either reduce the variance in results of an analysis or reduce the number of simulations required.

Subset simulation is an efficient sampling tool that can compute the probability of failure of rare events with a fraction of the cost of a traditional MCS. The procedure of SS is included to show how samples are generated within MCMC and an example is formulated to illustrate the efficiency of the method in searching for failing realisations. This is significant when considering multiple random variables in the analysis as the most critical combinations can be identified. The link to a real life scenario is realised when examining the stability of slopes and possible methods to combine probabilistic methods with slope stability are evaluated. Uncertainty, probabilistic methods and slope stability all come together when formulating the RFEM. Both parametric uncertainty and spatial variablity can be incorporated within the method as random fields can be generated for a number of input parameters. Finally, a review of cross-correlation indicates that generating correlation matrices will depend on generated correlation coefficients between input parameters. An example is formulated to illustrate how cross-correlation can be combined with spatial correlation functions to produce spatially variable correlated soil properties. However, the review has also shown that limitations such as positive definiteness may influence the sampling process for correlation coefficients in any stability analysis.

3

IMPLEMENTATION

3.1. INTRODUCTION

Reliability analysis will be performed in Fortran using a modified Subset Simulation approach that computes the failure probability of a slope using the Random Finite Element Method (section 2.8). The standard procedure of SS was presented in chapter one in section 2.6. This procedure was modified by van den Eijnden and Hicks (2017) to reduce computation time by avoiding the calculation of exact FOS for each realization. SS is an efficient sampling technique that makes it possible to compute the probability of failure for rare events of slope instability, and the aim of this paper is to expand the aprroach used by van den Eijnden and Hicks (2017) to take into account uncertainty in soil properties, uncertainty in the distribution of these properties and uncertainty in their dependence and cross-correlation.

Uncertainty in soil stems from various factors including inherent variability and geological depositions processes (section 2.2.2).Sources of uncertainty that stem from natural processes are referred to as aleatory. With efficient methods such as SS, it becomes possible to include such uncertainties in an analysis, even when considering rare events of failure. In the analysis, **cohesion, unit weight and friction angle** will be modelled using random fields. This is done to account for spatial variability in the three properties. Random values are usually generated based on a given mean and standard deviation for each parameter. The random variables are modelled based on a distribution to account for the inherent uncertainty or randomness of the soil. In typical studies, the point statistics (μ and σ) are determined based on laboratory or in-situ testing. Section 2.2.1 describes how sources of uncertainty exist in the determination of such parameters as well. This type of uncertainty is classified as epistemic and can be improved upon with better knowledge. Therefore in this analysis, the **mean** for the input parameters will be treated as random variables as well.

Studies have been published that take into account the correlation between soil properties when applying a Monte Carlo simulation (Griffiths et al., 2009; Cho and Park, 2010; Javankhoshdel and Bathurst, 2015). With the introduction of more efficient sampling techniques such as subset simulation, cross-correlation of soil properties has rarely been included in such analysis, with the exception of cross-correlated c-phi in some studies(Ahmed, 2012; Liu et al., 2017).Although this can be applied between all input parameters, in this study it will be limited to **correlation between cohesion and friction angle, cohesion and unit weight, and friction angle and unit weight**.Given the inherent heterogeneity of soil, it is expected that the correlation between these parameters is uncertain as well. It is necessary to understand how sensitive is the formulation to not only the introduction of correlation, but also the variation expected in the correlation between these parameters.

Therefore in this analysis, **cross-correlation coefficients** (ρ's) will be treated as random variables.

Therefore the aim of this chapter is to describe:

- The distribution of random variables to be used in the analysis
- The general flow of the Subset Simulation code
- How uncertainty will be applied in the analysis

3.2. FLOW OF FORMULATIONS

van den Eijnden and Hicks (2017) developed a Fortran code that evaluated the reliability of cohesive slopes using a modified approach of subset simulation. In that study, only uncertainty in cohesion was considered as it was modelled as a random variable with a log-Normal distribution. Therefore the code is extended to implement uncertainty in cross-correlation, uncertainty in c , ϕ and γ and uncertainty in their mean values. The chart in Figure 3.1 indicates the flow of code within the framework of Subset Simulation.

3.2.1. GEOMETRY AND FEM MESH

The first process in the analysis is to define the geometry of the slope to be analysed, and the number of integration points in the finite element mesh. Figure 3.2 indicates the geometry of the slope, FEM mesh and boundary conditions applied in the analysis.

3.2.2. INPUT PARAMETERS

Next, constitutive parameters and properties of subset simulation are initialized. Table 3.1 indicates the 4 types of input required for an analysis and the parameters that correspond to each type. A choice is required for subset simulation settings such as target conditional probability and failures per subset. Furthermore, choices for initial strength reduction factor and number of predefined checks are necessary. The soil and material properties also have to be initialised in the analysis. For the parameters that are treated as uncertain, the range of values and type of distribution must be identified prior to running the analysis. The typical values shown in the final column of table 3.1 are an example of such input and correspond to the input values that will are used for the practical example in chapter 5.

3.2.3. STIFFNESS MATRIX INTEGRATION AND ASSEMBLY

Based on the input constitutive parameters, a stiffness matrix is determined for each integration point. These matrices are then assembled to generate an elemental stiffness matrix. Finally, the elemental stiffness matrices are assembled to generate the global stiffness matrix of the slope in question.

3.2.4. FOR EACH SUBSET-REALISATION

Random realisations are then generated for each subset until N_c failures occurs. At the first subset level this equates to a general Monte Carlo analysis (See Fig 3.1). For all following levels, Markov Chain Monte Carlo is applied to generate realizations. MCMC is highlighted in green to indicate the link to the next flow chart (Figure 3.3). In order to generate samples within MCMC, seed samples that correspond to the SRF level in question are first selected from initial MC samples. Proposal

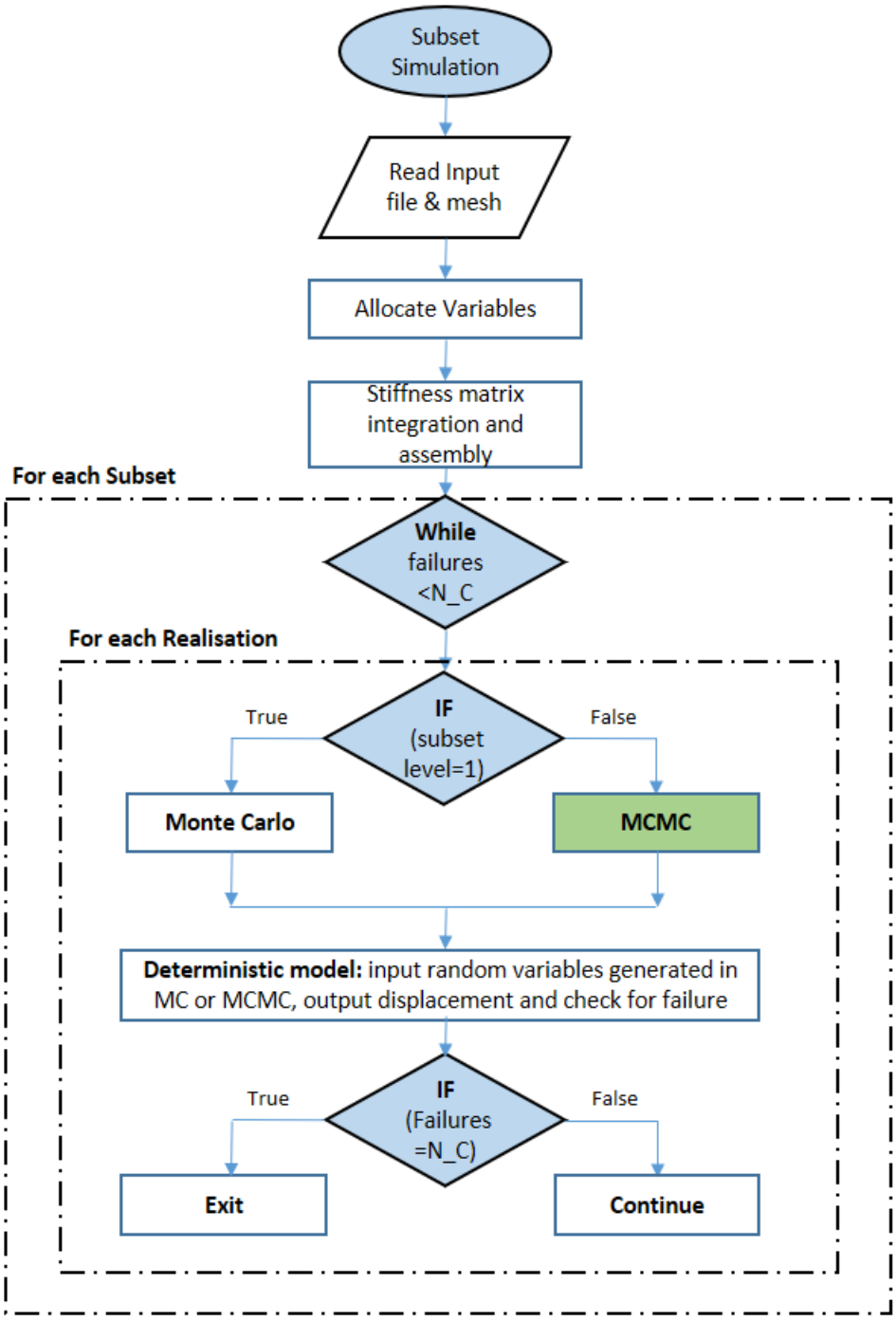

Figure 3.1: General flow of subset simulation procedure, for MCMC see Figure 3.3

Type	Input Parameters	Typical values (chapter 5)
SS settings	Failing realisations per subset (N_c)	400
	Maximum number of realisations per subset	20,000
	Maximum number of subset levels	30
	Target conditional probability	0.1
	Spread and type of proposal distribution	1, uniform
Analysis settings	Predefined FOS checks	3
	Initial SRF and prediction for second SRF	2.4, 2.1
	Final FOS check	1.0
	Convergence tolerance, displacement limit	0.0001, 0.05
	Maximum number of plastic iterations	2000
Soil and material properties	Constitutive parameters E, ν and ψ	table 3.2
	Range of μ for c (kN/m^2) , COV of c	15-60, 0.2
	Range of μ for ϕ (^{o}) , COV of ϕ	10-20, 0.2
	Range of μ for γ (kN/m^3) , COV of γ	15-20, 0.1
	Range of values for $\rho_{c,\phi}$	-0.7 to -0.3
	Range of values for $\rho_{c,\gamma}$	-1 to 1
	Range of values for $\rho_{\phi,\gamma}$	-1 to 1
	vertical and horizontal scales of fluctuation (m)	2.5 ,10
Type of dist for random	random μ? If yes, type of dist. of μ	yes, Normal
	random ρ's? If yes, type of dist. of ρ's	yes, Beta

Table 3.1: Input parameters for the analysis

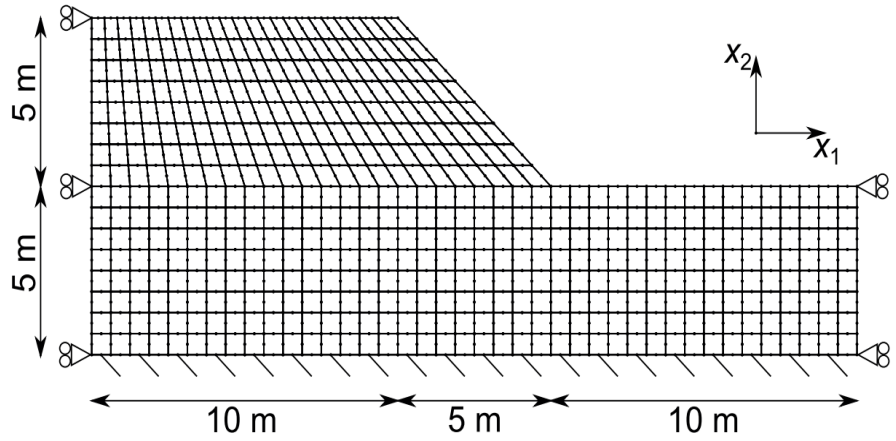

Figure 3.2: Slope geometry and FEM mesh

samples are then generated based on seed samples and are accepted and rejected according to the MMA in section 2.6.2.

3.2.5. DETERMINISTIC MODEL

The stability of the slope is determined based on Linear Elastic Perfectly Plastic constitutive behaviour with a Mohr Coulomb yield surface. c, ϕ and γ are treated as random and other soil constitutive properties are shown in table 3.2. The Young's Modulus of the soil (E) and poison's ratio (ν) will be treated as constants in the analysis with no dilation (ψ) taken into consideration. It must be mentioned that uncertainty exits in the determination of these properties as well, but the focus of this paper remains on uncertainty in c, ϕ and γ.

Property	**Set Value**
E	1x10^5 kPa
ν	0.3
ψ	0.0

Table 3.2: Input parameters for E,ν and ψ

3.2.6. INCLUSION OF UNCERTAINTY IN MCMC

As noted in section 2.6, the generation of samples from subset level 2 and onwards is performed using Markov Chain Monte Carlo. Therefore the modifications to include a general uncertainty approach must be applied within the framework of MCMC. This means that all generated samples must go through the same procedure of whether to be accepted or rejected, based on the Modified Metropolis Algorithm.

This procedure is shown in Figure 3.3, a flow chart for the generation of proposal states within MCMC (Subset level 2 to end). Based on the user input for type of distribution, random numbers are generated for all uncertain parameters. These random values are referred to as proposal states.

Each state is then individually accepted or rejected based on the two checks performed in MMA (see section 2.6.2). The modified procedure is as follows:

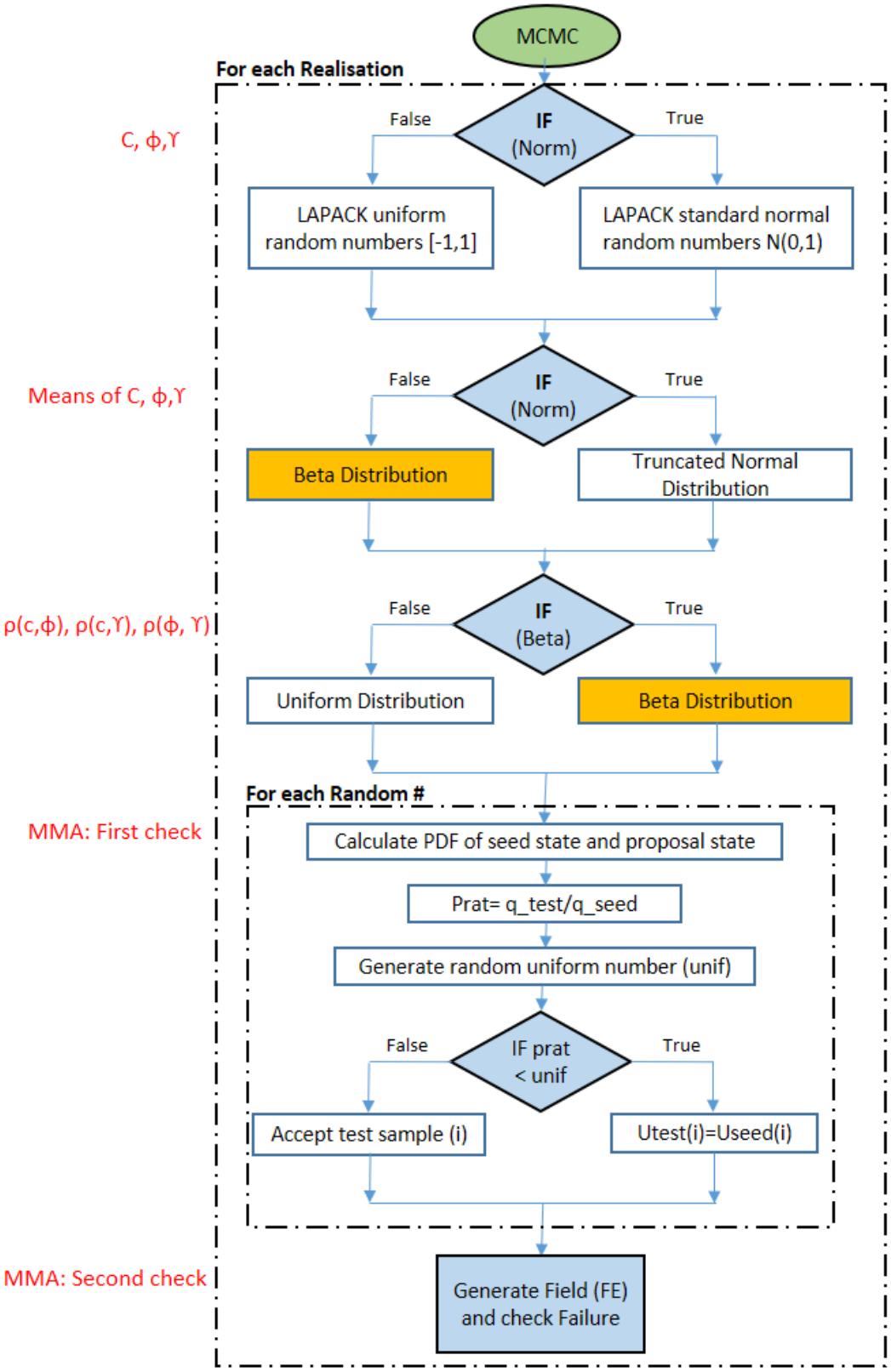

Figure 3.3: Flow Chart for MCMC, for Beta see Fig 3.7a

3.2.7. UNCERTAIN PARAMETERS

Based on distribution type, first either uniform or standard normal values are generated for c,phi and gamma. Distribution of these values is shown in section 3.3.1.The number of generated values for each property equals the number of integration points in the FEM mesh. Next, based on the choice of distribution of random means and standard deviations(section 3.3.2), random values are generated for μ of c,ϕ and γ. Finally based on the choice of distribution of correlation coefficients, 3 random values are generated for $\rho_{c,\phi}$, $\rho_{c,\gamma}$, $\rho_{\phi,\gamma}$ (see section 3.3.3). Beta distributions are highlighted in Figure 3.3 to indicate the link to the next flow chart (figure 3.7a).

MMA FIRST CHECK

The procedure for the Modified Metropolis algorithm is outlined in section 2.6.2. The first check includes accepting and rejecting proposal samples based on the ratio of PDF of proposal/PDF of seed (*prat* in Fig 3.3) against a generated uniform random number (*unif* in Fig 3.3). In MMA, this is performed for each component separately.

MMA SECOND CHECK

MMA second check is performed to determine if accepted samples belong to the same subset as that of the seed. This is done by generating the random fields of c, ϕ and γ and checking for failure. Correlation is introduced between fields before checking for slope failure. This is performed based on the cross-correlation matrix and procedure shown in section 2.9.

3.3. DISTRIBUTION OF RANDOM VARIABLES

This section describes the different distributions considered for each random variable. More than one option is identified for each uncertainty to examine the influence of distribution type on the formulation of subset simulation.

3.3.1. DISTRIBUTION OF SOIL PROPERTIES

A lognormal distribution will be used to model cohesion, friction angle and unit weight as random variables. This is the case since the three parameters are non-negative soil properties. While a normal distribution may sufficiently represent the randomness of the soil parameters, there is a possibility of generating a negative value for either c, ϕ or γ. Therefore, a lognormal distribution must be used to insure that the generated variables will remain positive. In order to study the influence of this log-normal transformation, a simple MATLAB code was used to simulate 10000 random samples of c, ϕ and γ. The chosen point statistics for the underlying normal distribution of the soil properties were as follows:

Property	**mean**	**standard deviation**
C	30 kN/m^2	8 kN/m^2
ϕ	15^o	3^o
γ	20 kN/m^3	3 kN/m^3

The transformation was achieved by:

1. Generating standard normal random samples (μ=0, σ=1)

2. Transforming the normal point statistics to log normal parameters using:

$$f\mu_x = log\Big(\frac{\mu_x}{\sqrt{1+\frac{\sigma_x}{\mu_x}*\frac{\sigma_x}{mu_x}}}\Big) \tag{3.1}$$

$$f\sigma_x = \sqrt{log\big(1+\frac{\sigma_x}{\mu_x}*\frac{\sigma_x}{\mu_x}\big)} \tag{3.2}$$

where X is a random variable, μ_x and σ_x are point statistics for the normal distribution of X and $f\mu_x$ and $f\sigma_x$ are parameters used as input for the log-normal distribution.

3. Transforming the standard normal random variables to the log-normally distributed variables given their point statistics by using:

$$X = exp(f\mu_x + f\sigma_x * rand_x) \tag{3.3}$$

where $rand_x$ are the standard normal samples of X.

In figure 3.4 the bars represent the histograms of log-normally distributed 10,000 random samples of c, ϕ and γ. The lines on the other hand represent the underlying normal distributions. Figure 3.4 indicates that even after the transformation, the underlying normal distributions are maintained while insuring that no negative values will be included in the analysis.

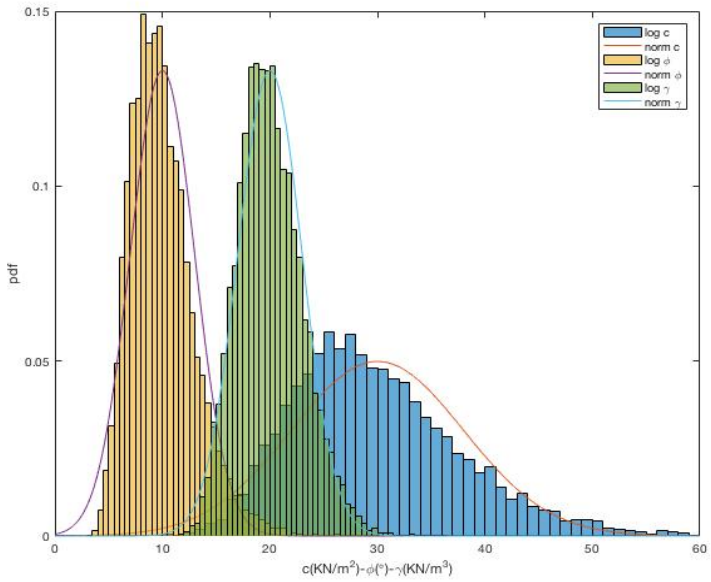

Figure 3.4: Normal vs log-Normal distributions for c, ϕ, γ

3.3.2. DISTRIBUTION OF MEANS

In order to generate a random mean value, two different distribution types are included in the analysis: Normal and Beta distribution (See Figure 3.3). The process for generating a random μ or σ for the case of a **Beta distribution** is as follows:

1. A range of values is defined for μ for all input parameters(eg. $\mu_{\text{c-min}}$ and $\mu_{\text{c-max}}$)

2. A random number x is generated (Beta[0,1])

3. The distribution is shifted based on the range defined in step 1. For example μ_c is determined as follows:

$$\mu_{\text{c-Beta}} = x * (\mu_{\text{c-max}} - \mu_{\text{c-min}}) + \mu_{\text{c-min}} \tag{3.4}$$

The process for generating a μ or σ for the case of a **Normal distribution** is as follows:

1. A range of values is defined for μ and σ for all input parameters. μ of parent distribution is determined as follows:

$$\mu_{\text{parent}} = \frac{\mu_{\text{max}} + \mu_{\text{min}}}{2} \tag{3.5}$$

2. A random number (x) is generated (N(0,1))

3. The standard deviation for μ or σ is determined based on the given range and the 6σ rule (99.7% of samples fall within 6σ)

4. The distribution is shifted based on μ of parent distribution and σ determined in step 3:

$$\mu_{\text{T-Normal}} = x * \sigma + \mu_{\text{parent}} \tag{3.6}$$

Table 3.3 is an example of ranges chosen for μ_c, μ_ϕ, and μ_γ. In order to demonstrate the difference between generating x using a Normal or a Beta distribution and why both choices are provided, consider a CDF(x)=0.95. This means that only 5% of generated values will be higher. For a standard normal distribution, this number corresponds to x=1.65. For a beta distribution, x=0.87. Using the ranges provided in Table 3.3, and based on procedure outlined above, equations 3.7 to 3.10 are an example for the determination of μ_c using both Beta and Normal.

$$\mu_{\text{parent}} = \frac{20+40}{2} = 30 kN/m^2 \tag{3.7}$$

$$\sigma = \frac{40-20}{6} = 3.33 \tag{3.8}$$

$$\mu_{\text{Norm}} = 1.65 * 3.33 + 30 = 35.5 kN/m^2 \tag{3.9}$$

$$\mu_{\text{beta}} = 0.87x(40-20) + 20 = 37.4 kN/m^2 \tag{3.10}$$

This indicates why more than one type of distribution was included in the analysis. For the same CDF value, Truncated Normal provides a lower μ than the one generated using a Beta distribution. This means that using a Normal distribution will lead to narrower distributions. Figure 3.5 shows the difference between the two distributions for the range of values provided above.

3.3.3. DISTRIBUTION OF CORRELATION COEFFICIENTS

Correlation coefficients ($\rho_{c,\phi}$, $\rho_{c,\gamma}$, $\rho_{\phi,\gamma}$) are treated as random variables in the analysis. Given that the objective of applying random ρ's is to be able to study the influence of different correlations on the output of SS, a uniform distribution is appropriate for the analysis. However, the use of a uniform distribution means that all samples will be accepted in the Modified Metropolis Algorithm of MCMC (see section 2.6.2). This is the case as all samples will have an equal probability density. The

μ	**Min**	**Max**
C	20 kN/m^2	40 kN/m^2
ϕ	10^o	20^o
γ	15 kN/m^3	25 kN/m^3

Table 3.3: Example of ranges for μ of c,ϕ and γ

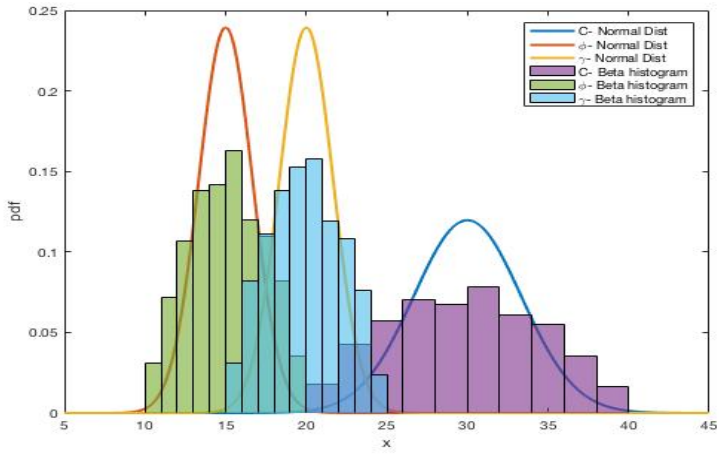

Figure 3.5: Normal distribution vs Beta distributions for μ of c, ϕ, γ

algorithm for accepting and rejecting samples is illusrated in Figure 3.3.

As a result, Beta was chosen as a second distribution for the generation of correlation coefficients. Figure 3.6 indicates the difference between the PDF for a uniform [0,1] and beta (α=2, β=2) distributions. The generation of a random beta sample is explained in detail in section 3.3.4.

The procedure to generate and assemble the cross-correlation matrix is as follows:

1. Generate 3 random numbers [0,1]
2. Shift the numbers based on user input for range of ρ's (eg[-1,1])
3. Generate correlation matrix and check for positive definiteness. If matrix is not positive definite, repeat steps 1 to 3

3.3.4. GENERATING RANDOM NUMBERS FROM BETA DISTRIBUTION

In the linear algebra libraries (LAPACK) used for computations in the Fortran code, there is no included subroutines to generate a Beta distributed random number. However a subroutine is included that can determine a Beta sample (x) based on its CDF. Therefore in the case of beta distributions, Inverse Transform Sampling was used to generate a random beta value between [0,1]. The method is a type of pseudo-random sampling where random values are generated based on CDF. Furthermore, the MMA algorithm requires that the PDF of generated samples is computed in the

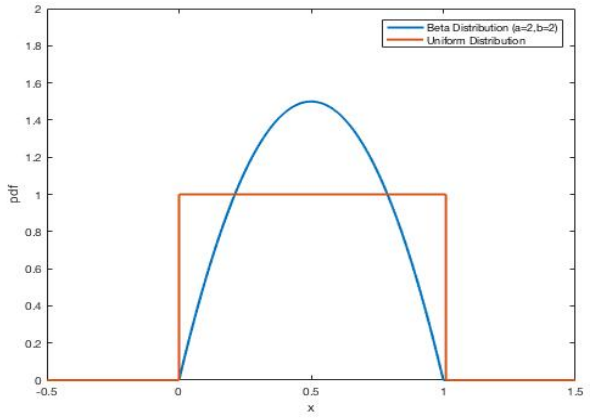

Figure 3.6: PDF's of Beta and Uniform distributi0n for ρ's

analysis. Therefore when generating a Beta distributed random number using Inverse Transform Sampling, the PDF of this number is calculated as well. The process is highlighted in Figure 3.7.a. and the procedure for generating a random number (x) from a beta distribution and its PDF using inverse sampling is as follows (PDF is equal to slope value):

1. For each random value, generate a random number (u) from a uniform distribution
2. Set CDF of x equal to u (F(x)=u)
3. Add and subtract small increments to F(x) to get F_min and F_max
4. Use subroutine Beta_CDF to calculate x_min and x_max
5. Calculate x based on slope of CDF function (see approximation in Figure 3.7.a)

This was tested using a simple MATLAB code as shown in Figure 3.7.b. The blue line indicates the PDF of a Beta distribution (α=2, β=2) and the histogram indicates 10000 beta-generated random values using the inverse sampling method shown in Figure 3.7.a. This indicates that little or no accuracy is lost by applying this type of sampling.

3.4. CONCLUSION

The generation of random variables for c , ϕ and γ is implemented in this section. This includes random variables for the mean of these properties and their cross-correlation coefficients. Flow charts are used to illustrate how these additions can be implemented in the procedure of subset simulation. Furthermore, all input required in order to perform such an analysis is described and the deterministic model used to evaluate slope stability is defined. Possible distributions for the random variables are identified and compared using simple examples. With the implementation of this method, it becomes possible to evaluate the influence of each random variable on the probability of failure and the influence of the chosen type of distribution on the sampling within an analysis.

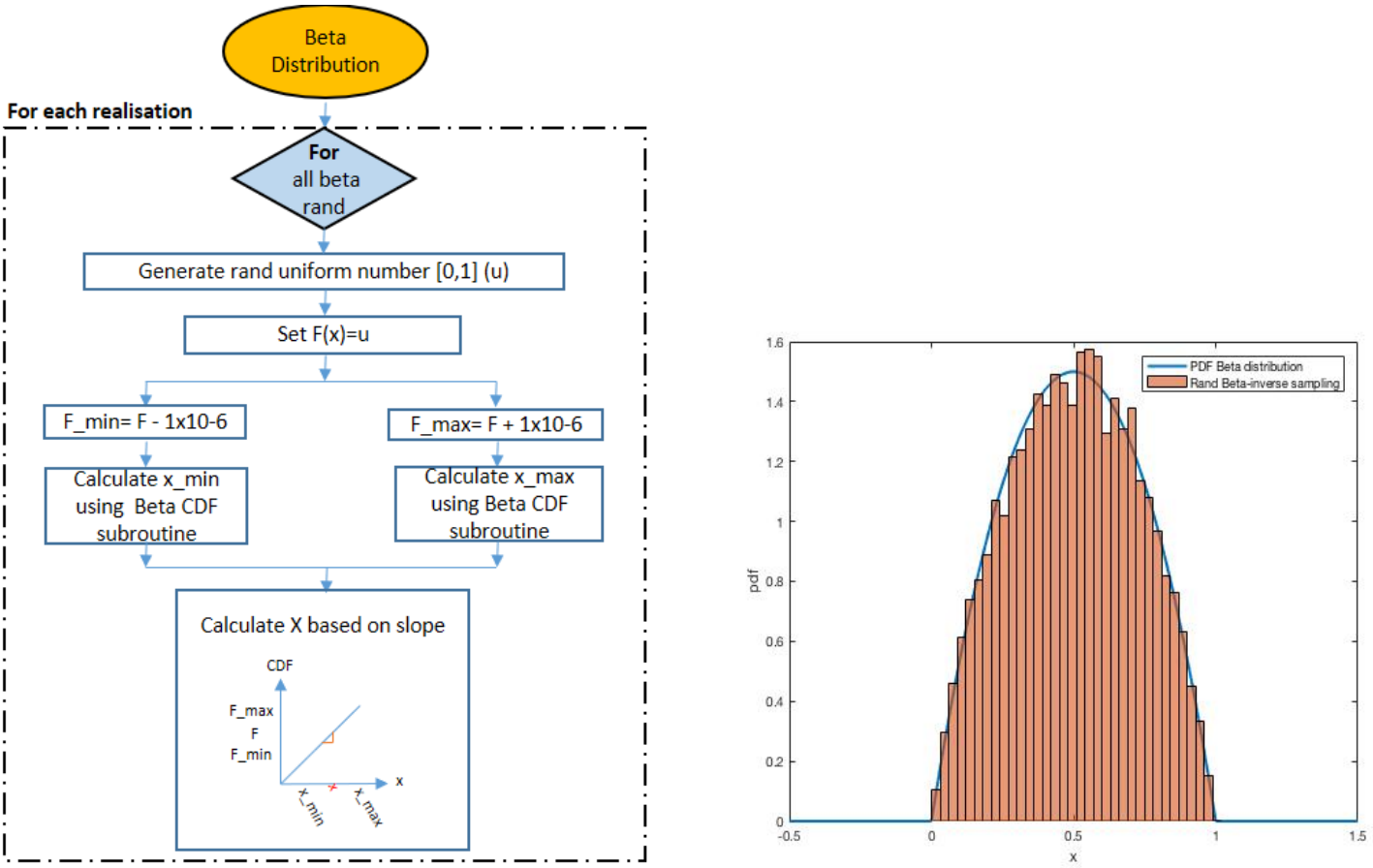

Figure 3.7: a) Flow chart for generation Beta random numbers b)Inverse sampling check

4

SENSITIVITY ANALYSIS

4.1. INTRODUCTION

Before introducing uncertainty in the mentioned input parameters, it is first necessary to determine the effect of each parameter individually on the outcome of the results. If the output is sensitive to changes in an individual parameter and this parameter is believed to be uncertain, then the methodology of treating it as random is supported. Therefore, a sensitivity analysis is performed for the proposed random parameters before they are treated as uncertain. Individual parameters will be altered while keeping all other input constant, and effect on output (p_f) will be evaluated. A sensitivity analysis is performed for:

- mean of c, ϕ, and γ
- correlation coefficient between c-ϕ, c-γ, and ϕ-γ

With a sensitivity analysis for the six soil properties above, it is possible to evaluate the effect of parameter and model uncertainty . However, uncertainty in soil is not restricted to the determination of soil properties and it includes other factors such as spatial variability. For example, it is expected that results will vary depending on the chosen input values for vertical and horizontal scales of fluctuation. Therefore, to illustrate the effect of other types of uncertainty on the output, sensitivity of p_f to changes in θ_V and θ_H is considered as well. Table 4.1 is a summary of input parameters used for each individual analysis. For each investigation a single COV value is used for the three parameters (c, ϕ and γ). This is done to insure that the relative spread of distributions is maintained as COV is not treated as a random variable in the analysis. In addition, maintaining one value for the three parameters will help in determining which parameter is the output most sensitive to. Given that the probability is failure is influenced by the choice for COV, each analysis is performed multiple times, each with a different COV for possible values of c, ϕ and γ.

Investigating the sensitivity of the model to an individual parameter does not give an indication of the effect of randomising this parameter. In table 4.1, properties are individually altered which means that each analysis consists of one set of values for μ's and ρ's. On the other hand, treating these parameters as random will lead to different μ's and ρ's for each realisation within one analysis. Therefore, an additional sensitivity investigation is performed where results are compared for the cases of:

- set means with no correlation
- random means with no correlation

- set means with set correlation
- set means with random correlation
- random means with random correlation

Furthermore, A choice has to be made on type of distribution before the generation of a random parameter. Chapter 3.3 in Part 3 summarises the different distribution types considered for means (c, ϕ and γ) and their cross-correlation coefficients. In order to determine the influence of altering the distribution type, a sensitivity analysis is performed where the following distributions are compared:

- Beta vs Truncated Normal for μ of c, ϕ and γ
- Beta vs Uniform distribution for ρ's

Results are compared in terms of influence of distribution type on sampling and parameter combinations that lead to failure. Figures for this investigation are explained in section c, ϕ and γ and are included in Appendix A.

Sensitivity analysis	C (kN/m^2)	ϕ(^{o})	γ (kN/m^3)	$\rho_{c,\phi}$	$\rho_{c,\gamma}$	$\rho_{\phi,\gamma}$	θ_V (m)	θ_H (m)
1) μ of C	15-25	10	20	0	0	0	4	10
2) μ of ϕ	20	5-15	20	0	0	0	4	10
3) μ of γ	20	10	15-25	0	0	0	4	10
4) $\rho_{c,\phi}$	20	10	20	-0.8 - 0.8	0	0	4	10
5) $\rho_{c,\gamma}$	20	10	20	0	-0.8 - 0.8	0	4	10
6) $\rho_{c,\gamma}$	20	10	20	0	0	-0.8 - 0.8	4	10
7) θ_V	20	10	20	0	0	0	0.6-4	10
8) θ_H	20	10	20	0	0	0	4	1-20

Table 4.1: Parameter set for each sensitivity analysis (red indicates altered parameters for each analysis)

4.2. MEAN OF C, ϕ AND γ

Figures 4.1a, 4.1b and 4.1c are results for the sensitivity of probability of failure to changes in the mean of c, ϕ and γ, respectively. For each figure, the red line indicates the results for the initial set of means (c= 20 kN/m^2, ϕ= 10 ^{o}, γ= 20 kN/m^3) while the blue and yellow line shows results after changes in each individual parameter. The x-axis corresponds to set COV values for the distribution of C, ϕ and γ.

As anticipated, increases in μ of c and ϕ and a decrease in μ of γ lead to a lower p_f. The first two contribute to resisting forces in the slope while the driving force of failure depends on the latter. The output was most sensitive to changes in μ at lower COV values (eg. 0.1) but the trend remains constant even at higher values. For the set of values reported in table 4.1, p_f is equally sensitive to changes in μ of c and γ and less to changes in ϕ. An increase of 5^o leads to a decrease in p_f from

10^{-10} to 10^{-15}. On the other hand, an increase of 5 kN/m^2 for c and a decrease of 5 kN/m^3 for γ both lead to a decrease in p_f from 10^{-10} to 10^{-20}. Furthermore, by comparing changes in output between one line to another (sensitivity to μ of parameters) and then comparing changes within one line (sensitivity to COV of parameters), it becomes clear that at low parameter values (eg. c=15kN/m^2 to c=15kN/m^2), p_f is more sensitive to changes in relative spread of distribution rather than changes in mean of distribution.

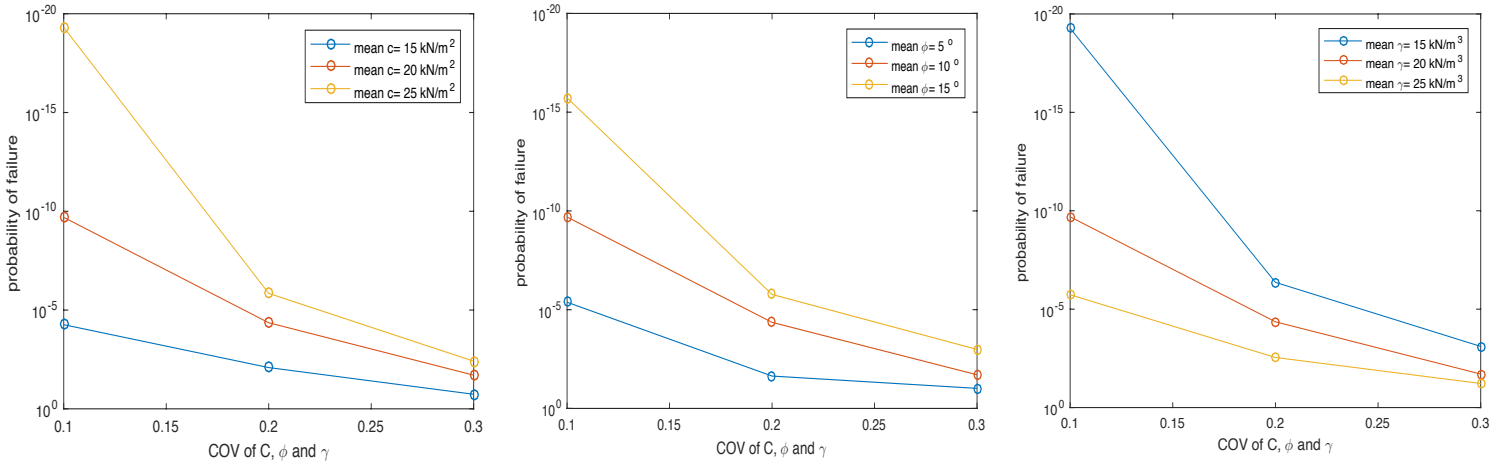

(a) (b) (c)

Figure 4.1: Sensitivity of p_f to changes in μ of (a)c (b)ϕ and (c)γ

4.3. CROSS-CORRELATION COEFFICIENTS

Figure 4.2 indicates the influence of cross-correlation coefficients on the calculated probability of failure. Each line in the figure shows a separate analysis for the sensitivity of p_f to changes in one ρ value while the remaining ρ's are kept constant at 0. The overall trend shows that negative values for $\rho_{c,\gamma}$ and $\rho_{\phi,\gamma}$ lead to an increase in probability of failure and positive values to a decrease in output. This is expected as an increase in driving forces corresponds with a decrease in resisting ones and vice versa. On the other hand, negative $\rho_{c,\phi}$ lead to a slight decrease in p_f and positive values lead to the opposite. By comparing p_f values in 4.2 to results in figures 4.1a, 4.1b and 4.1c, it is clear that the output is significantly more sensitive to changes in μ values than to changes in ρ. However, this is the case when only correlation between two parameters is considered and results will differ if cross-correlation is included between all three parameters (see section 4.5).

When comparing the three plots to each other, it is clear that the sensitivity of p_f to changes in input is different when considering a different ρ. For example, the calculated p_f increases from 10^{-4} to 10^{-2} when applying a $\rho_{\phi,\gamma}$=-0.8 while a smaller decrease is evident with a $\rho_{c,\gamma}$=-0.8. Furthermore, the sensitivity of p_f to positive values of a correlation coefficient is different than sensitivity to negative ones. While it is evident that negative values of $\rho_{\phi,\gamma}$ lead to an increase in p_f, positive values lead to little or no change at all.

4.4. SCALE OF FLUCTUATION

Figures 4.3a and 4.3b indicate the effect of changing the vertical and horizontal scale of fluctuation on the calculated probability of failure. In both cases the analysis is performed twice, once with a COV for c,ϕ and γ equal to 0.2 and once with a COV=0.3. For both θ_V and θ_H the sensitivity of p_f

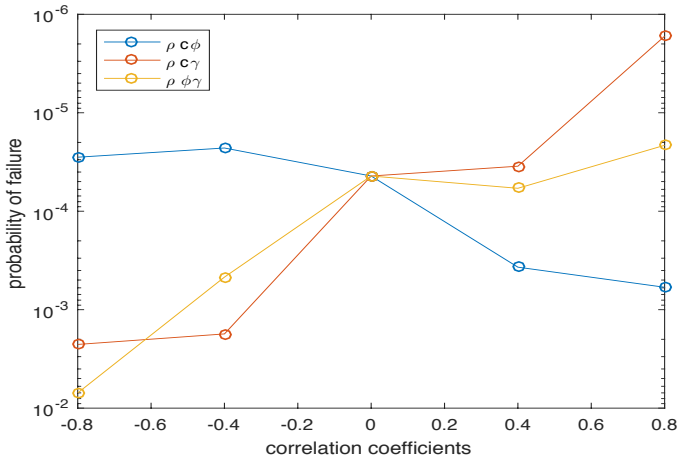

Figure 4.2: Influence of values of $\rho_{c,\phi}$, $\rho_{c,\gamma}$ and $\rho_{\phi,\gamma}$ on probability of failure

depends on the range of values considered. A θ_V between 0.6 and 1m leads to noticeable changes in p_f while for values more than 2.5m, the p_f becomes constant. This is also the case with θ_H as p_f is very sensitive to values between 1 and 5m while no sensitivity is evident in values higher than 7m. However, it is worth mentioning that the values of θ_V and θ_H where p_f becomes constant is heavily dependant on the geometry, boundary conditions and other properties of the slope in question.

Furthermore, p_f is more sensitive to the scales of fluctuation when considering lower COV value for c,ϕ and γ. This is evident when examining the difference between the slope of COV=0.2 vs COV=0.3 in figures 4.3a and 4.3b. In addition, when considering the shift between both lines in each figure, it is evident the p_f is more sensitive to changes in COV than to changes in θ_V and θ_H. When comparing to the parametric analyses of sections 4.2 and 4.3, it is clear that the output is as sensitive to other types of uncertainty (eg. spatial variability) as it is to uncertainty in parameters.

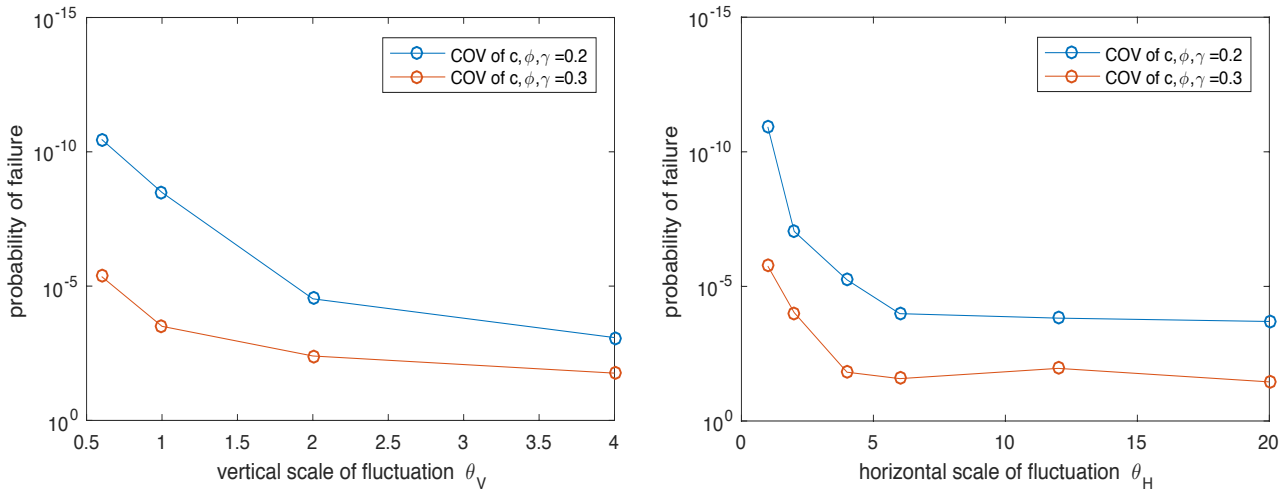

(a) (b)

Figure 4.3: Influence of (a) θ_V and (b) θ_H on p_f

4.5. RANDOM VARIABLES

Figure 4.4 indicates the influence of randomising mean values and correlation coefficients for c, ϕ and γ. The blue line shows probability of failure results for the basic case with c= 20 kN/m^2, ϕ= 10^o, γ= 20 kN/m^3 and no correlation between the properties. It is clear from the figure that including random means in the analysis (red and green lines) lead to a significantly higher p_f. This is especially the case when considering low COV values for c, ϕ and γ. Therefore, if there is uncertainty in the determination of mean values, randomisation must be included, as the outcome will differ considerably.Furthermore, when examining the change in p_f values in the x-axis versus changes in the y-axis, it is apparent that p_f is more sensitive to randomising the μ of properties than to a change in COV of these properties.

The effect of setting values for correlation coefficients is also included, where an investigation is performed with $\rho_{c,\phi}$=-0.7, $\rho_{c,\gamma}$=0.6 and $\rho_{\phi,\gamma}$=-0.5. These ρ values are selected arbitrarily and the analysis is carried out to highlight the difference in sensitivity of p_f, to set and random correlation. It is evident when comparing the basic case and the plot for random correlations that introducing uncertainty in all ρ's has little or no effect on p_f. However, when considering the case with set correlations, the p_f is significantly lower. It is clear that the change in p_f depends on the magnitude and combination of the ρ's. Nevertheless, this shows that certain combinations will lead to a drastic change in the calculated p_f. This illustrates the need for including cross-correlation, especially if dependence between properties is expected in certain types of soil.

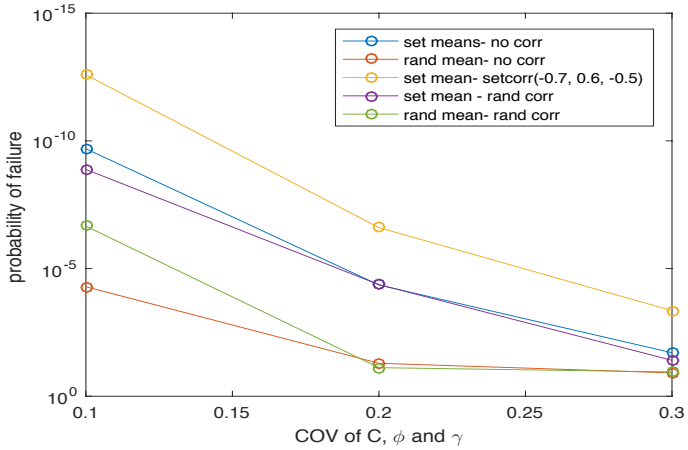

Figure 4.4: Influence of random μ's, random ρ's and set ρ's on p_f

4.6. TYPE OF DISTRIBUTION

In part 3, a number of distribution types are considered for the random variables in the analysis. Before a choice can be made on the most suitable distribution, its first necessary to investigate their influence on the outcome of results. Therefore an analysis is carried out where the type of distribution is altered and the outcome is evaluated. Simulations are performed with random μ's for c, ϕ and γ and random correlation between the three parameters. Furthermore, the COV for the soil properties is also considered as random. This is done to evaluate how random samples are generated for different distributions.

It is expected that changing the distribution type has minimal influence on the calculated probability of failure. However, parameter combinations that lead to failure at different p_f levels will de-

pend on the chosen initial distribution. In the subset simulation procedure, each generated subset corresponds to a lower strength reduction factor and lower p_f level. This means that samples generated for each subset will differ as weaker combinations are required for failure. For example in the case of SRF=1.5 vs SRF=1.0, weaker samples are required for the slope to fail under its own weight (SRF=1.0). Therefore results are compared with the use of scatter plots and fitted PDF distributions to illustrate the evolution of sampling from one p_f level to another. Results for this investigation are included in Appendix A.

4.6.1. BETA VS UNIFORM ρ'S

First the influence of distribution of correlation coefficients is investigated. The two considered options are beta and uniform distributions. The p_f for the slope considered in both cases is 0.013 for beta distributed ρ's and 0.014 for uniform distributed ρ's. Figures A.1a and A.1b in Appendix A are scatter plots for ρ samples generated using a beta distribution, A.1a for samples generated in first subset (SRF=1.5 and p_f=0.29) and A.1b for samples generated in last subset (SRF= 1.0 and p_f=0.013). On the other hand, figures A.2a and A.2b are scatter plots for ρ samples generated using a uniform distribution, A.2a for samples in the first subset (SRF=1.5 and p_f=0.31) and A.2a for samples in the last subset (SRF= 1.0 and p_f=0.014).

In the case of a beta distribution, gaps in the scatter plots indicate that less random samples are generated at the limits for ρ's (-1 and 1). This is not the case for samples generated using a uniform distribution as a sampling space of -1 and 1 is well covered for both p_f levels considered (figures A.2a and A.2b). Furthermore, by searching for critical combinations, the SS procedure generates samples from the tail ends of distributions for lower p_f levels in the case of a beta distribution (figure A.1b) as most samples of $\rho_{c,\gamma}$ and $\rho_{\phi,\gamma}$ are positive. However, when initial distribution is uniform, different SRF factors and lower p_f levels did not lead to a shift in sampling as most samples are generated around a mean value of zero. This is the case because in SS, samples are generated using MMA (see part 2, section 2.6.2). Based on seed samples from the first subset, proposal samples are generated and then accepted and rejected based on a ratio between PDF values of seed and proposal state. In the case of a uniform distribution, the PDF will almost always be constant:

$$PDF_{\text{uniform}} = \frac{1}{max - min} \tag{4.1}$$

This means that all samples will be accepted during the procedure. As such, it becomes more difficult to search for the most critical combinations if all generated samples for ρ are accepted. This is not an issue with a beta distribution as the PDF will vary from one sample to another.

4.6.2. NORMAL VS BETA μ'S

Next the distribution type for μ of c, ϕ and γ is considered. The two options investigated are normal and beta distributions. The procedure of how these samples are generated is highlighted in part 3, section 3.3.2. The calculated p_f in both cases is similar, 0.02 for the case of normally distributed μ values and 0.01 for the case of beta distribution. Figure A.3 in Appendix A shows fitted distributions for c, ϕ and γ in the case of normal and beta distributions. Based on all samples generated within a subset (p_f level), the PDF of these samples is estimated. Each plot contains PDF plots for all subsets within one simulation. The plots show samples in their initial form before being transfomred, N(0,1) for normal distribution and beta(0,1) for beta. For example, figure A.3a indicates fitted normal PDF plots for c for all p_f levels used to calculate the final p_f.

When examining samples of c, a shift in the point statistics of a distribution is evident as generated samples at lower probability levels are lower. This is expected as lower values of c are required

to induce failure at lower p_f levels and SRFs. However, this shift is more pronounced in the case of a normal distribution (figure A.3a) than with a beta distribution (figure A.3b). Sampling in both distributions lead to an increase in values for ϕ and γ with a clear shift in samples for beta towards the upper tail of the distribution (highest PDF value at ϕ and γ=0.8). It is clear that in the case of random μ's, both normal and beta distributions produce similar combinations of parameters that lead to failure at a certain SRF or p_f. This is consistent with the behaviour of a soil slope as for example, lower values of c and higher values of γ will lead to a less stable slope. However, the different characteristics of each distribution means that it may be easier to find these unstable combinations for a certain type of distribution. It is evident that lower values are generated for c in the case of a normal distribution. This should translate to a difference in calculated p_f of slope as more critical combinations are sampled. However, for the examples considered here, the difference in calculated p_f between both cases is negligible.

4.7. CONCLUSION

A sensitivity analysis is performed to evaluate the influence of different parameters on the outcome of the results. Before treating a soil property as random, it is necessary to first establish how sensitive is the outcome to changes in this property. The sensitivity of probability of failure to changes in μ of c, ϕ and γ is first examined. Altering the μ value of c, ϕ and γ leads to significant changes in the calculated p_f, especially if COV of these properties is less than 20%. In addition, the outcome is more sensitive to changes in c and γ than to changes in ϕ. This means that possible ranges for these values should be examined carefully if they are to be treated as random variables. Furthermore, the calculated p_f is heavily influenced by the coefficient of variation of the 3 soil properties. This must be considered when applying this method for a practical example or an existing slope and it is recommended that COV values are set initially in any future investigation.

Randomising the mean of c,ϕ and γ leads to a much higher calculated p_f, and a decrease in sensitivity of p_f to changes in COV of the three properties. When the COV was set to higher than 20%, no changes in p_f occurred which means that the outcome becomes more influenced by including uncertainty in μ values. This is particularly the case when including random values for μ of c as generating lower values becomes more possible which will ultimately lead to a higher p_f. This indicates that treating μ as a random variable, with a broad range of possible values, will lead to more conservative results in the analysis.

When considering cross-correlation between c, ϕ and γ, p_f was less sensitive to changes in individual correlation coefficients than to changes in mean values of the soil properties. Nevertheless, there is a clear trend that the magnitude of ρ will influence the calculated p_f. For example, positive correlation between c and ϕ ($\rho_{c,\phi}$) lead to a higher p_f. This is consistent with results presented in other studies (eg.Griffiths et al. (2009)) and means that assuming positive correlation between the two properties will lead to more conservative results. On the other hand, certain combinations of the correlation coefficients considered lead to a significant change in calculated p_f, as was the case in figure 4.4 with $\rho_{c,\phi}$=-0.7, $\rho_{c,\gamma}$=0.6 and $\rho_{\phi,\gamma}$=-0.5. This combination lead to almost a 100% decrease in p_f when compared to the base case with no correlation. This leads to the conclusion that if unless a site investigation points to a clear dependence between the properties, uncertainty in the determination of ρ values must be accounted for to avoid inaccurate results.

Furthermore, setting the 3 variables as random and considering all possible combinations (-1 to 1 for all ρ's) leads to little or no changes in the outcome. Although perfect positive and negative correlation is possible between two data sets, there is little or no data to support perfect correlation

between soil properties. Therefore it is recommended that if site specific information is available regarding inter-dependency between values of c, ϕ and γ, then possible ranges of ρ's should be limited according to this information.

An additional sensitivity analysis is performed to test the influence of spatial variability on the calculated p_f. Results show that within certain ranges, the output is heavily influenced by the magnitude of θ_V and θ_H. For example at θ_H<5m, p_f is very sensitive to changes and this should be considered when determining the input parameters for spatial variability in any future analyses. It is recommended that if information is limited for the slope conditions considered in this analysis, θ_V is set to a value >2m and θ_V>5m to avoid underestimating the p_f.

Finally the influence of distribution type is also considered in this analysis. Little information is available in literature about possible distributions for mean values and correlation coefficients of c, ϕ and γ. Therefore, this investigation is carried out to determine how sampling is influenced by the initial type of distribution, and if this influence will lead to a change in outcome. For the case of uniform distributed correlation coefficients, it becomes more difficult to find the most critical combinations as all samples are accepted during the SS procedure. This is significant as a high acceptance ratio will lead to inefficient sampling within a subset (van den Eijnden and Hicks, 2017). Therefore, for future investigations it is recommended to use other types of distributions. Sampling from a beta distribution is one possible alternative as the range of possible values is covered without forcing the acceptance of proposal samples.

When considering the distribution type for μ values of c, ϕ and γ the calculated p_f was similar for the case of a normal and beta distribution. However, the combination of parameters that lead to failure is slightly different between one distribution to another. This indicates that for a different set of input parameters than what was used in the analysis, the type of distribution may lead to a difference in the calculated p_f. Therefore, the type of distribution for μ values will influence the analysis and should be chosen based on expected variation in these properties according to site and model specific conditions.

5

PRACTICAL EXAMPLE

5.1. INTRODUCTION

In chapter 3, a general uncertainty approach is implemented to model means of c, ϕ and γ as random variables. The approach is extended to include cross-correlation between these parameters and to treat correlation coefficients as uncertain. In chapter 4, the influence of each individual parameter on the outcome is evaluated and the effect of randomising these parameters is investigated. The same geometry and boundary conditions applied in chapter 4 is considered for the practical example and are shown in chapter 3, figure 3.2. This means that sensitivity results presented can be used to determine ideal input parameters for the analysis. Therefore, based on results of chapter 4 and ranges of values reported in literature, a practical example of evaluating slope reliability is carried out while treating mean values and correlations as random. While a sensitivity analysis evaluates the influence of individual parameters, it is insufficient to determine the implications of the uncertainty approach in the case of real life scenarios. Therefore an analysis is performed based on practical values and results are interpreted according to:

1. Probability of failure p_f
2. Combination of parameters that lead to failure at different p_f levels
3. Mode of failure (depth and location of slip surfaces)
4. Random fields of c, ϕ and γ

The variability in the considered soil parameters can be attributed to inherent variability, measurement error and model transformation uncertainty, and the extent of contribution of each category to the total uncertainty will depend on the specific site and soil conditions (Phoon and Kulhawy, 1999). As there is little statistical data available regarding measurement and transformation error, it is more difficult to define uncertainty in these categories than to evaluate the inherent variability of the soil. Therefore, ranges of mean c, ϕ and γ are chosen based on reported values in literature for inherent soil variability. Phoon et al. (1995) conducted an extensive literature review and presented a general summary of statistical data for inherent variability in soil, and table 2.3 in part 2 is an example of values reported for mean and COV of c and ϕ. More recently, Kim et al. (2012) provided a similar summary for tests conducted on silty clay. On the other hand, limited information is available regarding possible values for correlation coefficients for c, ϕ and γ. Lumb (1970) and Yucemen et al. (1976) reported negative ranges for $\rho_{c,\phi}$, while other studies assumed positive

values for $\rho_{c,\gamma}$ and $\rho_{\phi,\gamma}$ (Javankhoshdel and Bathurst, 2015). Values reported in these studies in addition to results of part 4 will be used as a basis for decisions on input within the analysis.

5.2. INPUT PARAMETERS

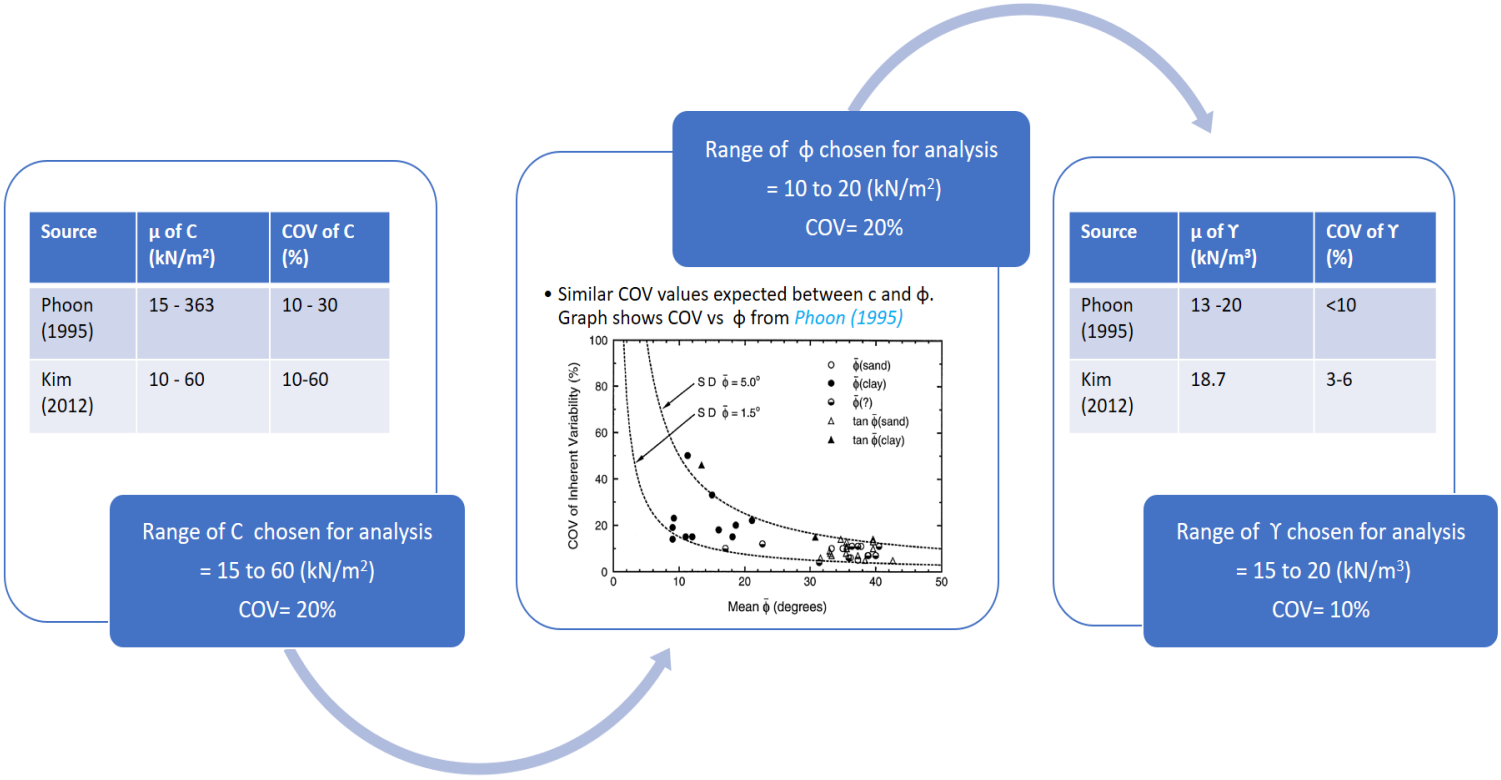

Figure 5.1: Determining ranges of c, ϕ and γ for practical example

Figure 5.1 indicates how decisions are made regarding ranges of mean values and COV's for c, ϕ and γ. Parameters are selected to represent a stable silty clay soil slope for which failure would be considered a rare event. Based on values presented in Phoon et al. (1995) and Kim et al. (2012), a choice is first made for range of μ of c and COV of c (15-60kN/m^2 and 20%). The maximum is limited to a value of 60 kN/m^2 as in part 4, it was shown that a μ for c higher than 25 kN/m^2 will lead to a very low probability of failure. A similar COV value is expected between c and ϕ and therefore 20% is used for both soil properties. Next based on the chosen COV, the range of ϕ is estimated according to the graph shown in figure 5.1. Finally, both studies show that inherent variability in the mean and COV of γ is less than in the case of c and ϕ. Therefore the set range for μ of γ is 15 to 20 kN/m^3 with a COV of 10%.

Next, based on values reported by Yucemen et al. (1976), Lumb (1970) and Javankhoshdel and Bathurst (2015) $\rho_{c,\phi}$ is expected be negative and therefore its range is set at -0.7 to -0.3. As there is little information available regarding $\rho_{c,\gamma}$ and $\rho_{\phi,\gamma}$ the maximum possible range of -1 to 1 is used in the analysis. Spatial variability is represented in the investigation with the use of vertical and horizontal scales of fluctuation. El-Ramly et al. (2002) and Phoon et al. (1995) reported values of 1-3 m for θ_V and 10-40m for θ_H. These ranges are considered appropriate for the slope in question as p_f is more stable in these ranges as shown in chapter 4, section 4.4. Therefore, the values chosen for θ_V and θ_H are 2.5 and 10 m, respectively. Table 5.1 is a summary of decisions regarding soil input

parameters for the practical analysis.

Parameter	Random ?	Range	COV	Distribution type
μ of C	✓	15 to 60 kN/m^2	0.2	Normal (log-normal for c)
μ of ϕ	✓	10-20^o	0.2	Normal (log-normal for ϕ)
μ of γ	✓	15-20 kN/m^3	0.1	Normal (log-normal for γ)
$\rho_{c,\phi}$	✓	-0.7 to -0.3	-	Beta
$\rho_{c,\gamma}$	✓	-1.0 to 1.0	-	Beta
$\rho_{c,\gamma}$	✓	-1.0 to 1.0	-	Beta
θ_V	X	2.5 m	-	-
θ_H	X	10 m	-	-

Table 5.1: Summary of input parameters for practical example

5.3. RESULTS AND DISCUSSION

5.3.1. PROBABILITY OF FAILURE

Table 5.2a shows the strength reduction factors applied for each subset during the analysis and the corresponding subset and cumulative p_f. The number of failures per subset (N_c) is set at 400 which leads to analysis with a total of 19151 realisations. To assess the accuracy of the applied method, an individual Monte Carlo simulation is performed at SRF=2.1, 1.8, 1.6 and 1.4. The MC simulations are performed until 100 failures are reached for each examined SRF. This is only carried out up to a SRF of 1.4 as 100 MCS failures at a SRF=1.0 will require approximately 12.5 million realisations.

Figure 5.2b is a plot of SRF versus cumulative p_f and shows results for both SS and MCS at different strength reduction factors. The resulting p_f from SS for the considered slope at a SRF=1.0 is $7.96 * 10^{-6}$. This is consistent with the results of the sensitivity analysis (part 4) where introducing a random mean lead to a higher probability of failure than in the case with set parameters. Furthermore, figure 5.2b indicates that the results between SS and MCS correspond up to at least a SRF=1.4. Therefore, not only does SS give a reasonable output, it does so at a fraction of the computational cost of a traditional MCS.

5.3.2. COMBINATIONS THAT LEAD TO FAILURE

Given that the means and correlation coefficients of c, ϕ and γ are treated as random, it is of interest to evaluate the critical combination of properties that lead to failure. Failing realisations within a subset are samples that fail at a certain strength reduction factor (eg. 2.4) and do not fail when applying the next SRF (eg. 2.1). Therefore these samples make up the combination of properties that leads to failure at the subset's cumulative p_f level. In order for the slope to fail at lower p_f levels, it will require either an increase in driving forces or decrease in resistance or both. This may be in the form of a reduction in shear strength (c and ϕ) or increase in unit weight (γ). The sensitivity

Subset	SRF	p_f	Cumulative p_f
1	2.4	0.096	0.096
2	2.1	0.29	0.028
3	1.8	0.26	0.0072
4	1.6	0.28	0.0016
5	1.4	0.26	4.34e-4
6	1.2	0.19	8.0e-5
7	1.1	0.29	2.3e-5
8	1.0	0.49	*7.9e-6*

(a) Results for each subset and cumulative p_f

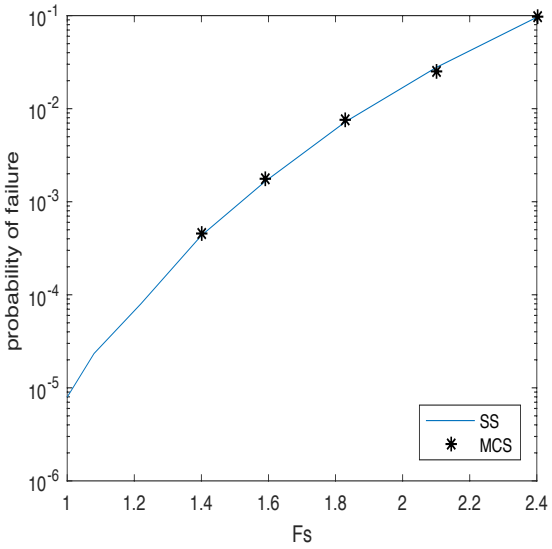

(b) SRF versus p_f

Figure 5.2: probability of failure results

analysis in part 4 indicated that p_f is almost equally influenced by c and γ and less so to changes in ϕ. By evaluating the combination of properties that leads to failure for this practical slope, it becomes clear if this holds even when correlation is introduced and properties are treated as random. Furthermore $\rho_{c,\phi}$ is restricted to a negative range (-0.7 to -0.3) without limiting possible values of $\rho_{c,\gamma}$ and $\rho_{\phi,\gamma}$ in the analysis. Evaluating generated samples at each p_f will provide insight on the influence of one correlation on the other. The aim of this section as a whole is therefore to examine generated realisations and determine the combinations of parameters that are more likely to result in a failing realisation at lower p_f's .

MEANS OF c, ϕ AND γ

Figure 5.3a indicates the average of standard normal generated means of c, ϕ and γ at each p_f level. It is clear that mean of c is the most critical parameter for generating failing realisations, as most samples of c are generated from the tail end of the distribution. On the other hand, the means of ϕ and γ are maintained throughout the analysis. To illustrate this trend in relation to the set ranges in table 5.1, figure 5.3b shows the means of c, ϕ and γ after they are transformed to normally distributed samples. The transformation procedure is explained in detail in chapter 3, section 3.3.1. While samples of mean ϕ and γ remain well within the average of the ranges set as input (table 5.1), any failing realisations at p_f of less than 10^{-1} required a mean of c around the set minimum or lower. Samples lower than the set minimum are possible as the standard deviation for the distribution of means is determined based on the 6 sigma rule. Therefore, to generate means of c lower than the set minimum (15kN/m^2), samples must be generated from the tail end of the distribution at a PDF of less than 0.15%. For the slope in question, this is the case at low p_f levels (10^{-4} and less).

Figure 5.3c shows fitted PDF distributions for generated samples of mean c in the first subset (initial distribution) versus samples in the final subset of the analysis. The latter distribution illustrates the values of mean c required for failure to occur at a p_f of $7.96 * 10^{-6}$. Figures B.1a, B.1b and B.2 in Appendix B indicate the fitted normal distributions of c, ϕ and γ at each p_f or subset level. Although results of the sensitivity analysis in part 4 show a similar influence of the three parameters

on p_f, fitted distributions show that a clear increase or decrease in magnitude is only apparent for means of c.

To better understand what combination of parameters leads to failure, figure 5.4a shows scatter plots for all samples generated for means of c, ϕ and γ, at each p_f level. The plots reaffirm that as the p_f decreases, the magnitude of mean of c decreases as well, while samples of ϕ and γ remain centred around the mean of the initial distributions. Furthermore, scatter plots of mean of ϕ versus γ indicate a clear positive correlation between the two soil properties. This becomes more evident at lower p_f's as dependence between the two parameters increases. It must be noted that this correlation is induced as a result of the procedure of SS searching for failing realisations rather than correlations according to the sampling of $\rho_{c,\phi}$, $\rho_{c,\gamma}$ and $\rho_{\phi,\gamma}$.

CORRELATION COEFFICIENTS OF c, ϕ AND γ

Figure 5.4b indicates scatter plots for generated samples of $\rho_{c,\phi}$, $\rho_{c,\gamma}$ and $\rho_{\phi,\gamma}$ at each p_f level. As shown in the list of input parameters (table 5.1), the range of $\rho_{c,\phi}$ is limited to -0.7 to -0.3 while ranges for the other two ρ's are kept at maximum (-1 to 1). The first observation is that at lower p_f levels, most samples of $\rho_{c,\phi}$ are generated closer to the maximum of the possible range (-0.3). This is consistent with the results of the sensitivity analysis (part 4) as the more negative $\rho_{c,\phi}$ is, the less likely the slope will fail. On the other hand a higher concentration of positive samples is evident for $\rho_{c,\gamma}$ and $\rho_{\phi,\gamma}$. This is especially the case when examining scatter plots of the latter as most samples are generated between 0 and 1. This reaffirms the observations of the previous section that most failing realisations at lower p_f levels have strong correlation between ϕ and γ.

Furthermore, some negative correlation is evident when examining the scatter plots of $\rho_{c,\gamma}$ versus $\rho_{\phi,\gamma}$. There is two possible explanations for this phenomenon: (1) the positive correlation between ϕ and γ, (2) limitations of a cross-correlation matrix (see part 2, section 2.9.4). In order to generate correlations between three different properties, the assembled correlation matrix must be positive definite. Given that $\rho_{c,\phi}$ is set to negative values in the analysis, this limits the range of possibilities for samples of $\rho_{c,\gamma}$ and $\rho_{\phi,\gamma}$, as it is difficult to achieve positive definiteness if all three ρ's are negative. Therefore, it is believed that the limitation of positive definitiness in addition to positive correlation between ϕ and γ will force negative correlation between $\rho_{c,\gamma}$ and $\rho_{\phi,\gamma}$.

Scatter plots of $\rho_{c,\gamma}$ versus $\rho_{\phi,\gamma}$ also indicate that generated samples are forming bands (vertical and horizontal concentration of points). This may be due to the size of the Markov steps within the procedure of subset simulation. A large Markov step leads to a continuous shift in sampling from positive to negative for each realisation, which might explain the trend detected in the samples of $\rho_{c,\gamma}$ and $\rho_{\phi,\gamma}$. In order to have efficient sampling in SS, large Markov steps are required in addition to a high acceptance rate in the Modified Meteropolis Algorithm van den Eijnden and Hicks (2017). Determining the optimum Markov step and acceptance ratio is not considered here and will require a separate investigation.

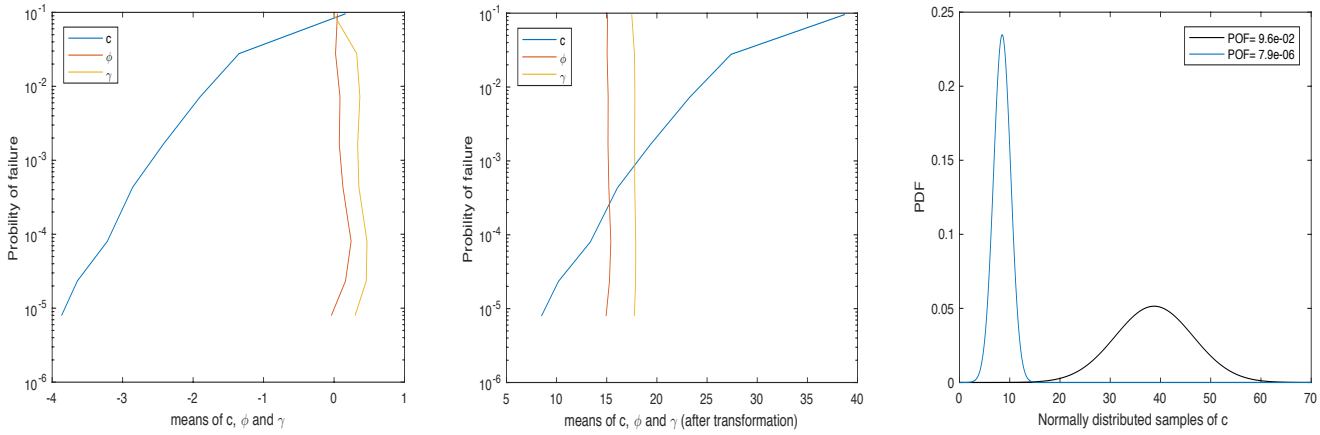

(a) (b) (c)

Figure 5.3: (a) mean of N(0,1) c, ϕ and γ at each p_f level (b) mean of c, ϕ and γ at each p_f level after transformation to Normal dist. (c) Fitted Normal distribution for samples of mean c at first and last subset

5.3.3. MODE OF FAILURE

Figure 5.5 is a plot of slip surfaces for all failing realisations within each subset. From examining the plots, it is evident that the mode of failure differs at different strength reduction factors. The mode of failure for an SRF=2.4 is considered deep with slip surface depths reaching up to 4m below the toe of the slope. On the other hand as the SRF decreases to a final SRF=1.0, the depths of slip surfaces decrease as well. The mode of failure when the slope is failing under its own weight(SRF=1.0) is considered as shallow failure with a significantly smaller sliding volume than in the case of SRF=2.4. Figure 5.6 is a plot of maximum slip surface depth below toe of slope versus the corresponding strength reduction factor, for each SRF level. It is reaffirmed from the plot that as the SRF reduces, so will the depth of sliding surfaces.

In order for failure to occur in the slope, the shear strength of the soil along a slip surface should be low. Therefore a long and deep slip surface will require weak strength along the whole line of shear. When considering a heterogeneous slope with spatial variability, such long weak shear bands are unlikely to occur. This explains the shallow slip surfaces shown for SRF=1.0. Similar results were reported by van den Eijnden and Hicks (2017) for a slope with cohesion as a random variable. They concluded that applying strength reduction methods to evaluate the stability of a slope may lead to overestimation of the sliding volume. The results in figures 5.5 and 5.6 are consistent with such conclusions, even when considering cross-correlated cohesion frictional slopes.

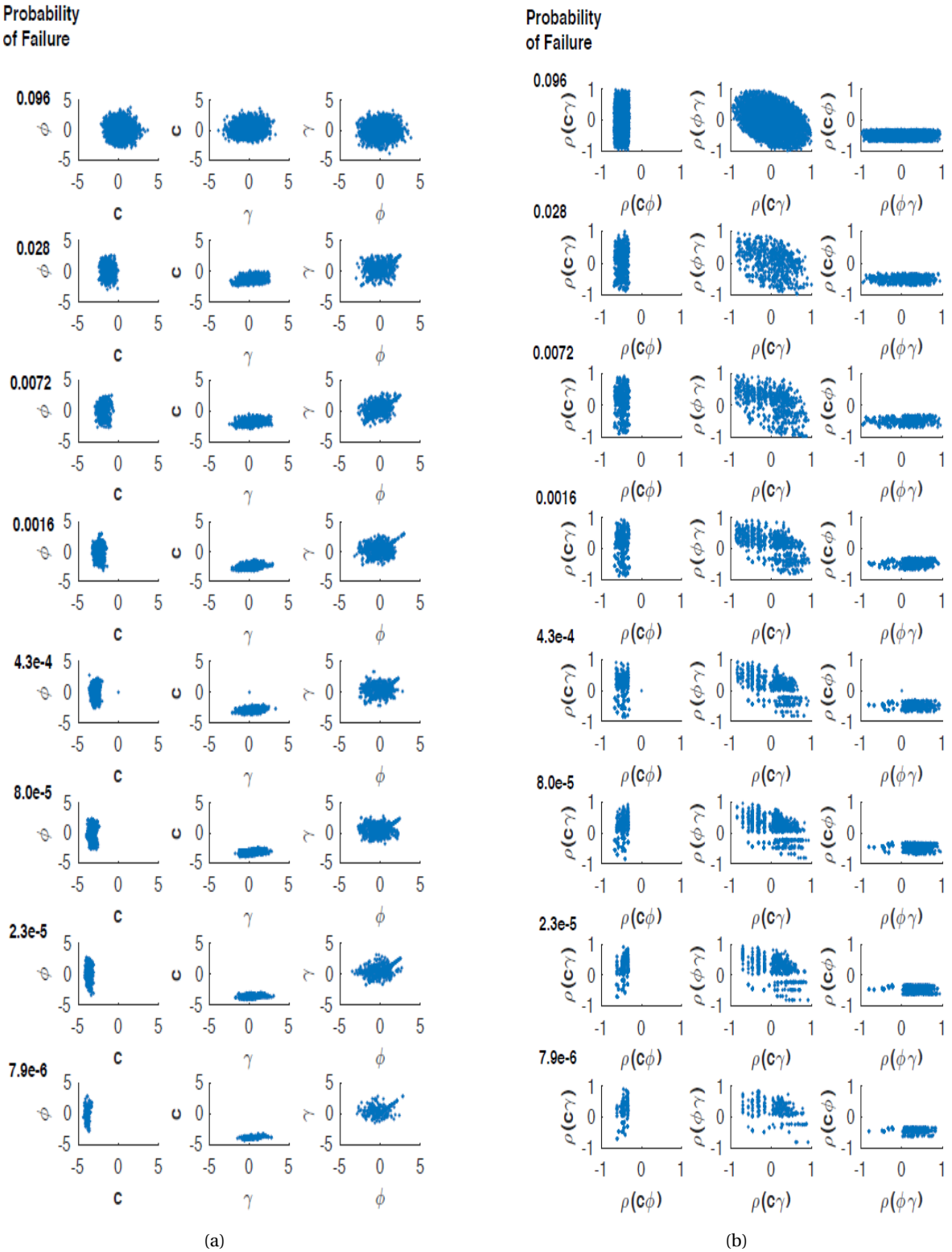

(a) (b)

Figure 5.4: (a) Scatter plots for means of c, ϕ and γ at each p_f level (b) Scatter plots of $\rho_{c,\phi}$, $\rho_{c,\gamma}$ and $\rho_{\phi,\gamma}$ at each p_f level

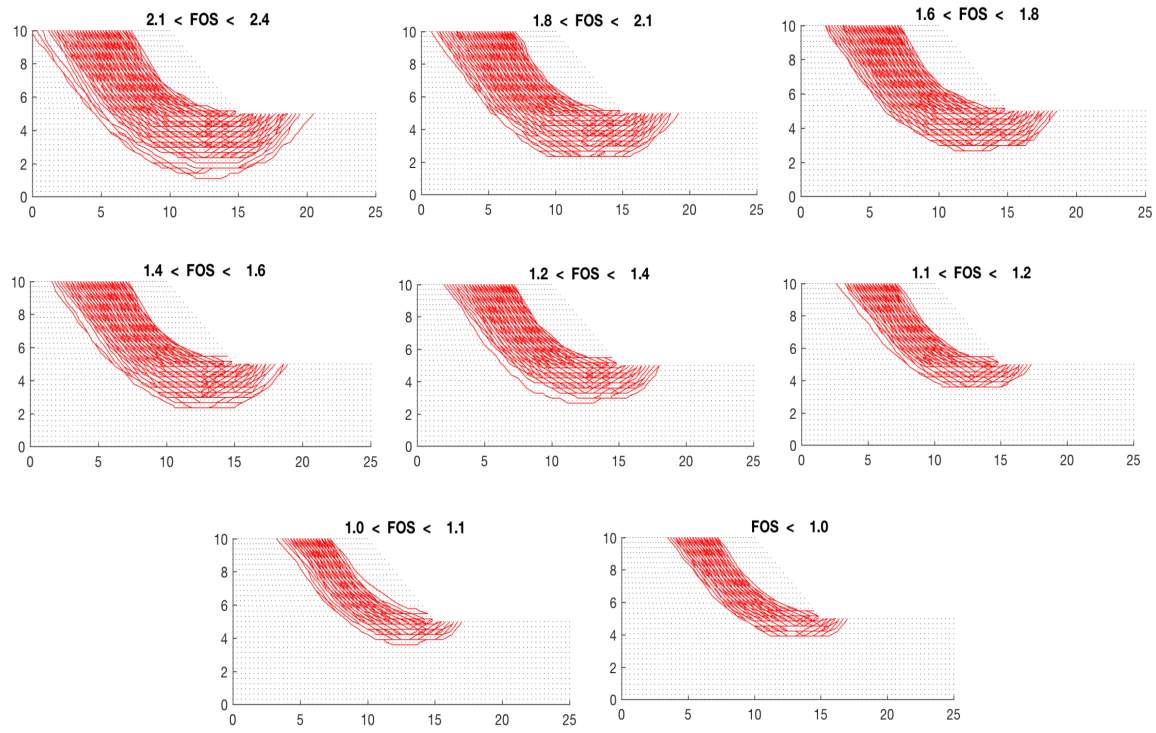

Figure 5.5: Slip surfaces for each subset

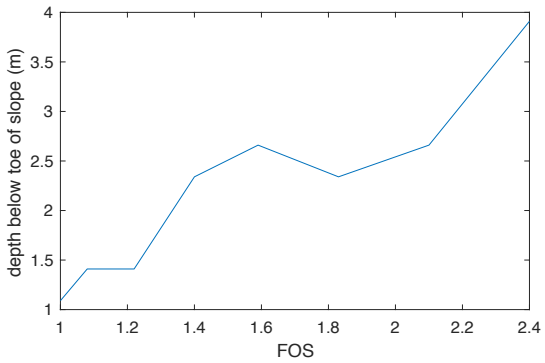

Figure 5.6: Maximum sliding surface depth below toe of slope versus factor of safety for each subset

5.3.4. RANDOM FIELDS OF c, ϕ AND γ

c, ϕ and γ are treated as spatially variable properties which means a random field is generated for each variable for every realisation within the analysis. These random fields are correlated according to the generated correlation matrix from values of $\rho_{c,\phi}$, $\rho_{c,\gamma}$ and $\rho_{\phi,\gamma}$ for each realisation. Figures 5.7a, 5.7b and 5.7c are the average values of failing random fields for the three soil properties during the whole analysis. The average of failing random fields at different probability of failure levels (each subset) are shown in Appendix C. Each plot has a different colour legend shown on the side which reflects the range of values at each p_f level.

When considering the average random field of c (figure 5.7a), weak zones are evident around the toe of the slope. Figure C.1 indicates the size of the weak zone is decreasing with decreasing probability of failure, which is consistent with the change in depth and location of sliding surfaces in figure 5.5. On the other hand random fields of ϕ and γ show strong regions above and around the toe of the slope. The distribution of strong and weak zones for c and γ is consistent with high driving forces at the top of the slope and low resistance around the toe, which is required for failure. Furthermore, the distribution of zones indicates that field values generated for the foundation (below toe of slope) have little influence on failure at lower p_f levels. This is the case as strong zones for γ at the top of the slope lead to a concentration of weak zones at the foundation level.

However, there is no such clear pattern when examining the random fields of ϕ (figures 5.7b and C.2). This indicates that given the restrictions on sampling such as positive definiteness and a negative $\rho_{c,\phi}$, failure within the analysis is not influenced by the distribution of strong and weak zones for ϕ. However, when considering the magnitude of mean of c, ϕ and γ (figure 5.3a), it can be concluded that p_f is more influenced by the reduction in mean of c than by the distribution of strong and weak zones at different p_f levels. Nevertheless, fields of c, ϕ and γ indicate that failure is driven by the weak zones of c around the toe of the slope and strong zones of γ above it.

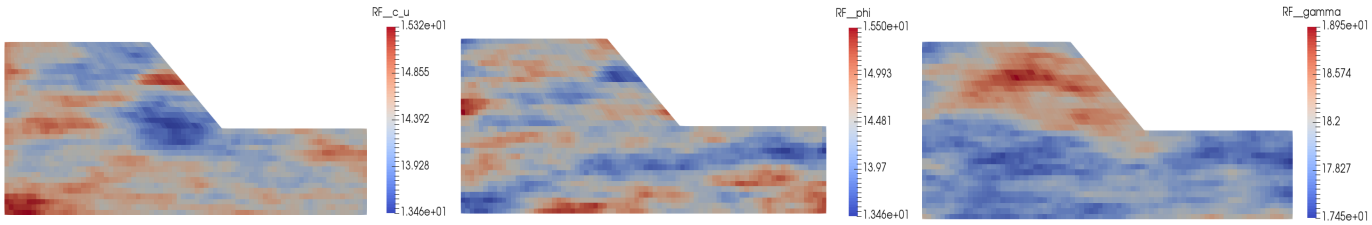

(a) (b) (c)

Figure 5.7: Average random field values for c, ϕ and γ

5.4. CONCLUSION

An analysis is performed using the introduced subset simulation uncertainty framework for an idealised slope. c, ϕ and γ and their mean values are treated as uncertain, and random cross-correlation is applied between the three parameters. Ranges for the material properties are chosen based on values in literature and the results of the sensitivity analysis of part 4. The slope fails with a $p_f = 7.96 * 10^{-6}$. Results are compared to a number of Monte Carlo simulations and show that accuracy and efficiency of SS is maintained even when introducing uncertainty in a number of input parameters.

Subset Simulation is a means to search for samples in the tail end of distributions, i.e. the most critical combinations for failure. When a number of parameters are treated as uncertain, the sam-

pling space and the number of possible combinations of properties increase significantly. This was the case with the practical example, and thus examining the combinations that lead to failure will give insight on the influence of each parameter within the analysis. Failure is most influenced by values of mean c, as at low p_f levels most samples are generated from the tail end of the distribution (PDF=0.015 and less) which is not the case for ϕ and γ. This indicates that for the ranges of values considered, rare events of failure can occur in slopes with low cohesion values, regardless of the magnitude of the friction angle in the analysis. Even though it is shown in part 4 that p_f is heavily influenced by mean of ϕ, this is not the case when treating the soil properties as random. Therefore, if the mean of c is believed to be uncertain, the type of distribution and possible ranges should be carefully chosen. For example the use of 6σ rule in determining the standard deviation for distribution of means may be ill advised if values are believed to strictly fall within a range. This is because although most samples should be generated with the selected range (99.7% of all samples), SS will search for the most critical combinations and may end up completely sampling from the tail end of distribution (0.015%).

Furthermore, a different mode of failure is evident at different strength reduction factors, ranging from deep failure at a SRF=2.4 to shallow failure at a SRF=1.0, or when slope is failing under its own weight. This is significant as it indicates that the use of strength reduction methods may lead to an overestimation of sliding volumes and therefore an overestimation of the risk of such a rare event. This relationship between SRF and mode of failure is consistent with the results of van den Eijnden and Hicks (2017) and must be taken into account when applying strength reduction method to analyse the stability of slopes. Finally, treating means as uncertain in the analysis with a wide range of possible values leads to an outcome that is more influenced by parametric and model uncertainty than by other types of uncertainty such as spatial variability. This is evident when examining the generated fields of c, ϕ and γ as failure is dominated by the magnitude of mean c rather than the distribution of strong and weak zones in the random fields within the analysis.

6

CONCLUSION AND RECOMMENDATION

6.1. CONCLUSION

This report describes a method to evaluate the reliability of a soil slope with cross-correlated uncertain soil properties. A review of literature, equations and conventions is first carried out in chapter 2. The method is then introduced and implemented in chapter 3. Subsequently, a sensitivity analysis is performed for all random variables accounted for in the procedure (chapter 4) before applying the method for an ideal slope with practical input parameters based on literature (chapter 5). The key research questions that were identified in the beginning of the report were as follows:

1. How can cross-correlation be implemented within Subset Simulation?
2. How can uncertainty in means and correlation coefficients of soil properties be implemented within Subset Simulation ?
3. What is the effect of type and range of distribution for these random parameters?
4. What are the most critical combinations of parameters that lead to failure?
5. Does it make sense to apply such an uncertainty framework?

The first two research question were answered in chapter 3 where a subset simulation code is modified to include cross-correlation between cohesion, friction angle and unit weight. This is followed by the implementation of an algorithm for random means of c, ϕ and γ as well as random correlation coefficients ($\rho_{c,\phi}$, $\rho_{c,\gamma}$ and $\rho_{\phi,\gamma}$) in the analysis. The influence of range and type of distribution of these properties is examined in chapter 4 and the critical combinations that lead to failure are evaluated using a practical example for an ideal slope in chapter 5. The probability of failure is heavily influenced by possible ranges of mean c, ϕ and γ with the minimum value for c being the driving force for failure. Furthermore, there was strong positive correlation between ϕ and γ in most failing realisation at low p_f levels. By combining the results of the practical example and sensitivity analysis, it can be concluded that in certain situations where it is believed that such uncertainty exists, it does make sense to model means and correlation coefficients as random variables. However,the sampling of one random parameter will influence sampling of the other and this must be accounted for, depending on the specific degree of uncertainty expected in each parameter. From the multiple investigations carried out in this report, the following conclusions can be made as well:

- Subset simulation is a robust sampling technique that provides the opportunity to compute the p_f for rare events of instability. It was demonstrated that in order to compute p_f with similar confidence using traditional sampling techniques, such as Monte Carlo simulations, the number of samples required to generate failing realisations will increase significantly.

- Subset simulation is a means of accessing the tail end of distributions. Therefore, in an uncertain analysis with a large number of possible parameter combinations, it can identify the most critical combinations that lead to failure for p_f <<<1. However, the success of SS will depend on choices for proposal density, conditional p_f for subsets and other required input for the method (Au and Beck, 2001). These choices are not evaluated in this paper.

- Realisations in SS are generated with Markov chains using MMA and therefore some correlation is anticipated within the chains (van den Eijnden and Hicks, 2017). The size of the Markov chain steps and the acceptance ratio in MMA will influence this correlation. This means that care is required when deciding on type of distribution for the random parameters . The acceptance of samples in MMA is dependant on a ratio between PDFs of seed and proposal states and in the case of a uniform distribution, these are both equal.

- A Beta distribution was considered the best option for modelling uncertainty in correlation coefficients between c, ϕ an γ as it was possible to identify critical combinations of ρ's that lead to failure. As explained in the previous point, this was not the case with a Uniform distribution as most samples were accepted and therefore sampling did not shift from its initial distribution.

- Both Beta and Normal distributions are able to properly model uncertainty in mean values of c, ϕ an γ. However, if sampling must be restricted to a range of possible values, a Beta distribution is the better option. This is the case, as applying a Normal distribution with a standard deviation based on a given range and the 6σ rule, means that samples are generated even below the minimum set value. This can also be avoided with the use of a Truncated Normal distribution.

- The sampling for ρ's is heavily influenced by the fact that the generated correlation matrix must be positive semi-definite. For example, by restricting the range of $\rho_{c,\phi}$, the possible values of $\rho_{c,\gamma}$ and $\rho_{\phi,\gamma}$ will become restricted as well and correlation will be introduced between the two properties. Therefore, if dependence is believed to exist between parameters and it can be quantified, then it may be better to set or restrict values for all ρ's included in the analysis.

- p_f is very sensitive to ranges of means of c, ϕ an γ. Care has to be taken especially in determining the minimum possible value for c. Furthermore, when means are treated as random variables, p_f is less sensitive to uncertainty in correlation coefficients. It was demonstrated that some combination of set ρ's (eg. $\rho_{c,\phi}$=-0.7, $\rho_{c,\gamma}$=0.6 and $\rho_{\phi,\gamma}$=-0.5) will lead to much lower p_f and therefore if such correlation is believed to exist, it must be set in the analysis to avoid conservative results.

- The mode of failure encountered when using strength reduction methods is different than in the case of the slope failing under its own weight. The prior leads to deep failures and the latter are predominantly shallow. This means that the use of such strength reduction methods may be conservative as it leads to overestimation of the depth and volume of sliding.

- Finally, the effectiveness of such an approach is driven by the input parameters used in the analysis. For example, uncertainty in the determination of mean can be categorised as epis-

temic. A proper site investigation will lead to more knowledge regarding an uncertain parameter which will improve the input for such an analysis and in turn, lead to a more accurate determination of p_f for the slope in question.

6.2. RECOMMENDATION

A method is introduced in this paper to model soil properties and correlation coefficients as random variables, adopting the procedure of subset simulation. However, in order to fully establish the effectiveness of such a method, further improvements and investigations should be performed. The following are recommendations for future work as well as any recommendations that arise from the implementation and investigation of the method in this report:

- The efficiency of SS after the implementation of the method should be examined and quantified. By repeating the analysis a significant number of times and computing the coefficient of variation of the results, it is possible to evaluate the efficiency of the method in comparison with a Monte Carlo simulation. This can be done by calculating number of samples required for same COV using equation 2.19 and comparing the computation cost of the methods.
- To limit correlations within consecutive samples in a Markov chain, a full analysis of optimum Markov step size for each random variable should be investigated. This should include an investigation of the optimum combination between Markov step size and acceptance ratio in MMA.
- A sensitivity analysis shows that p_f is heavily influenced by changes in vertical and horizontal scales of fluctuation. Therefore, it is recommended that the approach is extended to include random values for these, as it should not be limited to parametric uncertainty as other sources exist, such as spatial variability.
- A quantitative analysis of the effect of positive definiteness on the sampling of correlation coefficients might be required. This may include determining the number of samples rejected within SS due to this limitation. Such an analysis may provide insight on how to better generate random values for ρ's .
- Evaluating the effect of distribution type on sampling within SS may be also extended. This can include other possible distributions such as Gamma. Furthermore, a sensitivity analysis of effect of distribution type on p_f may be necessary before selecting the optimum type for each random variable.
- The study can be extended to include uncertainty in geometry, boundary conditions and other factors that may influence the p_f of the slope. In order to do so, a literature review will be required to determine if there is a basis for the inclusion of such sources of uncertainty.

BIBLIOGRAPHY

Ahmed, A. (2012). *Simplified and Advanced Approaches for the Probabilistic Analysis of Shallow Foundations*. PhD thesis, Universite De Nantes.

Alonso, E. (1976). Risk analysis of slopes and its application to slopes in canadian sensitive clays. *Geotechnique*, 26, No.3:453–472.

Au, S.-K. and Beck, J. L. (2001). Estimation of small failure probabilities in high dimensions by subset simulation. *Probabilistic Engineering Mechanics*, 16 (4):263–277.

Brehier, C.-E., Goudenege, L., and Tudela, L. (2016). Central limit theorem for adaptive multilevel splitting estimators in an idealized setting. In *Monte Carlo and Quasi-Monte Carlo Methods*, pages 245–260. Springer.

Cao, Z., Cao, Y. W. Z., Wang, Y., and Li, D. (2016). *Probabilistic Approaches for Geotechnical Site Characterization and Slope Stability Analysis*. Zhejiang University Press.

Cerou, F., Moral, P. D., Furon, T., and Guyader, A. (2012). Sequenctial monte carlo for rare event estimation. *Stat Comput*, 22:795–808.

Cho, S. E. (2010). Probabilistic assessment of slope stability that considers the spatial variability of soil properties. *Journal of Geotechnical and Geoenvironmental Engineering*, 136(7).

Cho, S. E. and Park, H. C. (2010). Effect of spatial variability of cross-correlated soil properties on bearing capacity of strip footing. *International Jouranal for Numerical Methods in Engineering*, 34:1–26.

Cornell (1969). A probability-based structural code. *ACI-Journal*, 66:974–985.

Das, B. M. (2006). *Theoretical Foundation Engineering*. Ross Publishing Inc.

El-Ramly, H., Morgenstern, N., and Cruden, D. (2002). Probabilsitc slope stability analysis for practice. *Canadian Geotechnical Journal*, 39(3):665–683.

Elkateb, T., Chalaturnyk, R., and Robertson, P. K. (2002). An overview of soil heterogeneity: quantification and implications on geotechnical field problems. *Canadian Geotechnical Journal*, 40:1–15.

Fenton, G. A. (2014). Simulation. In *ALERT Doctoral School, Stochastic Analysis and Inverse Modelling*, pages 127–181.

Fenton, G. A. and Griffiths, D. (2003). Bearing-capacity prediction of spatially random c - ϕ soils. *Canadian Geotechnical Journal*, 40(3):54–65.

Fenton, G. A. and Vanmarcke, E. H. (1990). Simulation of random fields via local average subdivision. *Journal of Engineering Mechanics*, 116(8).

Glasserman, P., Heidelberger, P., Shahabuddin, P., and Zajic, T. (1999). Multilevel splitting for estimating rare event probabilities. *Operations Reserach*, 47(4):585–600.

Griffiths, D. and Fenton, G. A. (2004). Probabilsitc slope stability analysis by finite elements. *Journal of Geotechnical and Geoenvironmental Engineering*, 130(5).

Griffiths, D., Huang, J., and A.Fenton, G. (2009). Influence of spatial variability on slope reliability using 2-d random fields. *Journal of Geotechnical and Geoenvironmental Engineering*, 135(10).

Griffiths, D., Huang, J., and A.Fenton, G. (2010). Comparison of slope reliability methods of analysis. In *GeoFlorida*.

Griffiths, D. and Lane, P. (1999). Slope stability analysis by finite elements. *Geotechnique*, 49.

Hasofer, A. M. and Lind, N. C. (1974). An exact and invariant first order reliability format. *Journal of engineering mechanics division*, 100:111–121.

Hassan, A. M. and Wolff, T. F. (1999). Search algorithm for minimum reliability index of earth slopes. *Journal of Geotechnical and Geoenvironmental Engineering*, 125(4).

Heidelberger, P. (1995). Fast simulation of rare events in queueing and reliablity models. *ACM Trans. Modeling and Computer Simulation*, 5:43–85.

Hicks, M. A. (2014). Application of the random finite element method. In *ALERT Doctoral School, Stochastic Analysis and Inverse Modelling*, pages 181–207.

Hicks, M. A. (2016). Lecture notes cie4395.

Hicks, M. A. and Samy, K. (2002). Influence of heterogeneity on undrained clay slope stability. *Quarterly Journal of Engineering Geology and Hydrogeology*, 35:41–49.

Huang, S., Quek, S. T., and Phoon, K.-K. (2001). Convergence study of the truncated karhunen–loeve expansion for simulation of stochastic processes. *International Jouranal for Numerical Methods in Engineering*, 52, Issue 9(1029-1043).

Janbu, N., Hirschfeld, R., and Poulos, S. (1973). *Slope Stability Computations, In Embankment-dam Engineering*. John Wiley and Sons.

Javankhoshdel, S. and Bathurst, R. (2015). Influence of cross-correlation between soil parameters on probability of failure of simple cohesive and c-phi slopes. *Canadian Geotechnical Journal*, 53(5):839–853.

Jonkman, S., Steenbergen, R., Morales-Napoles, O., Vrouwenvelder, A., and Vrijling, J. (2016). Lecture notes cie4130.

Juneja, S. and Shahabuddin, P. (2006). Rare-event simulation techniques: An introduction and recent advances. *Handbooks in Operations Research and Management Science*, 13:291–350.

Karandeniz, H. and Vrouwenvelder, T. (2003). Overview reliablity methods.

Kim, D., Kim, K.-S., Ko, S., Choi, Y., and Lee, W. (2012). Assessment of geotechnical variability of songdo silty clay. *Engineering Geology*, 133-134:1–8.

Kiureghian, A. D. and Ditlevsen, O. (2007). Aleatory or epistemic? does it matter? In *Special Workshop on Risk Acceptance and Rick Communication, Stanford University*.

Kulhawy, F. (1992). On evaluation of static soil properties. In *Stabilitiy and performance of slopes and embankments II*.

Liang, R., Nusier, O., and Malkawi, A. (1999). A reliability based approach for evaluating the slope stability of embankment dams. *Engineering Geology*, 54:271–285.

Liu, L.-L., cheng, Y.-M., and Zhang, S.-H. (2017). Conditional rnadom field reliability analysis of a cohesion-frictional slope. *Computers and Geotechnics*, 82:173–186.

Lumb, P. (1970). A probabilistic study of safety and design of earth slopes. *Canadian Geotechnical Journal*, 7:225–242.

Metropolis, N., Rosenbluth, A., Rosenbluth, M., Teller, A., and Teller, E. (1953). Equation of static calculations by fast computing machines. *Journal of Chemical Physics*, 21 (6):1087–1092.

Nguyen, V. U. and Chowdhury, R. N. (1985). Simulation for risk analysis with correlated variables. *Geotechnique*, 35(1):47–58.

Owen, A. B. (2013). *Monte Carlo theory, methods and examples.* Stanford.

Phoon, K.-K., Kulhawy, F., and Grigoriu, M. D. (1995). Reliability- based design of foundations for transmission line structures. *Computers and Geotechnics*, 26(3-4):169–185.

Phoon, K.-K. and Kulhawy, F. H. (1999). Characterization of geotechnical variability. *Canadian Geotechnical Journal*, 36(4)(612-624).

Robert, C. P. and Casella, G. (2010). *Introducing Monte Carlo Methods with R.* Springer.

Rocscience (2001). Application of the finite element method to slope stability.

Schueller, G. and Pardlwarter, H. (2009). Uncertainty analysis of complex structural systems. *International Jouranal for Numerical Methods in Engineering*, 80:881–913.

Shahabuddin, P. (1995). Rare event simulation in stochastic models. In *Proceedings of the 1995 Winter Simulation Conference*, pages 178–185. IEEE Computer Society Press.

Soubra, A.-H. and Bastidas-Arteaga, E. (2014). Advanced reliability analysis methods. *ALERT Doctoral School, Stochastic Analysis and Inverse Modelling.*

Suchomel, R. and Masin, D. (2010). Comparison of different probabilistic methods for predicting stability of a slope in spatially variable c-phi soil. *Computers and Geotechnics*, 37:132–140.

Sudret, B. and Kiureghian, A. D. (2000). Stochastic finite element methods and reliability a state-of-the-art report. *Department of Civil and Environmental Engineering at University of California, Berkeley.*

van den Eijnden, A. and Hicks, M. (2017). Efficient subset simulation for evaluating the modes of improbable slope failure.

Vanmarcke, E. (1983). *Random fields: Analysis and synthesis.* MIT Press, Cambridge, MA.

Verruijt, A. (2007). *Soil Mechnics.* VSSD.

Waarts, P. (2000). *Structural reliability using finite element analysis.* PhD thesis, TU Delft.

Wang, Y., Cao, Z., and Au, S.-K. (2010). Efficient monte carlo simulation of parameter sensitivity in probabilistic slope stability analysis. *Computers and Geotechnics*, 37:1015–1022.

Wright, S. G., Duncan, J. M., and Brandon, T. L. (2014). *Soil Strength and Slope Stability.* John Wiley and Sons.

Yu, W. and Au, S.-K. (2014). *Engineering Risk Assessment with Subset Simulation*. Wiley.

Yucemen, M. S., Tang, W., and Ang, A.-S. (1976). A probabilistic study of safety and design of earth slopes. *Canadian Geotechnical Journal*, 13(3):201–214.

Zwick, D. (2012). Positive definitive matrices.

Appendices

A

Sensitivity to Distribution type (Chapter 4)

A.1. BETA VS UNIFORM ρ'S

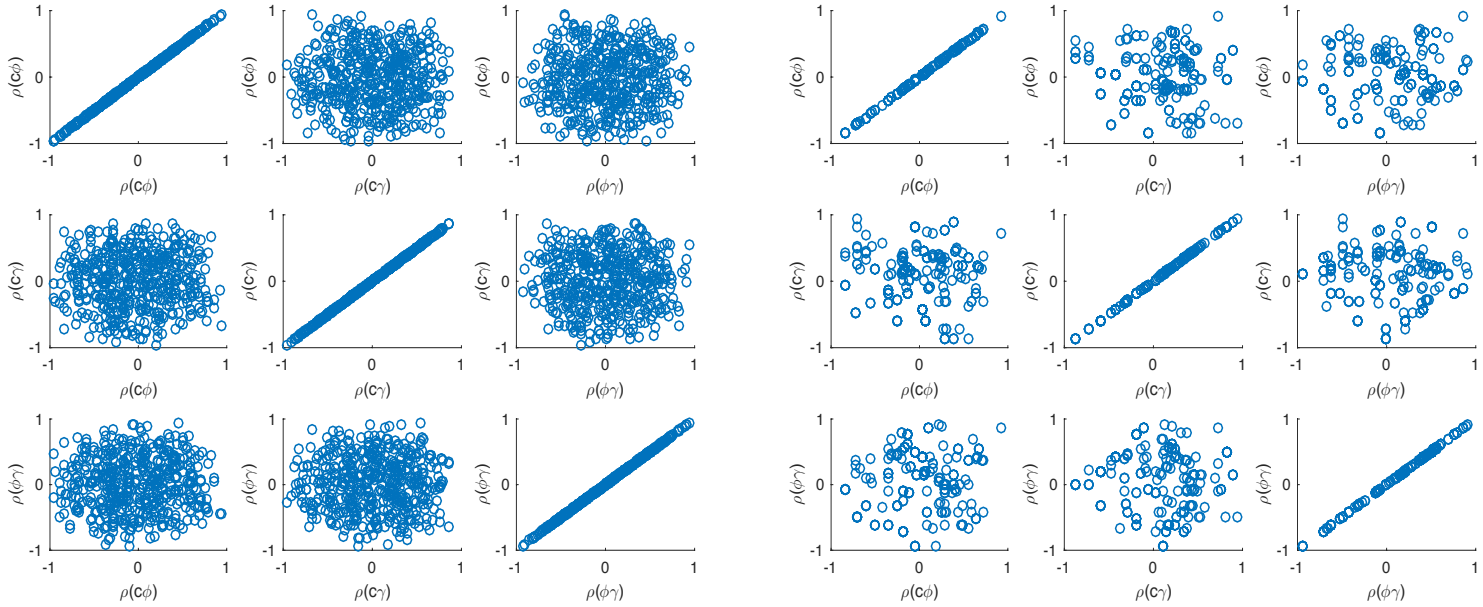

(a) (b)

Figure A.1: Scatter plot for Beta generated ρ's at p_f= (a)0.29 (b)0.013

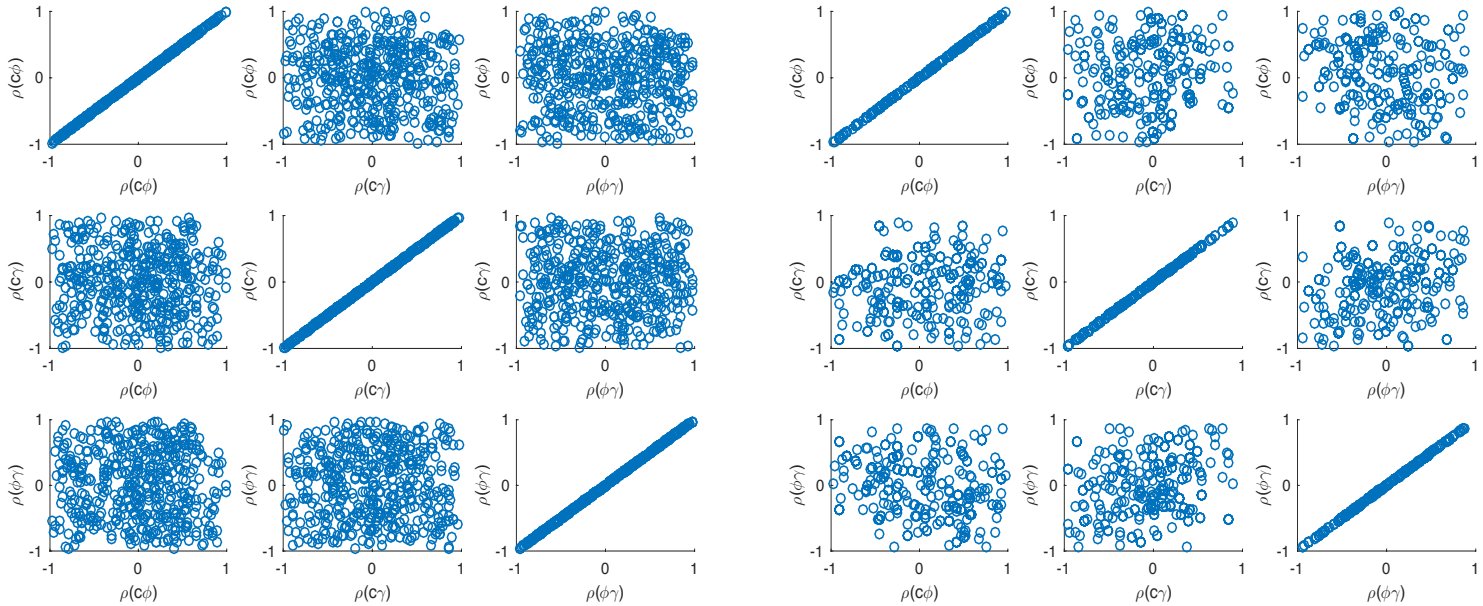

(a) (b)

Figure A.2: Scatter plot for Uniform generated ρ's at p_f= (a) 0.31 (b) 0.014

A.2. NORMAL VS BETA MEAN

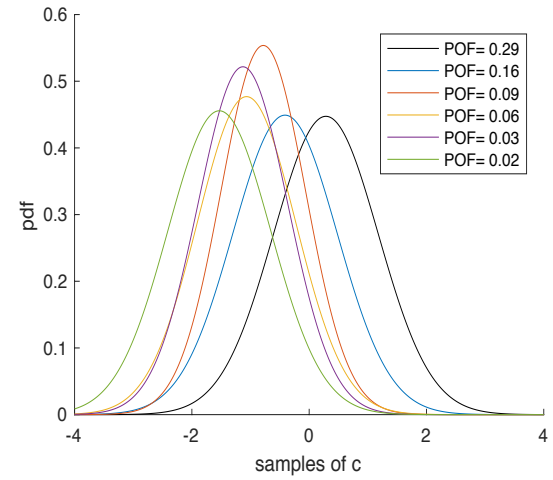

(a)

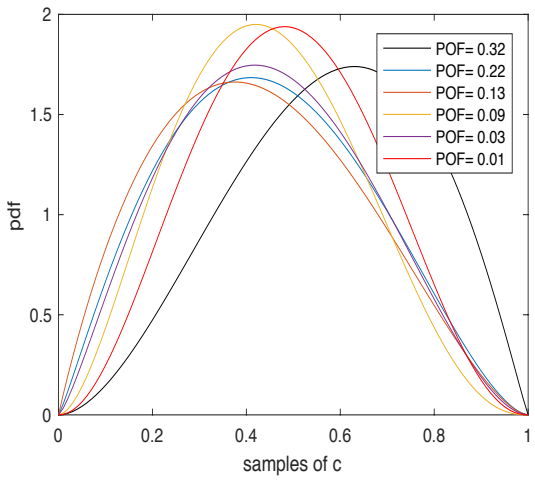

(b)

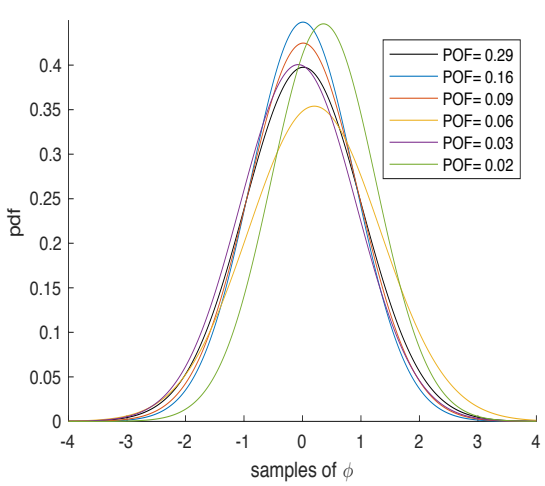

(c)

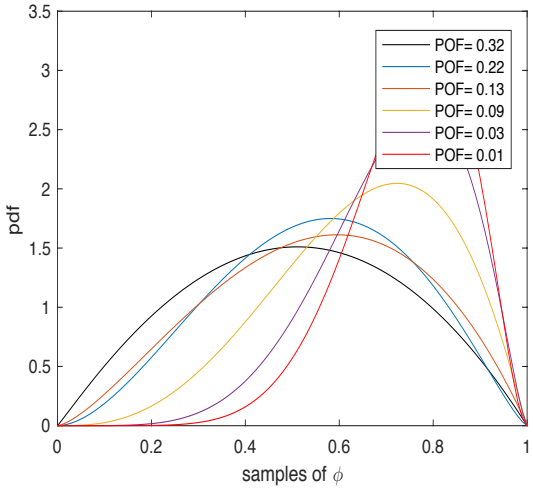

(d)

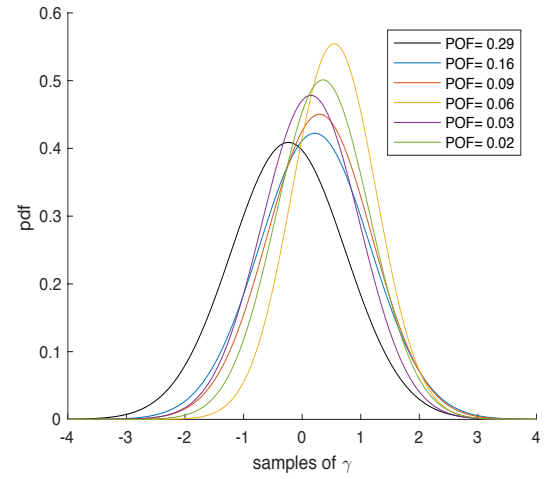

(e)

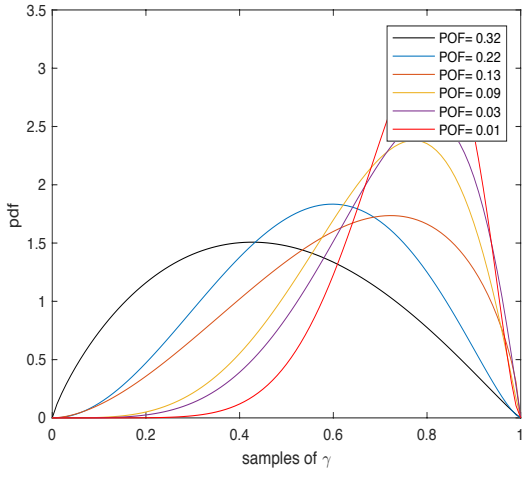

(f)

Figure A.3: **Left column:** N(0,1) samples of c,ϕ and γ, **right column:** Beta(0,1) samples of c,ϕ and γ

B

FITTED DISTRIBUTION PLOTS (CHAPTER 5)

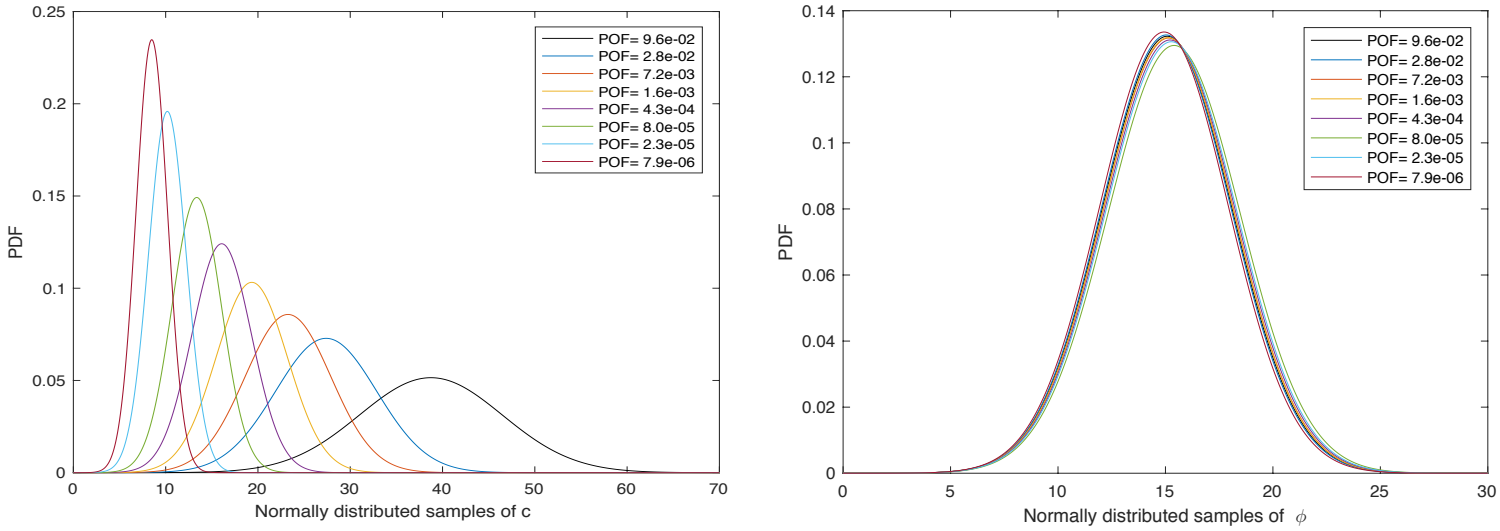

Figure B.1: (a) Normally distributed samples of c (after transformation) (b) Normally distributed samples of ϕ (after transformation)

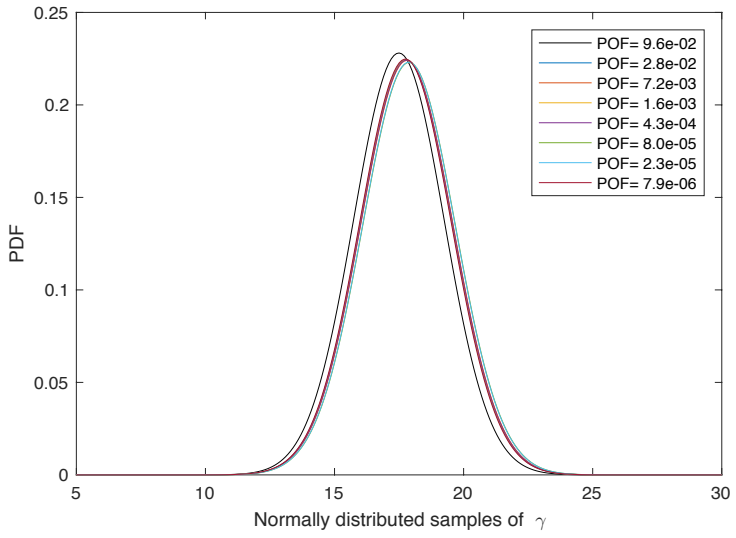

Figure B.2: Normally distributed samples of γ (after transformation)

C

Random Fields (Chapter 5)

C.1. COHESION

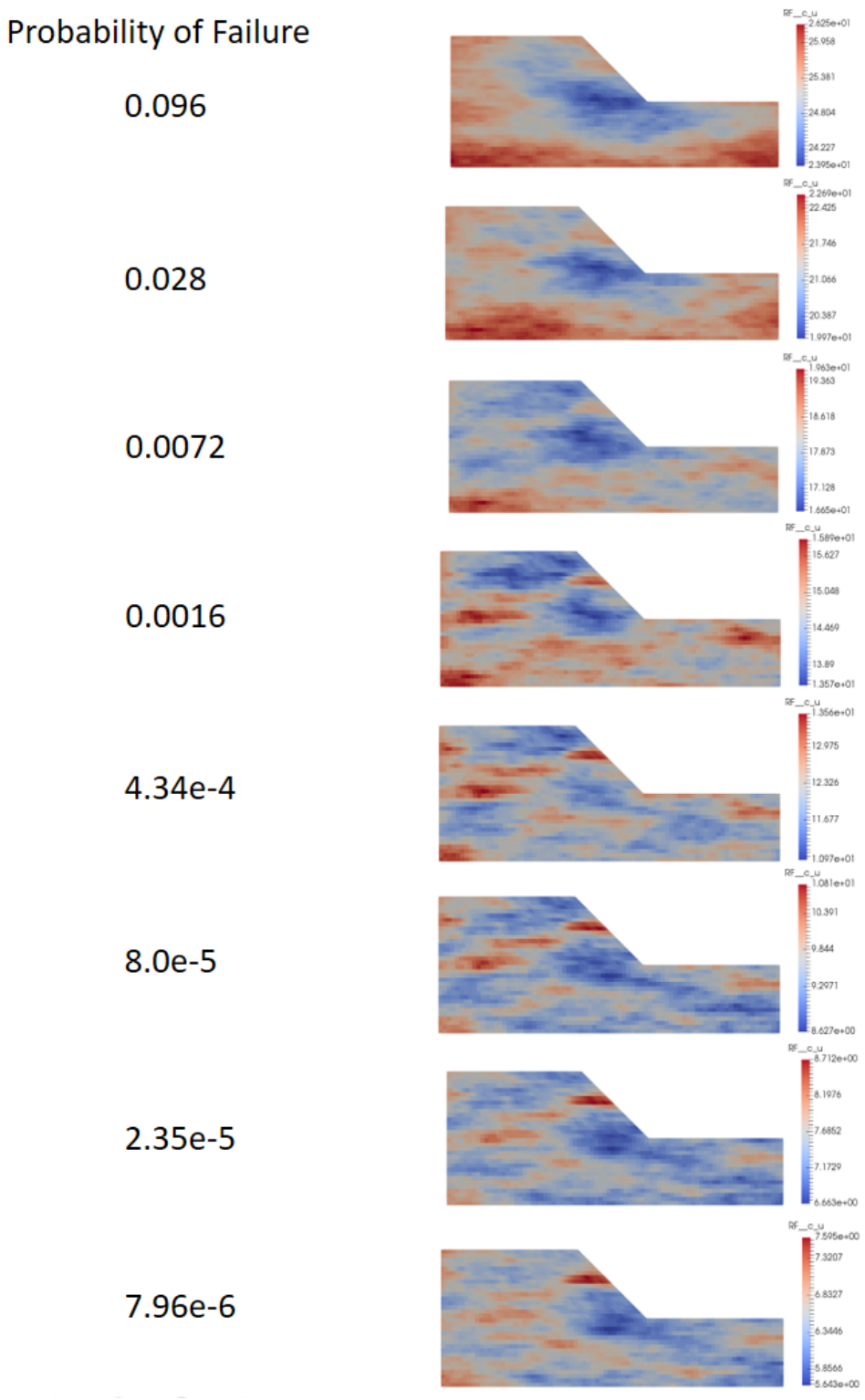

Figure C.1: Random field for c at each corresponding p_f level

C.2. FRICTION ANGLE

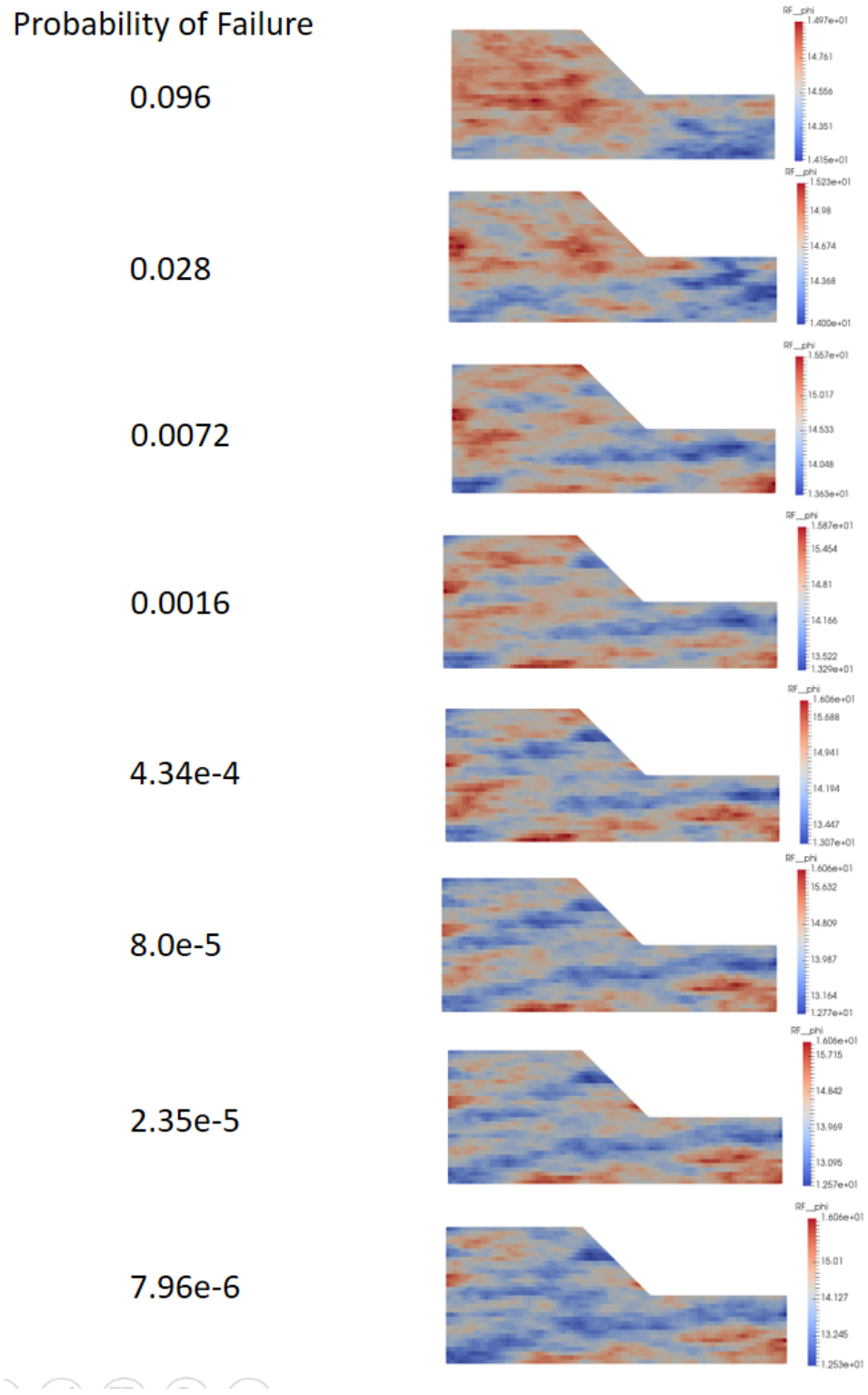

Figure C.2: Random field for ϕ at each corresponding p_f level

C.3. UNIT WEIGHT

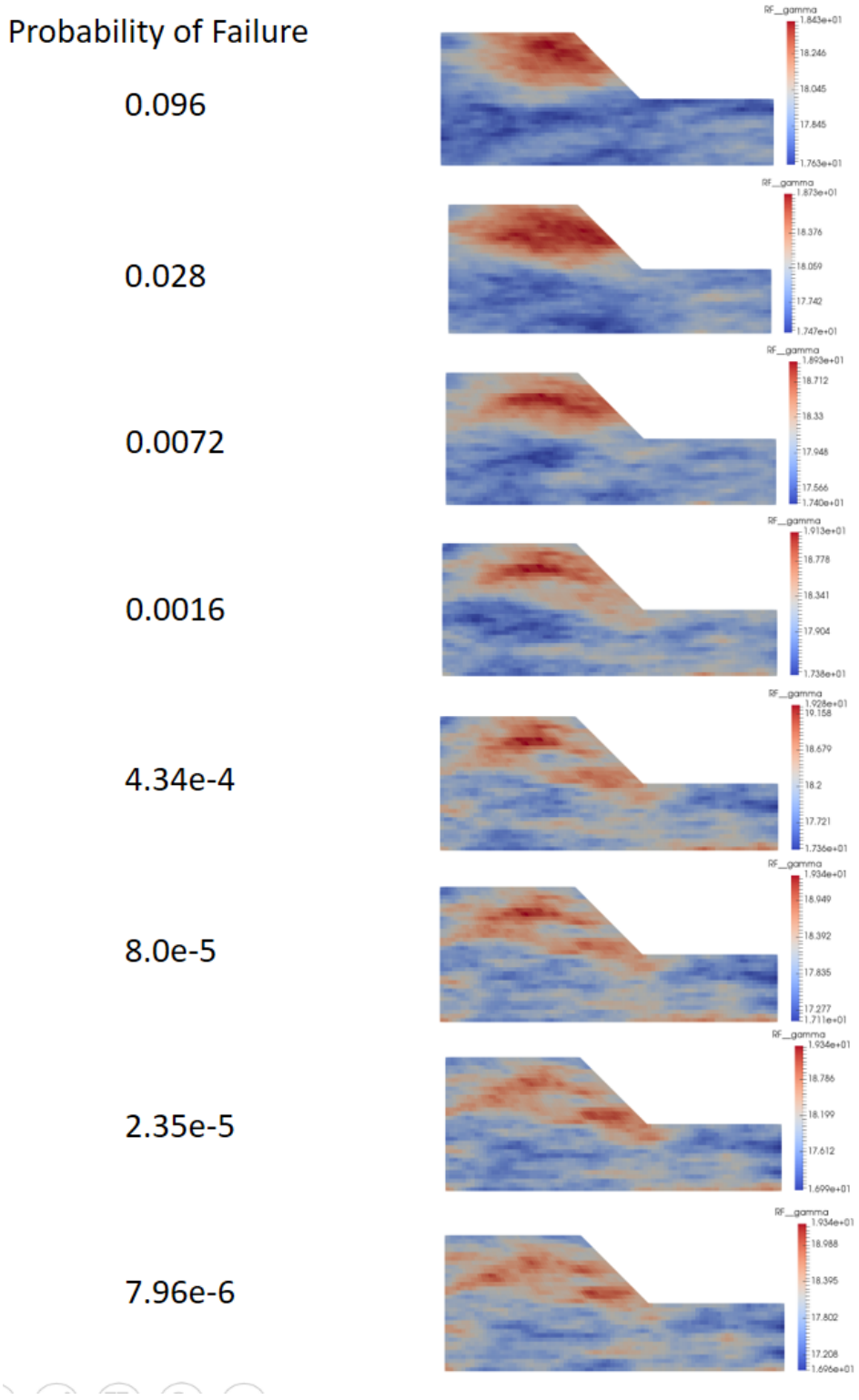

Figure C.3: Random field for ϕ at each corresponding p_f level